

**INVESTIGATION OF THE RELATIONSHIP BETWEEN
ATMOSPHERIC ELECTRICITY
AND THE ENVIRONMENT**

Thesis submitted to the
COCHIN UNIVERSITY OF SCIENCE AND TECHNOLOGY
for the Degree of
DOCTOR OF PHILOSOPHY
under the
FACULTY OF SCIENCE

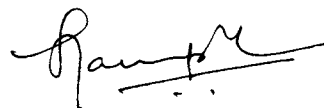
V. SASI KUMAR

ATMOSPHERIC SCIENCES DIVISION
CENTRE FOR EARTH SCIENCE STUDIES
THIRUVANANTHAPURAM-695 031

JANUARY 1994

CERTIFICATE

This is to certify that this Thesis is an authentic record of research work carried out by Mr. V. Sasi Kumar under my supervision and guidance in the Centre for Earth Science Studies for Ph.D. Degree of the Cochin University of Science and Technology, and no part of it has previously formed the basis for the award of any other degree in any University.



Dr. S. Sampath
(Research Guide)

Head

Atmospheric Science Division
Centre for Earth Science Studies
Thiruvananthapuram - 695031

Thiruvananthapuram
January, 5, 1994.

CONTENTS

1. INTRODUCTION	1
1.1 THE ATMOSPHERIC ELECTRICAL CIRCUIT	1
1.1.1 The spherical capacitor theory	3
1.2 ION PRODUCTION IN THE ATMOSPHERE	9
1.2.1 Sources of ionization	9
1.2.2 Ionization due to radioactivity	11
1.2.3 Formation and recombination of ions	14
1.2.4 Effect of aerosols	16
1.3 DIURNAL AND SEASONAL VARIATIONS	19
1.3.1 Temporal variation of conductivity	20
1.3.2 Temporal variation of the vertical electric field	22
1.4 RADIOACTIVITY IN THE ATMOSPHERE	27
1.4.1 Radioactivity at the surface and in the atmo- sphere	27
1.4.2 Studies on relationship between radioactivity and atmospheric electricity	31
1.5 PRESENT STUDY	34
2. INSTRUMENTATION	35
2.1 INTRODUCTION	35
2.2 THE GERDIEN CONDENSER	36
2.2.1 Theory	37
2.2.2 Sources of error	43
2.2.3 The Gerdien sensor	47
2.2.4 The ground-based instrument	48

2.3 THE FIELD MILL	57
2.3.1 Theory	59
2.3.2 The sensor	60
2.3.3 The electronics	62
2.4 THE SYSTEM CONSOLE	65
3. THE EXPERIMENTS	66
3.1 INTRODUCTION	66
3.1.1 The study region	67
3.2 MEASUREMENTS AT THE SURFACE	72
3.2.1 Monitoring sites	72
3.2.2 Operation and maintenance	75
3.2.3 Data reduction and analysis	77
3.3 JEEP-BORNE AND AIR-BORNE SURVEYS	79
4. CONDUCTIVITY VARIATIONS AT THE SURFACE	81
4.1 INTRODUCTION	81
4.2 DIURNAL VARIATION OF POLAR CONDUCTIVITIES	82
4.3 EFFECT OF SURFACE RADIOACTIVITY ON CONDUCTIVITIES	86
4.4 DIURNAL VARIATION OF CONDUCTIVITY AT A RADIOACTIVE SITE	91
4.5 EFFECT OF RAINFALL ON CONDUCTIVITY	95
4.5.1 Effect of pre-monsoon rainfall	95
4.5.2 Effect of monsoon rainfall	96
4.6 DIFFERENCE BETWEEN COASTAL AND INLAND SITES	100
4.7 DIURNAL VARIATION OF CONDUCTIVITY - TOWARDS AN ALTER- NATIVE EXPLANATION	101
4.7.1 Need for an alternative explanation	101
4.7.2 Harmonic analysis of conductivity	104
4.7.3 Towards an alternative explanation	107

5. SPACIAL VARIATION OF CONDUCTIVITY	111
5.1. INTRODUCTION	111
5.2 PAYLOAD DETAILS	112
5.2.1 Design of the sensor	113
5.2.2 Design of the electronics	113
5.3 GROUND SURVEYS	119
5.4 RESULTS OF AERIAL SURVEYS	121
5.4.1 Survey 1 : Trivandrum - Alleppey	123
5.3.2 Survey 2: Trivandrum - Kanyakumari	127
5.3.3 Survey 3: Trivandrum - Kottarakara - Chavara	128
6. SUMMARY AND CONCLUSION	133
6.1 RESUMÉ	133
6.2 HIGHLIGHTS OF RESULTS	134
6.3 SUGGESTIONS FOR FURTHER STUDIES	136
REFERENCES	139
PUBLICATIONS	148

LIST OF FIGURES

Figure 1.1	Variation of positive polar conductivity between the earth's surface and 35 km altitude measured from Hyderabad, India (after Murali Das, <i>et al.</i> , 1990).	5
Figure 1.2	Schematic diagram of the atmospheric electric circuit.	7
Figure 1.3	Variation of small ion concentration with aerosol concentration.	18
Figure 1.4	Diurnal variation of the vertical electric field over the oceans observed in the cruise of the research vessel <i>Carnegie</i> .	20
Figure 1.5	Examples of (a) single and (b) double oscillation types of diurnal variation of positive polar conductivity.	22
Figure 1.6	Examples of the three types of diurnal variation of the vertical electric field (after Israel, 1971).	25
Figure 1.7	Theoretical profile of the concentration of radon above and below the soil surface (after Junge, 1963).	29
Figure 2.1	Theoretical current-voltage characteristic of a Gerdien condenser.	40
Figure 2.2	Trajectory of an ion inside a Gerdien condenser.	41
Figure 2.3	Sectional elevation of the Gerdien condenser used for ground-based measurements.	49
Figure 2.4	Block diagram of the electronic circuit of the Gerdien condenser used for ground based measurements.	51
Figure 2.5	The control circuitry used for switching the driving voltage.	52
Figure 2.6	Detailed circuit diagram of the electronics of the ground-based Gerdien condenser.	54
Figure 2.7	The circuitry used for eliminating the transients from the recorded data.	56
Figure 2.8	Calibration of the Gerdien condenser system.	57
Figure 2.9	Current-voltage characteristic of the Gerdien condenser used in the monitoring stations.	57
Figure 2.10	Schematic diagram of the field mill sensor.	61
Figure 2.11	Block diagram of the electronic circuitry of the field mill.	62

Figure 2.12 Detailed circuit diagram of the electronics of the field mill.	64
Figure 2.13. Schematic diagram of the ground station console.	65
Figure 3.1 Map showing physiography of Kerala State.	68
Figure 3.2 Map of the southern part of Kerala State and the adjoining regions of Tamil Nadu, showing the distribution of radioactivity in terms of the intensity of terrestrial radiation.	70
Figure 3.3 Map showing the locations of the monitoring stations.	76
Figure 3.4 Sample portion of a day's record of conductivity.	78
Figure 4.1 Diurnal variation of conductivity at Kottarakara for the months of May, June, July, August and September, 1991.	83
Figure 4.2 Diurnal variation of conductivity at Ambalapuzha for the months of June, July, August, September and October, 1991.	84
Figure 4.3 Percentage variances of the monthly mean hourly values of polar conductivities at Chavara plotted against monthly mean temperatures for Alleppey.	89
Figure 4.4 Monthly mean diurnal variation of polar conductivities at Chavara for the months of March, April, May and June, 1991.	93
Figure 4.5 Daily mean positive polar conductivity at Trivandrum for April and May, 1993, and the daily rainfall.	96
Figure 4.6. Variation of daily mean positive polar conductivity at Chavara during May and June, 1991.	97
Figure 4.7 Variation of daily mean conductivity at Trivandrum during May and June, 1993. The daily rainfall is also shown.	98
Figure 4.8. Monthly mean diurnal variation in the ratio of polar conductivities at Chavara for May and June, 1991.	99
Figure 4.9 Diurnal variation of positive and negative polar conductivities at Athens for each month and for the year (from Retalis & Zervos, 1976).	103
Figure 4.10 Second harmonics of the mean hourly values for the three stations.	105
Figure 4.11 The second harmonics of the monthly mean diurnal variation of positive polar conductivity at Athens for every month of the year (computed using figures given in Retalis & Zervos, 1976).	106

Figure 4.12 Diurnal behaviour of atmospheric pressure in the tropics (from Nieuwolt, 1977).	108
Figure 4.13 Second harmonic of a typical day's pressure variation at Trivandrum and that of the mean value for Kottarakara for all the months.	108
Figure 5.1 The sensor used for aircraft measurements, along with the clamp for mounting it on the aircraft.	114
Figure 5.2 Block diagram of the measurement system for aerial survey.	115
Figure 5.3 Circuit diagram of the electronic circuitry used in the aircraft payload.	117
Figure 5.4 Calibration curves of the complete aerial survey system for the two gain stages which were used in the surveys.	119
Figure 5.5 Polar conductivity data from jeep-borne survey between Trivandrum and Manavalakkurichy.	120
Figure 5.6 Portion of the chart showing enhancement in conductivity near a quarry.	122
Figure 5.7 Map of the region showing the routes along which aerial surveys of polar conductivities were carried out.	124
Figure 5.8 Conductivity variation along the coast from Trivandrum to Alleppey.	125
Figure 5.9 Sample portion of the chart from the survey between Trivandrum and Alleppey showing the large fluctuations.	126
Figure 5.10 Conductivity values obtained in the survey between Trivandrum and Kanyakumari.	127
Figure 5.11 Conductivity data obtained in the survey between Trivandrum and Chavara via Kottarakara.	128
Figure 5.12 Map showing the positive polar conductivity values obtained from the three aerial surveys. The ranges are different for the Trivandrum-Kottarakara-Chavara survey because the flight was carried out at a different altitude.	131

CHAPTER I

1 . INTRODUCTION

1.1 THE ATMOSPHERIC ELECTRICAL CIRCUIT

The existence of electricity in the earth's atmosphere was first discovered by the French scientist T.F. d'Alibart on 10th May 1752 at Marly near Versailles, and reported three days later to the Académie des Sciences in Paris, although it is generally attributed to the renowned scientist-statesman Benjamin Franklin of the United States. Franklin, without knowing about the Frenchman's discovery, independently conducted the experiment in June of the same year and obtained similar results. Both these experimenters, and several others who repeated the experiment, had confined themselves to the observation of the electrical nature of lightning strokes. The discovery that the atmosphere exhibits certain electrical characteristics even on a day of very fine weather was made by another French scientist, L.G. Lemonnier. He soon concluded that electrical phenomena are a permanent property of the atmosphere. Another important discovery of the early phase was that of C.A.Coulomb, who found that a well-insulated conductor, exposed to air, soon lost its charge. He concluded that air must be slightly conducting. Although this discovery was made in 1785, it was not properly appreciated at that time and lay ignored until the experiment was repeated a hundred years later.

The first attempt to explain the observed atmospheric electrical phenomena was made by Alessandro Volta. He hypothesized that as

water evaporates from the surface, it carries away some positive charge, leaving the earth negatively charged. Although this theory was eventually found to be incorrect, it is interesting to note that his theory has, in common with the modern understanding of the generation process of the atmospheric electric field, the phase transition of water contributing to the generation of the electric field. Later, A. Peltier proposed a slightly modified version of the theory. He proposed that the earth had an acquired negative charge which is carried upward by water evaporating from the surface. However, since the resultant charge concentration is less in the atmosphere than on the earth, the lower negative charge was being observed as a positive charge. In spite of its limitations, his theory is considered to be remarkably clear and consistent, and it enabled the problem to be tackled mathematically. This apparently helped later investigators like W. Thomson (Lord Kelvin) to virtually revolutionize the investigation of atmospheric electricity.

The modern theory of the atmospheric electrical circuit was originally formulated by C.T.R. Wilson (1920, 1929) and A. Wigand (1927 a,b), who were the first to suggest that the driving force behind the atmospheric electric circuit was to be found in the so-called "disturbed" regions of the atmosphere - namely, the large number of active thunderstorms always present around the globe. The existence of ions in the atmosphere (Elster & Geitel, 1899), and that of the highly conducting layer in the upper atmosphere, the Kennelly-Heaviside layer, had already been established by then. Still the world was not very willing to accept the new theory, mainly because it conflicted with the existing knowledge about the thunderstorm at that time. Their theory has, however, come to stay, and the accepted model of the atmospheric

electric circuit largely follows the lines suggested by Wilson and Wigand. Generally known as the "spherical capacitor theory", an outline of the model is given below.

1.1.1 The spherical capacitor theory

Electrical processes in the earth's atmosphere have their origin in the production of ions in the air. Ionization of air below about 60 km is mainly due to galactic cosmic rays. As the cosmic rays penetrate deeper into the atmosphere, they produce greater ionization, down to about 15 km altitude. Below this altitude ionization is seen to decrease progressively down to about 2 to 3 km. Over land, from the surface up to 2 to 3 km, the dominant ionizing agent is radioactivity. Very close to the surface, the nuclear radiations from the radioactive minerals in the soil dominate. Their influence, however, is limited to a very short distance. At higher altitudes, radioactive gases released from the soil and their decay products which are radioactive, only are important. The concentration of these gases, and consequently the ionization produced by them, decreases with altitude.

The ionization of air results in air having a finite conductivity. The conductivity of air depends on the concentration and mobility of ions. Mobility is the drift velocity acquired by an ion in a unit electric field. It depends on the mass, being higher for lower masses. To be precise, the conductivity due to one type of ions is the product of the concentration n and mobility μ of the ions and the charge on the ions. If more than one type of ions are present, then the contribution from

each type will have to be accounted for. Thus the positive or negative polar conductivity can be written as :

$$\lambda^{\pm} = \sum n^{\pm} e \mu^{\pm} \quad (1.1)$$

where n^{\pm} , μ^{\pm} , and e are the number density, the mobility and the charge on the ions, respectively, and the summation is taken over the different types of ions present. Since both positive and negative ions are present in the atmosphere, the total conductivity of air is the sum of the polar conductivities, that is, $\lambda_{tot} = \lambda^{+} + \lambda^{-}$. Virtually all the ions found in the atmosphere are singly charged, so that the e in the equation becomes equal to the electronic charge. Ion number density does not vary very widely in the region of the atmosphere below about 70 km. On the other hand, ion mobility, being a function of mean free path, increases exponentially with altitude. Conductivity also consequently increases rapidly with altitude, except in the region from the surface up to 2 to 3 km. (This is the region where ionization is mainly due to radioactivity, and conductivity decreases with altitude). A typical conductivity profile from the surface up to 35 km, measured from Hyderabad, India (Murali Das, *et al.*, 1991) is shown in Figure 1.1. At an altitude of about 60 to 65 km, the conductivity is sufficiently high for any electrical disturbance at one point to be distributed all over the globe within a time period that is small compared to the time scales of the electrical processes in the atmosphere. This equalization layer is usually called the *electrosphere*. Often, the ionosphere is taken as the equalization layer.

The electrosphere and the earth's surface together form a spherical capacitor that acts as the main element in the atmospheric electrical circuit. This capacitor is charged continuously by the

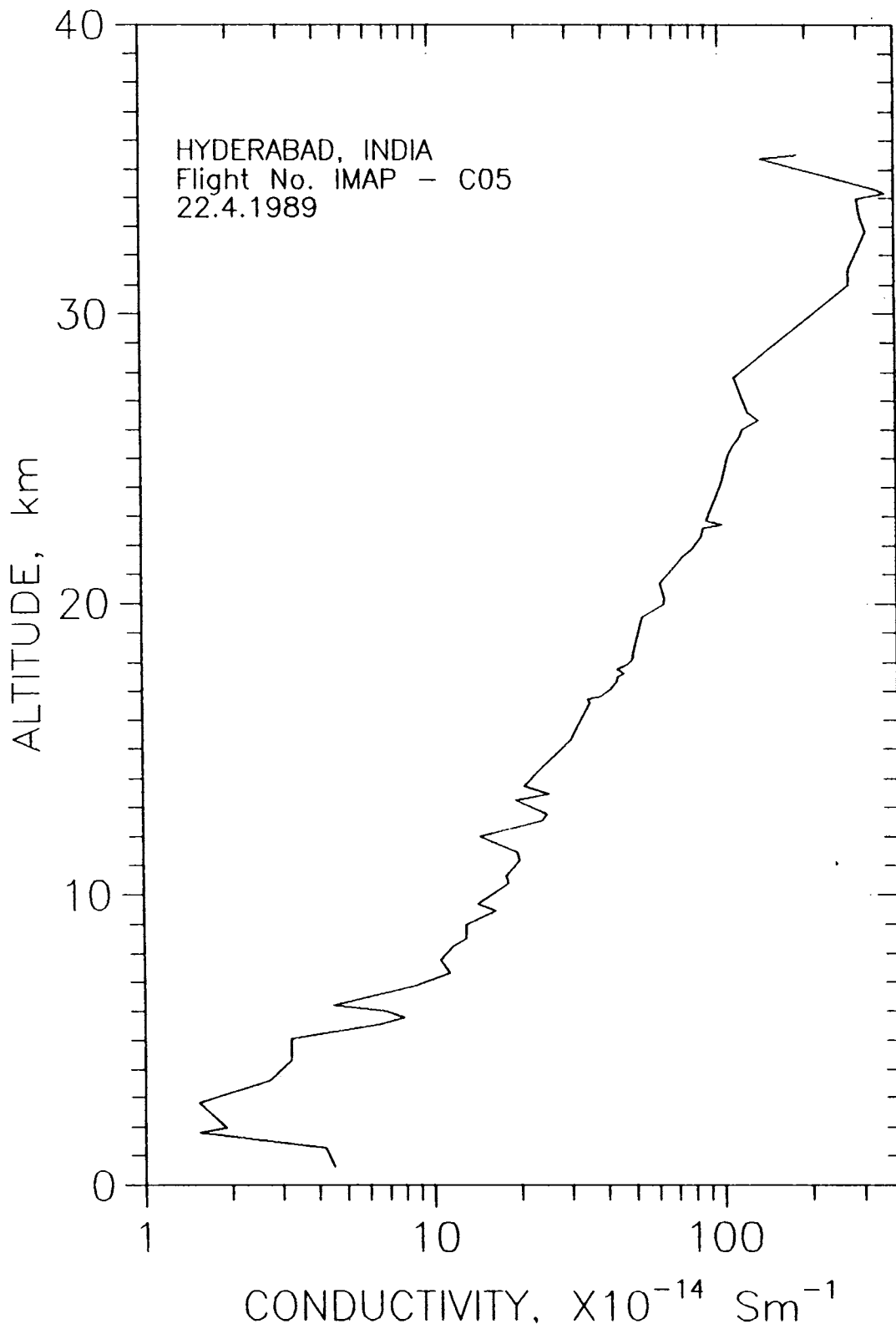


Figure 1.1 Variation of positive polar conductivity between the earth's surface and 35 km altitude measured from Hyderabad, India (after Murali Das, *et al.*, 1991).

roughly 1500 active thunderstorms present around the globe at any given moment. The electrospheric potential has been found to be about 250 to 300 kV (for instance, **Markson**, 1985). This is maintained by the charging current from the thunderstorms and a corresponding discharge current that flows through the fair weather region of the atmosphere. The charging current from the thunderstorms to the electrosphere is mainly a conduction current. Charge transfer from thunderstorms to the earth takes place in different forms. Lightning is the most obvious process. The rain from these clouds also carry some charge (**Chalmers**, 1951 a). Point discharge currents from pointed objects beneath the thunderstorm is also important (**Chalmers**, 1951 b; **Kamra & Varshneya**, 1967). Significant currents may be provided even by point discharge beneath dust storms (**Kamra**, 1969,b), which are known to be electrified. The discharge current is a conduction current that flows from the electrosphere to the earth, the magnitude of which at a given place depends upon the columnar resistance of the atmosphere at that place. Since it may be assumed, as a first approximation, that there are no current sinks in the atmosphere, the electrosphere-earth current can be considered to be constant with altitude. This, in combination with the varying conductivity, creates an electric field that varies with altitude in a manner that is opposite to that of conductivity. This electric field is almost entirely oriented in a vertical direction since horizontal gradients of electric charge are of a very small magnitude throughout the atmosphere. The electric field E , the conduction current density J , and the conductivity λ at any point in the atmosphere are related by the equation $J = \lambda E$. From the discussion above, it can be seen that the independent parameter here is the conductivity λ , the other two being dependent on it (and the electrospheric potential).

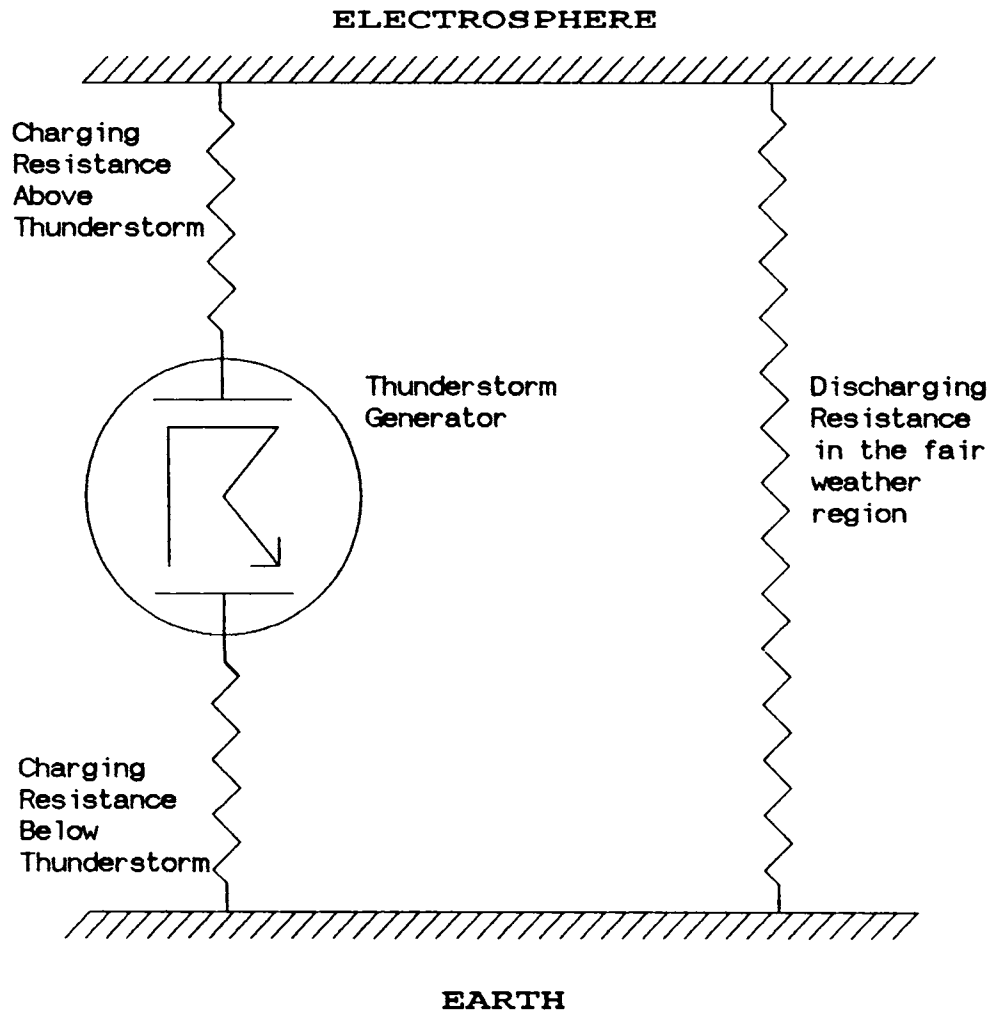


Figure 1.2 Schematic diagram of the atmospheric electric circuit.

The spherical capacitor consisting of the earth and the electro-sphere, the power source formed by the large number of active thunderstorms around the globe that charges this capacitor, and the fair weather region of the atmosphere that acts as a leaky dielectric and provides the discharge path together forms the *atmospheric electric circuit*. Figure 1.2 shows a schematic diagram of the atmospheric electric circuit. Analytical and numerical models of the whole circuit and parts of it have been constructed and studied by several workers, for instance, Hoppel (1967), Chand & Varshneya, (1973), Hays & Roble

(1979), Roble & Hays (1979), Willet (1979), Varshneya (1980), Tuomi (1982), Makino & Ogawa (1984) Nisbet (1985) and others.

The description given above is for an ideal situation where there are no external factors that influence the circuit. Since the earth and the electrosphere are considered to be almost perfect conductors of electricity, it used to be presumed that electrical influences from outside this region would not penetrate below the electrosphere. However, there is growing evidence to the contrary. For instance, coupling between ionospheric and lower atmospheric processes have been reported (Park & Dejnakintra, 1973; Park, 1976; Dutra *et al*, 1992). Solar flare has been found to modify electric fields in the stratosphere (Holzworth & Mozer, 1979) and at the surface (Cobb, 1967; Sao, 1967; Reiter, 1969; Reiter, 1971). Markson (1978), Muir (1979) and Markson & Muir (1980) have suggested the possibility of sunspots and other sun-related phenomena affecting the electrical processes on the earth and thereby even the weather.

1.2 ION PRODUCTION IN THE ATMOSPHERE

As mentioned in the previous section, the main reason for the existence of electrical phenomena in the earth's atmosphere is that air is a conductor of electricity, although a weak one. This is due to the presence of ions in the air. Both positive and negative ions are present in equal numbers so that on the whole the air is neutral. These ions are produced in air by the removal of one or more electrons from some of the air molecules. This is possible if sufficient energy for the removal of the electrons is supplied by some external source. After

ionization, the ions formed undergo changes very quickly, through electrostatic interactions with other molecules and aerosols present in the air, until a relatively stable structure is formed. This survives in a more or less unchanged form until two ions of opposite polarity meet and combine to form neutral species. A brief outline of the processes involved is given in this section.

1.2.1 Sources of ionization

In the earth's atmosphere, ionization is produced by different agencies in different regions. Above about 60–65 km altitude, the main source of ionization is electromagnetic radiations from the sun, ranging from X-rays to the ultraviolet. In the region below, galactic cosmic rays form the main source, except in a thin layer, of about 2 to 3 km, over land. In this region, the dominant sources of ionization are the nuclear radiations from radioactive minerals in the soil, and the radioactive gases released into the atmosphere from the soil and their daughter products. In the region where ionization is due to solar radiation, the rate of ionization shows large variations with time because of the variations in the incident radiation. Since galactic cosmic ray intensities remain more or less uniform over long periods, the ion production rate in the region of the atmosphere from about 2 to 3 km to about 60–65 km altitude remains constant with time; but it shows a variation with latitude. The occurrence of radioactive minerals varies widely from place to place, and the presence of radioactive elements in the air is also influenced by meteorological factors. Ionization due to radioactivity is therefore strongly dependent on the place and time. Since the present work is confined to a region close to the surface,

natural radioactivity and its atmospheric electrical effects will be discussed later in somewhat greater detail.

There are other sources in the atmosphere whose contribution to the total ionization is rather small, but may be important at specific places during specific time periods. The lightning discharge is one of them. Lightning is produced mainly as a part of thunderstorm activity, although similar discharges have been observed during volcanic eruptions, and even during a strong dust storm (Kamra, 1969,b). Snow storms and dust storms are known to be highly electrified (Kamra, 1972, a). Kamra (1972, b) observed sparks extending a few metres upward into the air over gypsum dunes in New Mexico when strong winds were blowing large quantities of sand into the air. Apart from these phenomena involving intense activity, it has been found that ions are generated in several common processes. For instance, it has been found that the water splashing at the bottom of a waterfall releases ions into the atmosphere (Lenard, 1892; Pierce & Whitson, 1965). Water drops falling from a height, for instance during rainfall, on different types of surfaces release ions at different rates (Chate and Kamra, 1992) . This mechanism does not produce ions of both polarities in equal quantities, so that a net space charge results. Sea surf is another mechanism that generates ions of one polarity, namely positive, preferentially (Muir, 1977). Human activities like industrial plants, automobile exhausts, etc. and structures like high voltage power lines and even tall buildings, communication towers, chimneys, etc. (Kamra, 1991) can also release ions into the atmosphere.

1.2.2 Ionization due to radioactivity

The earth's atmosphere contains radioactive elements that contribute to the ionization of air. Of these, the largest fraction is contributed by the radioactive elements present in the rocks and soils in the form of minerals. Rocks and soils contain radioactive elements like uranium and thorium. Nuclear radiations from them ionize air in a thin layer close to the ground. In addition, their decay products are radioactive gases which are released into the air and are transported vertically and horizontally, and contribute to ionization over a much larger region of the atmosphere. Another group of naturally produced radioactive nuclei are those generated in the atmosphere by the collision of cosmic rays with air molecules. These are insignificant in quantity and can be ignored for the purposes of atmospheric electricity. The third group is of recent origin and consists of radioactive elements released into the atmosphere due to human activity. Nuclear tests carried out in the atmosphere were a major source for this before such tests were banned in 1964. The effect of these explosions on atmospheric electric parameters have been studied, and are discussed in a later section. At present only the inadvertent leaks of radioactive gases into the atmosphere fall in this category, and can be ignored. However, large scale leaks, like the one from the ill-fated reactor at Chernobyl, do produce significant changes in the atmospheric electrical parameters, as discussed later. In this section, a brief account is given of the naturally occurring radioactive elements and their influence on atmospheric electricity.

The rocks and soil in the solid earth contain radioactive elements like uranium and thorium in the form of minerals like monazite and uraninite, their concentration varying from region to region. Decay of these elements releases α , β and γ radiations, along with daughter products, which themselves may or may not be radioactive. Some of the daughter elements are gases like radon and thoron. These gases either are released into the atmosphere or get trapped within the rock/soil, depending on the permeability of the surrounding material. The radioactive gases released from the soil get mixed with air and contribute to ionization during their decay. The concentration of these gases vary from place to place, and with altitude at any given place. The distribution of these gases with altitude depends on atmospheric stability. The decay products of these gases are mostly radioactive elements, and they also contribute to the ionization of air.

Apart from the radioactive gases released from the soil and their daughters, the nuclear radiations from the radioactive minerals in the soil also produce ionization in the air. However, only γ rays, and to a lesser extent β rays, are important in this respect. The α rays and much of the β and γ rays produced beneath the top most surface of the soil get absorbed in the soil itself. The α rays penetrate only a few centimetres into the atmosphere, losing their energy very fast through ionising interactions with air molecules. While β rays penetrate to a somewhat greater distance, γ rays have a much smaller interaction with air and thus penetrate several metres into the atmosphere. Several metres above the ground, the intensity of ionization due to the different ionizing radiations is as follows (Bricard, 1965):

Cosmic Rays	20 %
From air:	
α rays	44 %
β rays	0.3%
γ rays	1.5%
From soil:	
β rays	3 %
γ rays	32 %

Thus the land surface provides another source for atmospheric ionization. Ionization due to radioactivity decreases with altitude and becomes comparable to that due to cosmic rays at altitudes around 2.5 to 3 km. The vertical profile of conductivity is thus modified by the presence of surface radioactivity. It may also be mentioned here that surface radioactivity has no effect on the air above water bodies because the nuclear radiations cannot penetrate the water layer. Above the oceans, the total natural radioactivity is reduced to a few hundredths of its value above the ground (Bricard, 1965). Since atmospheric electrical conductivity is lowest in the bottom most portion of the atmosphere, the contribution to conductivity by radioactivity assumes significance as far as atmospheric electrical processes are concerned. And since this source of ionization is at the surface, it cannot be ignored during investigations at the surface. A brief description of the exhalation of the isotopes of radon from the soil and their distribution in the atmosphere is given in a separate section below.

1.2.3 Formation and recombination of ions

When ionizing radiation interacts with atmospheric air, the ions created are mostly nitrogen and oxygen molecular ions since these gases constitute about 99% of air. These ions cannot exist as such. Due to electrostatic interaction, they are soon surrounded by neutral molecules. The ions become stable only when each ion is surrounded by about 20 to 30 neutral molecules. This is known as a small ion, and has a mobility of the order of $10^{-4} \text{ m}^2\text{V}^{-1}\text{s}^{-1}$. The charge can also get transferred to other molecules or atoms present in the atmosphere by ion chemical reactions that have not been fully understood. The electron released during the ionization immediately attaches itself to a neutral molecule, forming a negative ion. This also undergoes growth and transformation like the positive ion, although the chemical species to which the negative ions get attached are different from that of positive ions. The negative ion has been observed to have a somewhat higher mobility, or in other words, a lower mass, than the positive one.

Ions in the air tend to adhere to aerosol particles, thus becoming considerably heavier and less mobile. The aerosol particle sizes involved are mainly between about $0.01 \mu\text{m}$ and $1 \mu\text{m}$. The mobility of these so-called large ions become as low as about $10^{-8} \text{ m}^2\text{V}^{-1}\text{s}^{-1}$ and their contribution to conductivity can be ignored for most purposes. Hence, from this point of view, it may be said that the small ions that get attached to large aerosol particles are effectively 'lost', so that attachment is often treated as one of the loss processes of atmospheric ions. Jonassen & Wilkening (1965), for instance, show that both positive

and negative polar conductivities are well correlated with the corresponding small ion densities.

The ultimate loss of both polarities of ions is by mutual recombination. This occurs during chance collisions between positive and negative ions during their Brownian motion. If recombination is the only mode of ion loss, then we can write an approximate equation for the ion balance in air. Let q be the ion pair production rate, n the number of positive or negative ions, and α the *recombination coefficient*. α is the number of ion pairs undergoing recombination per second per ion pair present, or the probability of an ion being lost through recombination. Then we can write:

$$\frac{dn}{dt} = q - \alpha n^2. \quad (1.2)$$

Since the left hand side of the equation will tend to zero under equilibrium conditions, we can solve for n to get:

$$n = \sqrt{(q/\alpha)}. \quad (1.3)$$

1.2.4 Effect of aerosols

Aerosols are small solid and liquid particles suspended in the air. They are of interest to the student of atmospheric electricity because atmospheric small ions tend to adhere to these particles and get converted to large ions having very low mobility. The simple picture presented in the previous section therefore is only that of an ideal situation, and the effect of aerosols has to be taken into account before a realistic picture can be formed.

The sizes of aerosol particles range from about 10^{-9} m to less than 10^{-4} m. They are generally classified into three, namely, (i) Aitken particles whose diameters are less than $0.1 \mu\text{m}$, (ii) large particles whose diameters range from 0.1 to $1 \mu\text{m}$, and (iii) giant particles which are larger. Their concentration can vary widely, depending on the type of environment. In marine air, especially in remote regions like the Antarctica, counts as low as 10^8 m^{-3} are seen. In continental areas, the concentration is around 10^9 to 10^{10} m^{-3} in relatively clean rural air. In urban areas, and close to industrial establishments, the count could go as high as 10^{11} to 10^{12} m^{-3} (Twomey, 1977, p18). Aerosol particles are generated mainly from two different mechanisms, namely dispersal of materials from the earth's surface, and chemical reaction and condensation from atmospheric gases and vapours (Mészáros, 1981, p98). Particles injected into the atmosphere from the bursting of gas bubbles at the surface of sea water, and mineral particles blown into the air by wind are examples of the former. These are usually larger than $0.1 \mu\text{m}$ and hence fall into the category of large particles. The smaller Aitken particles are usually generated by the second mechanism. Apart from these, there are other sources that may be insignificant on a global level, but could be important at specific locations or times. Volcanic eruptions, meteors, forest fires, industrial and automobile exhausts, etc. are some examples. Apart from these, particles of biological origin like pollen grains and bacteria also form important components in certain specific environments. Aerosol particles are usually composed of several materials, and the composition can vary with place and time. This is because the particles are continuously interacting with the surroundings and going through coagulation, condensation and gas adsorption processes. The composition is also different for the different size ranges.

Ammonium sulphate, sodium chloride, sulphuric acid, organic compounds, nitrates, etc. are some of the commonly encountered substances. The concentration of aerosols reduces rapidly with altitude.

The particles of interest in atmospheric electricity are the Aitken particles. They are the ones which contribute most to the conversion of small ions into large ions. The attachment coefficient of small ions to aerosol particles is different for different particle sizes. A theoretical analysis that takes into consideration the aerosol spectrum and the variation of attachment coefficient with particle size is very involved and many of the parameters required are still unknown. However an approximate calculation using total aerosol concentration and a suitable average attachment coefficient can be made. From such an analysis, the concentration of small ions in the presence of aerosols is given by the equation (Twomey, 1977):

$$n = \frac{-\eta_1 N_1 - \eta_0 N_0 \pm \sqrt{(\eta_1 N_1 + \eta_0 N_0)^2 + 4\alpha q}}{2\alpha}$$

where η_0 and η_1 are the recombination coefficients for an ion with a neutral particle and ion of opposite polarity respectively, and N_0 and N_1 are the concentrations of neutral and charged aerosol particles. The effect of aerosols on small ion concentration is illustrated in Figure 1.3. The values used are: $q = 20 \text{ cm}^{-3} \text{ s}^{-1}$, $\alpha = 1.6 \times 10^{-6} \text{ cm}^3 \text{ s}^{-1}$, and attachment coefficients are the highest and the lowest values given by Israel (1971), p 162.

Aerosols thus influence the concentration of small ions. Highly polluted regions therefore tend to have much lower electrical conductivity than regions having clear air. Ion lifetimes are reduced from about

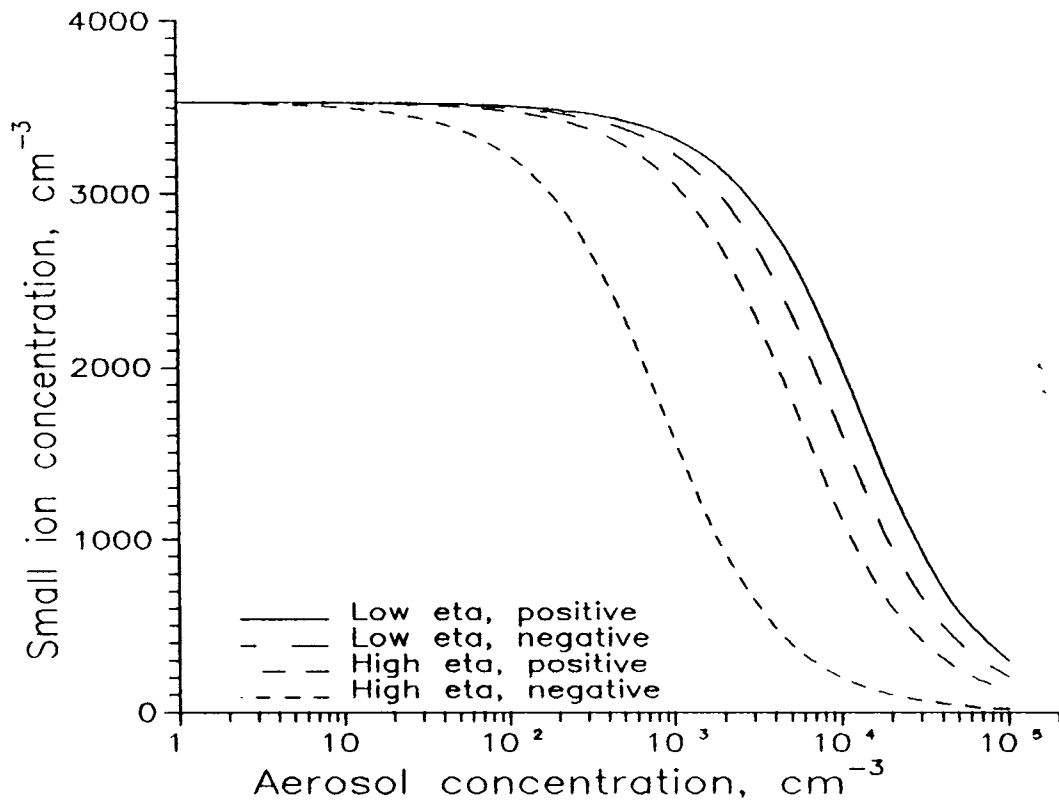


Figure 1.3 Variation of small ion concentration with aerosol concentration.

300 s in clear air to about 20 s in highly polluted air (Cobb, 1973). In polluted regions, therefore, atmospheric electrical measurements may have to be supplemented with aerosol measurements if any comparison is to be made with data from other regions.

1.3 DIURNAL AND SEASONAL VARIATIONS

The atmospheric electrical circuit described above does not remain in a constant steady state at all times. Various environmental factors influence the circuit so that the circuit parameters are constantly changing. Near the earth's surface, two different kinds of variations can be discerned. One is global in nature, felt uniformly all over the earth, and is mainly due to the variation in global thunderstorm activity

and the consequent variation in the electrospheric potential. The second is of local origin, and is due to local changes in weather, human activity, etc. Pollution is another parameter that varies not only with place, but also with time, and influences the electrical parameters. Traditionally, the study of atmospheric electrical phenomena has been divided into two different areas, namely, the fair-weather and the disturbed weather portions. In the former, only data pertaining to fair-weather periods, defined as periods without rainfall, with low cloud cover and wind speed, etc., are selected. Disturbed weather studies normally concentrate on periods of thunderstorm activity, including effects of lightning. Therefore the normal diurnal and seasonal variation patterns of the atmospheric electrical parameters usually refer to that during the fair-weather periods. A brief description of these variations is given below.

Global thunderstorm activity shows a clear diurnal pattern. This follows the movement of the sun across the major continental land masses where it initiates thunderstorm activity. A higher thunderstorm activity results in a larger flow of charging current, and thus to a higher electrosphere voltage. This is reflected in a well-defined diurnal variation pattern in the vertical electric field observed over the oceans and in remote areas like Antarctica. Since this global variation is usually masked by local effects, it cannot be easily observed from a land station, especially one that has a significant population. One of the earliest observations of the global diurnal variation of the vertical electric field was carried out during a cruise of the research vessel *Carnegie*. Since the observations were carried out entirely over the oceans, local perturbations that are present over land regions were

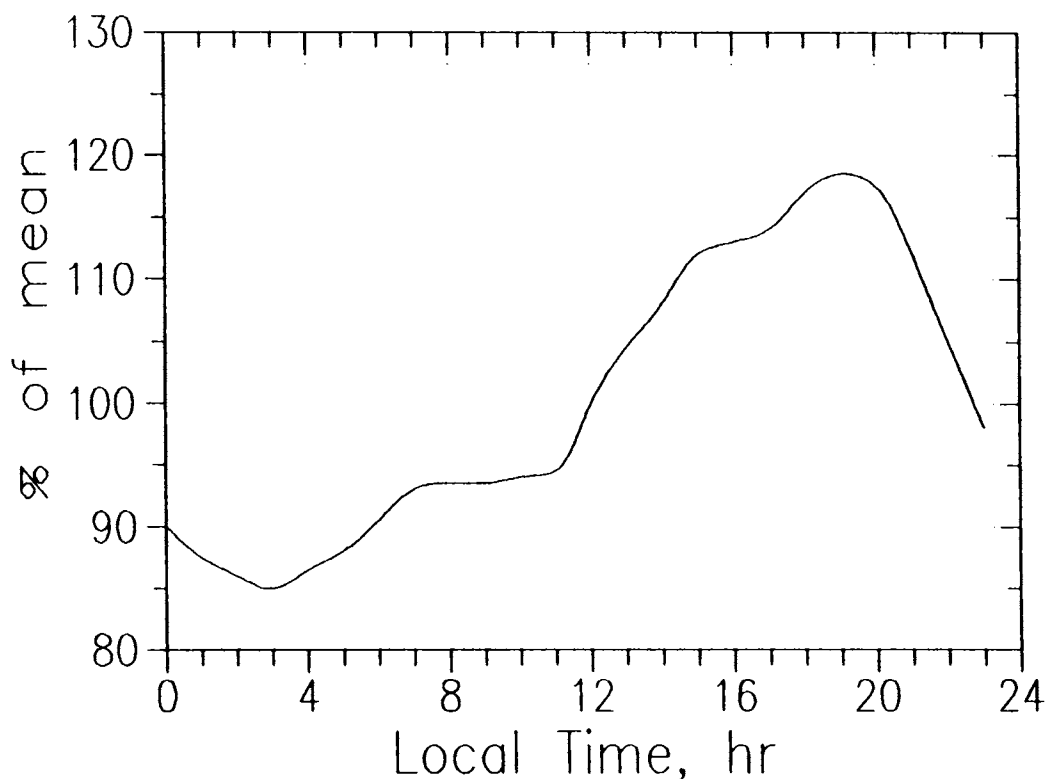


Figure 1.4 Diurnal variation of the vertical electric field over the oceans observed in the cruise of the research vessel *Carnegie*.

virtually avoided. The observed pattern, shown in Figure 1.4, has come to be known as the *Carnegie curve*, and is universally accepted as the standard diurnal variation of the electrospheric potential.

1.3.1 Temporal variation of conductivity

Near the earth's surface, electrical conductivity is not constant with time. Long period observations at various sites have shown that atmospheric electrical conductivity shows well defined diurnal and seasonal variations during fair weather periods. The exact nature of variation is different for different stations, and the mean values and amplitudes are also different. For a given station, the pattern of variation of conductivity at the surface normally remains more or less

constant during a year. The mean behaviour at each station may therefore be said to constitute a characteristic of the "atmospheric electric climate" for that station. But some similarities are seen in the diurnal behaviour of conductivity at most stations. For instance, conductivity is usually high during night time. This is possibly a reflection of the general rhythm of the atmosphere, since nights are usually calmer, with low winds and hardly any convective motion, and therefore conducive for the accumulation of radon and other radioactive species near the surface. A sharp fall associated with sunrise is seen at many stations. This is believed to be due to an increase in the aerosol concentration due to onset of circulation and human activity, and has often been called the "sunrise effect", although a slightly different and unexplained phenomenon is known as the sunrise effect, as explained later. The behaviour during the rest of the day differs from station to station. Some stations show a single oscillation type of pattern, with one maximum and one minimum, while some others show a double oscillation behaviour. Figure 1.5 shows typical examples of the diurnal variation of conductivity. The curve showing the single oscillation is for Gulmarg (Raina & Raina, 1988), and the other is for Athens, Greece (Retalis & Zervos, 1976).

The situation is different over the oceans, with hardly any change between locations. In marine air, the mean conductivity is slightly higher than that over land but the diurnal amplitude is very low. And unlike over land, conductivity is minimum in the late afternoon and early evening hours and remains low during night. It rises to a peak in the forenoon and is followed by a gradual decline. This is almost a mirror image of the pattern seen over continental stations. Further,

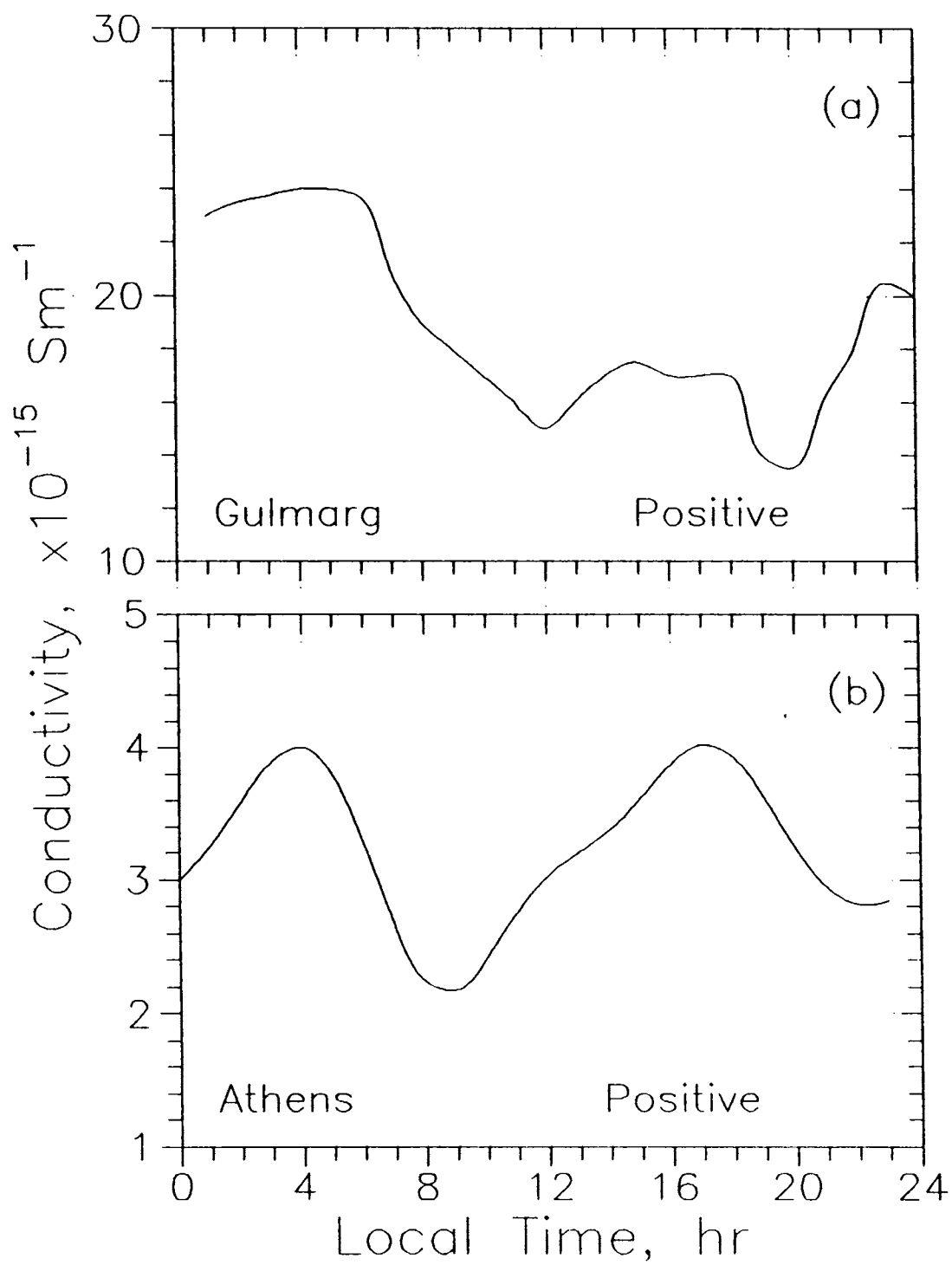


Figure 1.5 Examples of (a) single and (b) double oscillation types of diurnal variation of positive polar conductivity.

while the positive polar conductivity displays a clear variation in the manner described, the variation in the negative polar conductivity has a very low amplitude and is just discernible. The ratio of polar conductivities thus exhibits a clear diurnal pattern over oceans (Israel, 1971, p 97).

1.3.2 Temporal variation of the vertical electric field

Apart from the global variation observed in marine environment, described in the previous section, the vertical electric field measured at any continental station (other than Antarctica) shows a diurnal pattern that is due to local perturbations. If R is the columnar resistance of the atmosphere (the resistance of a vertical column of unit cross section) and V is the potential of the electrosphere, then the electrosphere-earth current density J will be V/R . Now if r is the resistance of an air column of unit height and unit cross section at the measurement site, then the potential drop across this height, equal to the vertical electric field at that point will be $E = J.r = (r/R)V$. The columnar resistance of air is almost constant in all fair-weather regions of the atmosphere, having a value of about 10^{17} ohms per square metre. The vertical electric field is thus seen to have a dependence on the specific resistance of air at the location, or in other words to the conductivity of air. As explained below, the conductivity of air at any land station shows a certain diurnal pattern that can vary from place to place, and is also affected by environmental factors like the weather, pollution, etc. This is consequently reflected in the vertical electric field also.

Electric field measurements have shown that the strength of the vertical electric field is more or less similar over land and sea. Marine measurements have indicated a certain latitude dependence, the field being higher at higher latitudes. Diurnal and seasonal variations have been observed over land stations. Israel (1971) classifies these into three types, namely,

- i) the *single oscillation continental type*, where the field strength passes through a single oscillation with the minimum around 0400 hr local time and a maximum in the late afternoon;
- ii) the *double oscillation continental type*, where it shows a double oscillation with the minima around 0400 and 1400 hr and maxima around 0900 and 2100 hr local time; and
- iii) the *universal time type*, where a single oscillation is seen with minima around 0400 hr UT and maxima around 1600 - 1800 hr UT.

The first two types are observed only over continental stations. The type of variation depends on the season, weather and locality. In winter, the single oscillation type and in summer the double oscillation type usually occurs. However, some stations have the same type of variation throughout the year. Type (iii) is seen only in the polar regions and also over the oceans (Israel, 1971). Some examples of the three types of variations are shown in Figure 1.6. Factors that alter the normal pattern of variation are solar eclipse (Anderson & Dolezalek, 1972), sea breeze (Trevitt, 1984), etc.

An interesting feature in the behaviour of the vertical electric field is a sharp increase seen after sunrise. Since a decrease in

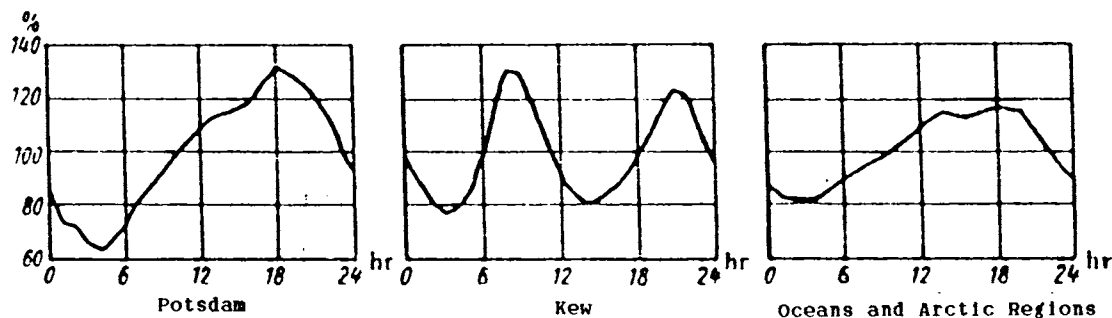


Figure 1.5 Examples of the three types of diurnal variation of the vertical electric field (after Israel, 1971).

conductivity is seen around this time, the increase in electric field is natural. What makes it interesting is the fact that the change in electric field is not commensurate with that of conductivity. In other words, it is accompanied by an increase in the air-earth current density. The increase in the electric field is in agreement with the decrease in conductivity and the increase in air-earth current density. The effect is more pronounced at low altitude stations in the plains and less evident at mountain tops. It shows a clear increase from winter to summer (Israel, 1971, p 405-8). A pseudo-sunrise effect has been observed at the end of a solar eclipse also (Anderson, 1972).

Although first observed by E.H. Nichols in 1916, and rediscovered by R.E. Holzer in 1955 (Chalmers, 1967), this phenomenon is yet to be explained fully. Kasemir suggested that the positive space charge that accumulates near the earth's surface at night is transported upward with the onset of circulation, thus constituting a current in the opposite direction from the one that normally flows, and that this may be the reason for the observed increase in electric field and air-earth current. Chalmers, however, showed that this cannot give a complete account of the phenomenon. Kamra (1969,a) argued that the effect was related to

the increase in air temperature in the morning rather than to sunrise, and that the cause is related to the increase in aerosols due to the onset of circulation. Muir (1975) suggested that the sunrise effect may be due to an increase in the electrospheric potential, and suggested a mechanism that could produce the desired effect.

1.4 RADIOACTIVITY IN THE ATMOSPHERE

As mentioned in Section 1.1, surface radioactivity plays an important role in atmospheric electrical processes near the earth's surface. While there have been some investigations into the behaviour of atmospheric electrical parameters under the influence of radioactivity, detailed studies have been very rare. This section gives a brief outline of atmospheric radioactivity and the studies carried out in relation to atmospheric electricity.

1.4.1 Radioactivity at the surface and in the atmosphere

Radioactive atoms in the earth's atmosphere can be divided into three groups based on how they are produced. The first, and by far the biggest, group consists of the radioactive gases released from the soil and their daughters. These are mainly the three isotopes of radon, namely, radon (Rn^{222}), thoron (Rn^{220}) and actinon (Rn^{219}), and their decay products, which are not all gases. The second group consists of the radioactive isotopes produced in air by the action of cosmic rays. The third group is of a relatively recent origin - that of isotopes released into the air by atmospheric nuclear explosions and other anthropogenic

causes. In the context of atmospheric electricity only the first group is important.

The earth's crust contains small quantities of uranium²³⁸, uranium²³⁵, and thorium²³² in the form of minerals. They are present everywhere in varying concentrations. All of them decay into isotopes of the same noble gas, namely radon. These gases accumulate inside the soil and slowly diffuse up into the atmosphere. The rate of diffusion depends on the porosity of the soil and other environmental conditions. Once the gases escape into the atmosphere, they are transported horizontally and vertically by atmospheric turbulence. The rate of transport then depends on the strength of the turbulence.

A simple model proposed by Israel (1958) and discussed by Junge (1963) for the exhalation and atmospheric mixing of the radioactive gases is useful to demonstrate the essential features of the processes. Let c_s be the concentration of the gas in the soil air, d its diffusion constant, and a its rate of production within the soil (in number of atoms per unit volume per second). If the soil is sufficiently porous, then the equilibrium condition within the soil can be expressed by the following equation:

$$\frac{\partial c_s}{\partial t} = 0 = d \frac{\partial^2 c_s}{\partial z^2} + a - \Lambda c_s \quad (1.5)$$

where z is the depth, t the time, and Λ the decay rate of the gas. The solution of this equation is :

$$c_s = (a/\Lambda) [1 - \exp(-\sqrt{\Lambda/d} z)] \quad (1.6)$$

where $c_{s0} = a/\Lambda$ is the concentration of the gas in undisturbed soil air in deeper layers of the soil. The exhalation rate is then given by:

$$E_r = \left(d \frac{\partial c_a}{\partial z} \right)_{z=0} = a \sqrt{d/\Lambda}. \quad (1.7)$$

The constants a and Λ being fixed for a particular kind of emanation, the exhalation rate naturally depends only on the diffusion constant in the soil, or, in other words, the porosity of the soil. The corresponding equation for the vertical transport of the gas in the atmosphere can be obtained from equation 1.5 by setting $a = 0$ and replacing d by the eddy diffusion coefficient D . Although D is highly variable over space and time, and also with altitude, we can assume it to be constant with altitude, as a first order approximation. The concentration of the gas in the air at any altitude h is then given by:

$$c_a = c_{a0} \cdot \exp(-\sqrt{\Lambda/D}h). \quad (1.8)$$

A typical profile of the concentration of radon in the air above the surface and in the soil is given in Figure 1.7.

The exhalation rate of radon depends on the soil conditions. Apart from the variations due to the porosity of soil, soil temperature and moisture, and meteorological factors like rainfall are known to influence the exhalation rate. Decreases of up to 70% due to rainfall have been observed. Seasonal variations generally show a minimum during summer and a maximum during winter. There are, however, several exceptions to this rule. In the eastern Alps, for instance, it shows a maximum in late spring. This is probably because the soil is frozen during winter, and radon is not able to escape (Junge, 1963, p217). Similar could be the case in the regions of our sub-continent where heavy rains during the monsoon could suppress radon exhalation.

There are several studies on the exhalation of radon from the soil and its distribution in the atmosphere. Schery *et al.* (1984) measured radon exhalation rate from a gravelly sandy loam in a semi-arid climate.

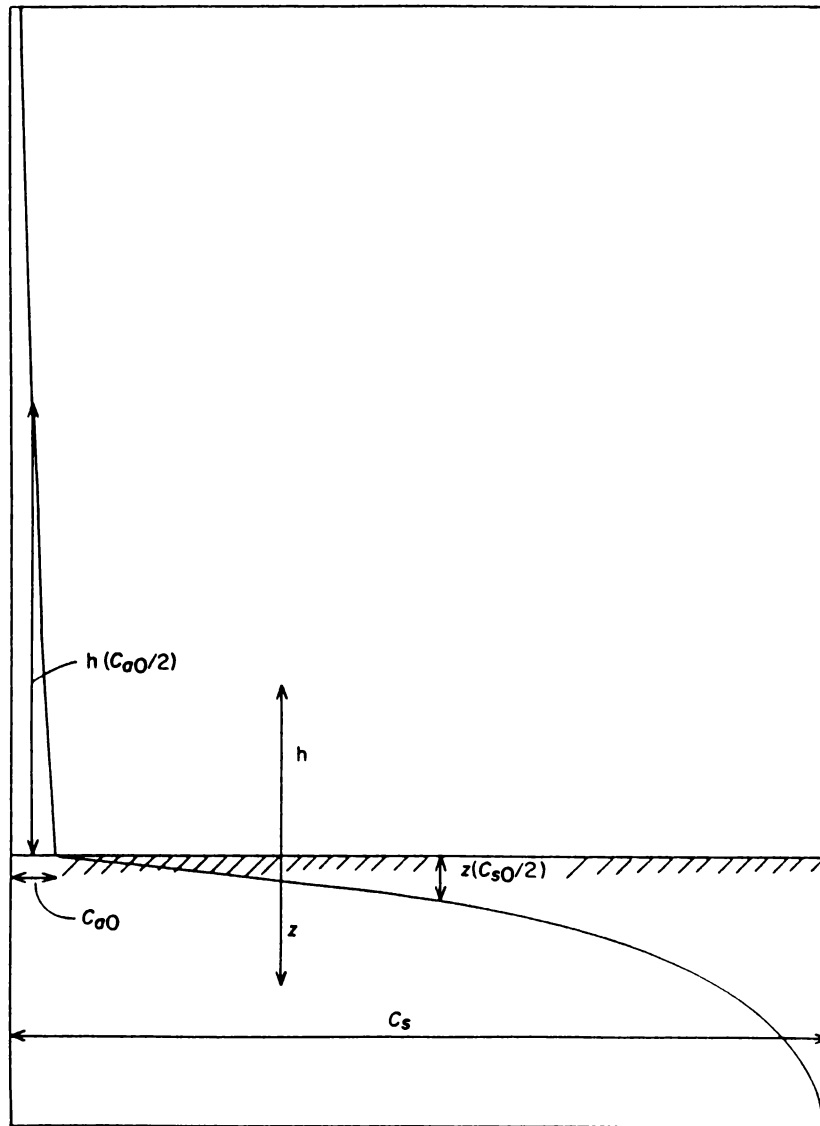


Figure 1.7 Theoretical profile of the concentration of radon above and below the soil surface (after Junge, 1963).

They found that the meteorological factors that affected the exhalation rate most were pressure and rainfall. Effects of other factors like temperature and wind were minor. The exhalation rate of Rn^{220} was seen to be less influenced by pressure variations than that of Rn^{222} .

The radon content of surface air depends on the exhalation rate and atmospheric turbulence, the latter being the dominant factor. During a quiet day, it shows a maximum around sunrise when turbulent mixing is minimum, and a minimum in the afternoon when mixing is at its maximum. **Wilkening** (1959), apart from observing this kind of a diurnal pattern, also reports a good correlation with the gustiness of air. A minimum in the radon concentration that he observes during spring is attributed to the higher average wind speed. **Moses et al.** (1960) studied the effect of meteorological variables on the vertical and temporal distribution of radon at the Argonne Meteorological Laboratory, and found a strong relationship between the stability of the atmosphere and the concentration of radon. **Liu et al.** (1984) analyzed the data from several reported measurements and showed that in summer, about 55% of the Rn^{222} is transported above the planetary boundary layer, which is considerably more than in the other seasons. They also found that in summer about 20% rises to over 5.5 km.

The decay products of these gases are heavy metals. They adhere to aerosols and are brought down by meteorological processes like rainfall.

1.4.2 Studies on relationship between radioactivity and atmospheric electricity

There have been several studies on the effects of radioactivity on the electrical structure of the atmosphere. Both natural and artificial sources of radioactivity have been objects of study. The former have mostly concentrated on ionization and the latter on the effect on the vertical electric field.

Pierce (1958) measured the variation in ion production rate with height from 1 cm to 1 m. He found that ion pair production rate decreased from about $60 \text{ cm}^{-3}\text{s}^{-1}$ at 1 cm to about 8 at 1 m. His results give a qualitative idea about the manner of variation with altitude of ionization by surface radioactivity.

Pierce (1957) studied the effect of nuclear explosions on the vertical electric field, and Pierce (1972) studied the secular effects of nuclear fallout. He found that for the period before 1952, the vertical electric field data shows no consistent change from year to year. After 1952, the field was found to decrease progressively to reach a minimum in 1959. A partial recovery was seen in 1960 and 1961 to be succeeded by a further decline in 1962-63. The vertical electric field started recovering to its earlier values from 1964 onwards. This behaviour corresponds to that of atmospheric testing of nuclear explosives carried out globally. Israelsson & Knudsen (1986) used polar conductivity, electric field and space charge data from Uppsala, Sweden, to identify the effect of the accident at the nuclear power plant at Chernobyl, USSR. They found that the conductivity increased about 11 times, the

electric field decreased about 10 times and the space charge density decreased about 10 times. These sudden changes were seen shortly after a rainfall on 29.4.1986, before which only a small and gradual change in the parameters was seen. They also found that after fairly heavy rainfall during May 11 to 13, the values recovered to normal. A similar study by **Retalis** (1987) showed that the small ion concentration started increasing on May 3rd and reached its highest daily mean value on May 5th. These maximum values were four times the normal for positive ions and 5 times for negative ions. **Retalis & Pitta** (1989) reported the effect of the Chernobyl accident on the vertical electric field, conductivity and small ion concentration at Athens. They also compared the results with radionuclide concentration and exposure rate in the air near the ground.

Wilkening & Romero (1981) measured the positive and negative ion densities, mobilities and polar conductivities in the Carlsbad caverns. Being unventilated, the air inside contained very high levels of Rn, although the surrounding rock strata contained only normal levels of uranium. They found the conductivities and ion densities to be two to three orders of magnitude higher than in the free atmosphere, indicating ion pair production rates higher by a factor of about 200. The small ion mobilities were found to be about half of that seen outside, possibly due to the high humidity inside.

Pierce & Whitson (1964) measured the vertical electric field in an area adjacent to the nuclear test site in Nevada, USA. The measurement was carried out both at the surface and up to 2 km using a balloon. They found the surface value to be about one third the normal. The

vertical profile also was seen to be very much different from that over uncontaminated ground. The electric field was found to increase from the surface value of about 30 Vm^{-1} to about 100 Vm^{-1} at about 1.1 km, and then decrease gradually with altitude. As per their calculations, the normal field should be around 100 Vm^{-1} at about 500 m altitude. The difference seen over the contaminated ground was explained as being caused by the enhanced ion concentration over that region.

Thus the study of the effects of radioactivity on atmospheric electricity has been limited to a few isolated observations in regions that had a relatively higher concentration of radioactive substances. In all these cases, except the measurements in the Carlsbad caverns, the radioactivity has been from man-made sources. There appears to have been no concerted study of the behaviour of atmospheric electrical parameters in regions of high natural radioactivity.

1.5 PRESENT STUDY

As mentioned earlier, the study of atmospheric electrical phenomena has been traditionally divided into the fair-weather and the disturbed weather portions. While studying fair-weather phenomena, all efforts were made to eliminate the effects of meteorological and other influences by monitoring these parameters also and selecting data for periods when the values of these parameters were within specified limits. The study of disturbed weather phenomena was almost exclusively confined to thunderstorms and lightning.

In the present study, polar conductivity data have been obtained from four environmentally different sites in all kinds of weather conditions. The data are then analyzed together with meteorological data obtained from stations of the India Meteorological Department to bring out the influence of these parameters on conductivity. Of the four sites, two are coastal, very close to the sea, with one having a large deposit of the radioactive mineral monazite. The second coastal site and one of the inland sites have very little radioactivity. The fourth site is inland, though not very far from the sea, and has a moderate level of background radioactivity. The data from three aircraft surveys of polar conductivities covering the region of study are also presented and discussed.

CHAPTER II

2 . INSTRUMENTATION

2.1 INTRODUCTION

The investigation reported here involved the measurement of atmospheric electrical polar conductivities in different environments. Attempt was also made to carry out measurements of the vertical electric field. The instruments for these measurements were identified based on the convenience of fabrication and maintenance and on the reliability of the data. The Gerdien condenser was adopted for the measurement of conductivities, since the instrument has been generally accepted as a standard for the measurement of conductivities, ion densities and ion mobilities. The field mill was used for measuring the vertical electric field. This was found to be better suited than other available techniques, like the radioactive potential equalizer and the agrimeter. The radioactive potential equalizer has several limitations, such as the strong influence of air motion. The field mill, in comparison with the agrimeter, is simpler in operation and maintenance since it does not involve any brush mechanism. However, one limitation of the field mill is the difficulty in identifying the sign of the field, which requires a synchronous detector. A field mill was designed, fabricated and test run at one station. The field trials were successful. However, some modifications were found necessary after the test run, which could not be completed during the period of this investigation. Each station had a system console, where the recorders were situated along with the

major part of the electronic circuitry and the power supply modules. The console also had provision for keeping a few tools and other small items. The principle of operation and the design of the instruments used in the ground stations are described in this chapter. The instruments used for surveys at ground level using a jeep and at higher altitudes using an aircraft are described, along with the data obtained, in Chapter 5.

2.2 THE GERDIEN CONDENSER

The Gerdien condenser is a simple instrument that has been used for long for the measurement of atmospheric electrical conductivities, ion densities and mobilities. Named after H. Gerdien (1905), the instrument is basically a cylindrical capacitor through which air is allowed to flow. A voltage (the *driving voltage*) is applied to one cylinder, known as the *driving electrode*, with reference to the other, known as the *collector*. This results in the generation of an electric field inside the condenser, which drives ions of one polarity towards the collector (and those of the other polarity towards the driving electrode). These ions give up their charge at the collector, constituting a current (the *collector current*). This current is measured using suitable electronic circuitry. For low applied voltages, the collector current is proportional to the voltage applied. For a sufficiently high driving voltage all the ions in the incoming air are collected. Thereafter the current becomes independent of the applied voltage and the condenser is said to be *saturated*. A detailed theory of the operation of the Gerdien condenser is given below. The discussion is largely based on Conley (1974) and Farrokh (1975).

2.2.1 Theory

In analysing the operation of the Gerdien condenser, the following assumptions are made:

- (i) The air flow through the condenser is plane parallel and streamlined;
- (ii) The thermal diffusion of ions can be ignored in comparison with the diffusion due to the applied electric field;
- (iii) Ion production and destruction processes are slow enough to be ignored for the duration of the flow through the condenser;
- (iv) The air is essentially neutral; that is, the concentration of positive and negative ions are equal in the ambient air.
- (v) Only one ion species is considered; that is, it is assumed that all the ions of one polarity have the same mobility. A similar treatment would be applicable to the ions of opposite polarity.

Considering the situation where the driving voltage is positive so that only positive ions are collected, the general equation of motion for the ions can be written as follows:

$$J = -eD \nabla n^+ + \mu^+ n^+ e \nabla \phi + n^+ e U \quad (2.1)$$

where J is the current density at the collector, D is the diffusion coefficient, μ^+ the mobility and n^+ the number density of the positive ions, ϕ is the potential at any point inside the condenser, U is the convection velocity of the ions inside the condenser and e is the electronic charge. The first term in the equation represents the contribution to the current from thermal diffusion. This can be neglected as per our

second assumption. The validity of this assumption is demonstrated in the next section. The third term represents the contribution from convective motion. This becomes negligible if our first assumption is satisfied. We are therefore left with only one term, namely the contribution due to the applied electric field. Assuming cylindrical symmetry, we may write this as a two-dimensional equation, namely:

$$J = \mu n^+ e \frac{d\phi}{dr} \quad (2.2)$$

where r is the radial distance. The gradient of the potential would depend on the space charge density inside the condenser. This is zero as per our fourth assumption. The gradient of the potential is then:

$$\frac{d\phi}{dr} = \frac{V}{r \ln(b/a)} \quad (2.3)$$

where a and b are the radii of the inner and outer cylinders of the condenser respectively. Substituting in the previous equation, and solving we get:

$$J = \frac{\mu^+ n^+ e V}{r \ln(b/a)} = \frac{\mu^+ n^+ e V C}{2\pi \epsilon_0 L r} \quad (2.4)$$

where L is the length of the electrodes, ϵ_0 is the permittivity of free space, and C is the capacitance of the condenser, given by :

$$C = \frac{2\pi \epsilon_0 L}{\ln(b/a)} \quad (2.5)$$

The current to unit length of the collector is $i = 2\pi r J$, so that the total current to the probe is:

$$I = 2\pi r J L = \frac{\mu^+ n^+ e C V}{\epsilon_0} \quad (2.6)$$

Equation 2.6 describes the current-voltage characteristic of the condenser in the conductivity mode, that is when only a part of the ions entering the condenser are collected. Here, the collector current is proportional to the driving voltage, so that this region of the characteristic is called the ohmic region. When the driving voltage is equal to or greater than the saturation voltage, all the ions entering the condenser are collected, and the collector current obtained can be written as:

$$I_s = n^+ e v \pi (b^2 - a^2) \quad (2.7)$$

where I_s is the *saturation current* and v is the speed of air flow through the condenser. The collector current is thus directly proportional to the driving voltage in the conductivity mode, and constant in the saturation mode. The theoretical I-V characteristic of a Gerdien condenser should therefore look as shown in Figure 2.1. The driving voltage at which the condenser saturates is known as the *saturation voltage*, and is given by the expression:

$$V_s = \frac{\epsilon \pi (b^2 - a^2) v}{C \mu^+} \quad (2.8)$$

which can be derived by analysing the motion of the ions in the electric field inside the condenser. Consider a positive ion entering the condenser at a distance R from the centre (see Figure 2.2), when the driving voltage is positive. The ion enters the condenser with an axial velocity equal to the velocity of air flow, $U(r)$. Under the influence of the electric field produced by the driving voltage, the ion acquires a drift velocity, U_r , in the radial direction given by:

$$U_r = \mu^+ E(r) \quad (2.9)$$

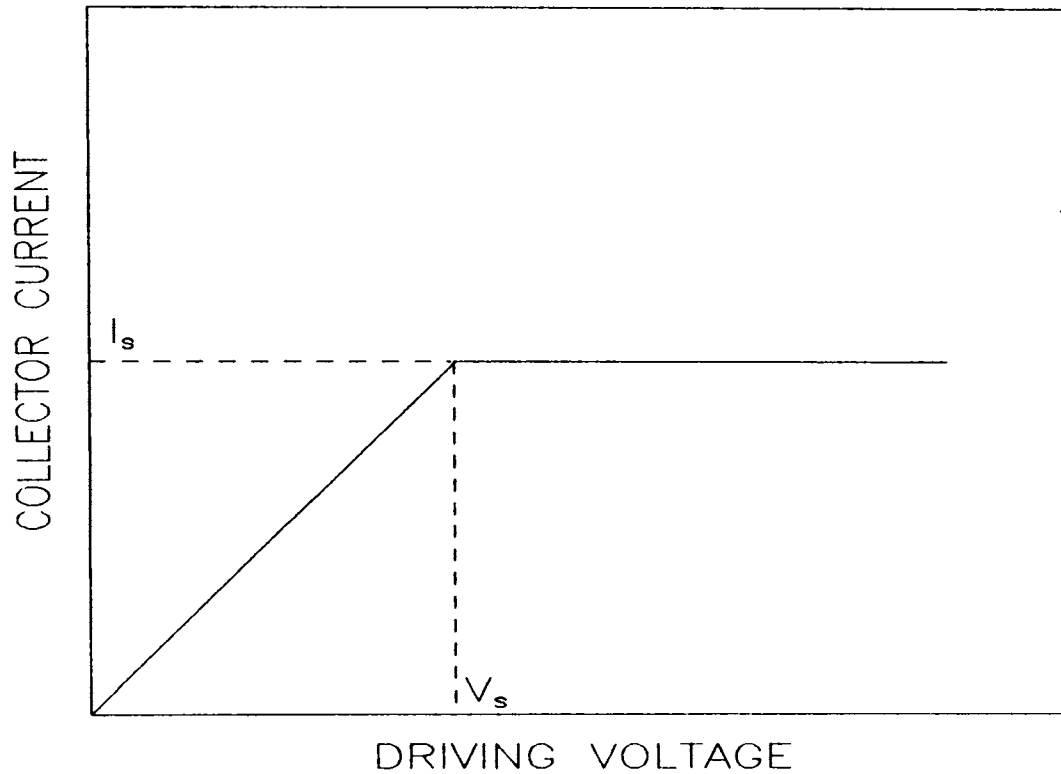


Figure 2.1 Theoretical current-voltage characteristic of a Gerdien condenser.

where $E(r)$ is the electric field at the point where the ion is situated, and μ^+ is the mobility of the ion. If V is the driving voltage, then the radial field at a distance r from the centre is given by:

$$E(r) = -\frac{V}{r} \cdot \frac{1}{\ln(b/a)}. \quad (2.10)$$

In a time interval dt , the axial distance travelled by the ion, dx , and the radial distance, dr , are proportional to the respective velocities. We can therefore write:

$$dt = dx/U(r) = dr/U_r.$$

Therefore,

$$dx = (U(r)/U_r) \cdot dr.$$

Substituting from equations 2.9 and 2.10 and integrating, we obtain:

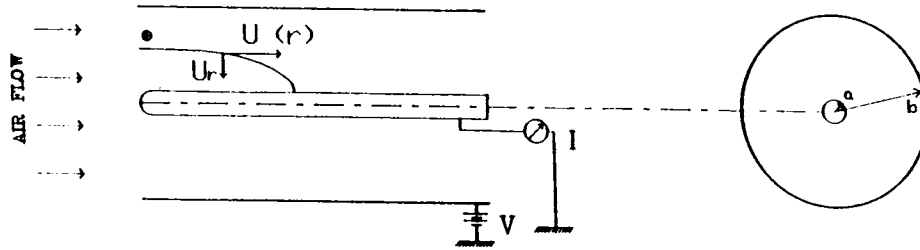


Figure 2.2 Trajectory of an ion inside a Gerden condenser.

$$x = \int_R^r \frac{U(r)}{\mu^+ E(r)} dr = \frac{-\ln(b/a)}{\mu^+ V} \int_R^r U(r) r dr \quad (2.11)$$

The integral in the last term is nothing but the volume flow rate of air through the area between radii R and r , say $U(R,r)$. Equation 2.11 can then be written as:

$$x = \frac{1}{2\pi} \frac{\ln(b/a)}{V\mu^+} U(R,r). \quad (2.12)$$

Now consider a positive ion that enters the condenser close to the driving electrode, that is at $R = b$. $U(R,r)$ is then the volume flow rate of air through the condenser, given by $\pi v(b^2 - a^2)$. If the mobility of the ion and the driving voltage are such that this ion is just collected, that is $x = L$, then the driving voltage corresponds to the saturation voltage. We can then write, from equation 2.12:

$$L = \frac{1}{2\pi} \frac{\ln(b/a)}{V\mu^+} \cdot \pi v(b^2 - a^2). \quad (2.13)$$

The saturation voltage is therefore given by:

$$V_s = \frac{\ln(b/a) \cdot v(b^2 - a^2)}{2L\mu^+}. \quad (2.14)$$

This is the same as equation 2.8 with the expression for the capacitance of the condenser substituted.

Alternatively, since the point at which the condenser just saturates may be considered to be still in the linear portion of the characteristic, we may substitute I_s for I and V_s for V in equation 2.6. Then, by substituting for I_s from equation 2.7 and solving, we obtain the expression given in equation 2.8. It may be seen that the saturation voltage and current will be higher for a higher flow rate. From the equations given above, the polar conductivity, ion concentration and ion mobility can be calculated, by determining the I-V characteristic of a condenser for a known air flow rate. Thus, from equation 2.6, we can write the expression for positive polar conductivity as:

$$\lambda^+ = n^+ e \mu^+ = \frac{e_0 I}{CV} \quad (2.15)$$

where λ^+ is the positive polar conductivity, equal to the product of the concentration and mobility of positive ions and the electronic charge. The expressions for ion concentration and mobility can similarly be obtained as:

$$n^+ = \frac{I_s}{e\nu\pi(b^2 - a^2)}, \quad (2.16)$$

and

$$\mu^+ = \frac{e\pi\nu(b^2 - a^2)}{CV_s}. \quad (2.17)$$

Similar equations are valid for negative polar conductivity, ion density and mobility.

2.2.2 Sources of error

The discussion given above of the principle of the Gerdien condenser is valid only in ideal conditions. Many of the assumptions

given at the beginning will not be valid in practice. This can lead to deviations from the theory derived above, and hence to errors in the measurement. Sufficient care has to be taken while making measurements so that these errors do not become too large. A brief examination of this problem is given in this section.

The first assumption made while deriving the expressions for the Gerdien condenser is that the flow through the sensor will be laminar. This means that the Reynolds' number for the configuration remains below a certain value that is dependent on the configuration. For two very long coaxial cylinders the Reynolds' number is defined as:

$$R_e = \frac{(b - a)U}{\nu} \quad (2.18)$$

where U is the average flow velocity across the cross section and ν is the kinematic viscosity. The critical value for such a configuration is 2000. The exact value for a given condenser has to be determined experimentally. For ground based instruments, where the flow rate is determined by the flow generator used, it can be ensured that the Reynolds' number remains below the critical value. However, there is bound to be turbulence at the inlet end of the sensor. In order to ensure that this does not affect the measurements, it is generally the practice to leave a certain portion of the cylinder at the inlet for flow stabilization. Care has to be taken here also to see that the ions that enter are not lost in this portion of the sensor.

The second assumption is that the thermal diffusion does not contribute significantly to the current. The validity of this assumption can be verified from Einstein's equation, $D/\mu = kT/e$, where k is

Boltzmann's constant, and T is the ambient temperature. For normal surface temperatures, the right hand side of the equation works out to less than 0.03. The contribution of diffusion is therefore less than 3 percent. This is within tolerable limits.

The third assumption is that the ion concentration in the air inside the sensor is the same as that in the outside air. That is, ion pair production and loss processes that take place inside the sensor are small enough to be ignored. Small ion life times in air are of the order of 100 s, which is significantly larger than the time the air parcel takes to move from the inlet of the sensor to the outlet. Ion production will be taking place inside the sensor due to radioactive elements that are present in the air. However, the ion balance will remain the same inside and outside since the conditions do not change when the air enters the sensor.

The question of charge neutrality inside the sensor is one that has to be addressed in detail. This assumption was used in deriving equation 2.3 which gives the variation of the electric field inside the sensor. In the presence of space charge, the electric field variation could be different. In order to determine the extent to which this could affect the measurement, Conley (1974) assumed a uniform charge distribution of one polarity inside the condenser and solved the corresponding Poisson's equation. He found that for charge densities as high as 10^{11} m^{-3} , the perturbation to the field is very small. This effect can therefore be ignored for most purposes.

The last assumption that all ions have the same mobility is not strictly valid. However, the ions that are detected by the Gerdien condenser are the small ions which have mobilities within a narrow range. The effect of having a range of mobility values is to modify the linear portion of the characteristic of the condenser. If ions of mobilities $\mu_1, \mu_2, \mu_3 \dots$ are present in the air, then there will be a saturation voltage for each of these ion species. The region of the characteristic between the origin and the point corresponding to the saturation voltage of the ions with the smallest mobility will therefore consist of several short straight line segments. This would not affect conductivity measurements if the driving voltage used is sufficiently small. The different mobilities can be obtained by determining the saturation voltages for each ion species. Conley *et al.* (1983) have done such an exercise for their measurements using a rocket-borne Gerdien condenser.

Apart from the points discussed above, errors can occur due to the fringing of the electric field at the inlet to the sensor. These field lines can deflect some of the incoming ions to some portion of the sensor other than the collector, resulting in the collector current being less. This effect is clearly seen when the driving voltage is gradually increased from zero to a value that is much higher than the saturation voltage, V_g . The collector current can be seen to reach a broad maximum around $V = V_g$ and then decrease. The effect is small for small driving voltages. For conductivity measurements, when the driving voltage used is small compared to the saturation voltage, the error introduced can be ignored. Moreover, near the surface the low mobility of the ions also helps to keep the error due to fringing of the electric field low.

Modifications to this basic design has been attempted by several workers. In the modified McClelland method, for instance, the driving voltage is kept fixed at a high value and the collector current is measured for different air flow rates. Whipple (1960) suggested a method to obtain a single characteristic from the current obtained by varying either the driving voltage or the airflow rate. This has been extended to include the capacitance of the sensor so that the characteristic becomes valid for any Gerdien condenser (Dhanorkar & Kamra, 1991). Rosen & Hofmann (1981) used a pumped Gerdien condenser having two separate parts for the collector to measure conductivity and ion concentration. The instrument used in the present investigation is the normal type without any basic modification.

2.2.3 The Gerdien sensor

The Gerdien instrument consists of the sensor and the electronic circuits for generating the driving voltage and measuring the collector current. The sensor basically consists of two cylindrical electrodes. The one that is used as the collector has to be insulated from the rest of the sensor using a material that can give very high impedance. Both the electrodes are usually mounted inside another cylinder that is earthed. This outer cylinder protects the sensor from external disturbance, prevents the driving voltage from being accidentally short circuited, and often acts as a flow stabilizer and guard ring (to reduce the effect of fringing fields). The guard ring has also been found to reduce pickup at the collector. For a ground-based system, since the currents obtained are very low, of the order of 10^{-13} ampere, the measuring electronics has to be very sensitive, and consequently

susceptible to external disturbances. Therefore, it is desirable to have at least the front end of the amplifier close to the sensor.

When the instrument is used for ground-based measurements, it should incorporate some provision for generating the required air flow. A suitable air-blower or fan can be used for this purpose. When used on moving platforms like aircraft, balloon or rocket, the airflow can be generated by the movement of the vehicle. While this arrangement is satisfactory for measuring conductivities over limited altitude regions, pressure changes over large height ranges in balloon measurements create errors due to the variation in Reynolds' number, as reported by Paltridge (1965). A force-aspirated condenser is preferred for accurate measurements on balloons. In the present investigation, ground-based, jeep-borne and air-borne measurements have been conducted. The sensor was force aspirated for measurements at the surface. For jeep-borne and air-borne measurements, self-aspirated sensors have been used. These are discussed in Chapter 5 where the results of the measurements are presented.

2.2.4 The ground-based instrument

The Gerdien condenser for ground-based measurements was designed to be operated at three stations, two of which were near the coast and hence susceptible to severe corrosion. They were to be used for measuring both positive and negative polar conductivities alternately. The design also took into consideration the fact that the instruments were to be maintained by technicians who may not be very skilled in handling sophisticated instruments.

A sectional elevation of the Gerdien condenser sensor developed for the study is shown in Figure 2.3. The dimensions are as follows: radius of collector, $a = 8$ mm; radius of driving electrode, $b = 32$ mm; length of the electrodes, $L = 500$ mm. The driving electrode is fixed inside a longer cylinder with high voltage insulating sheet between them. The diameters of the two cylinders are such that, with the sheet between them, the inner cylinder fits tightly into the outer one. The shield along with the driving electrode can easily be removed when the collector assembly inside has to be accessed. The outer cylinder extends about 300 mm beyond the driving electrode at the inlet side. This helps to stabilize the air flow through the sensor. The bottom end of the outer cylinder is fixed onto a base with the help of flanges. The base has a horizontal tube with short vertical tubes at either end. The driving electrode assembly is bolted onto the top of the vertical tube at one end. The bottom end of this vertical tube is closed and holds the collector. The collector is insulated from the body of the instrument with the help of a PTFE sleeve. The collector and the sleeve pass through a conical tube fixed on the metal plate that closes the bottom end of the vertical tube of the base, mentioned above. The bottom end of the collector projects below the metal plate where a nut threaded onto it and insulated using a PTFE washer holds it in position.

The top end of the other vertical tube is also closed, and the bottom portion contains an instrument cooling fan that draws air through the sensor. The actual sensor part and the flow generator are thus separated. This configuration was adopted for three reasons. First, this enables the collector to be fitted firmly at the bottom end of the sensor. Secondly, the electrometer can be mounted just beneath the

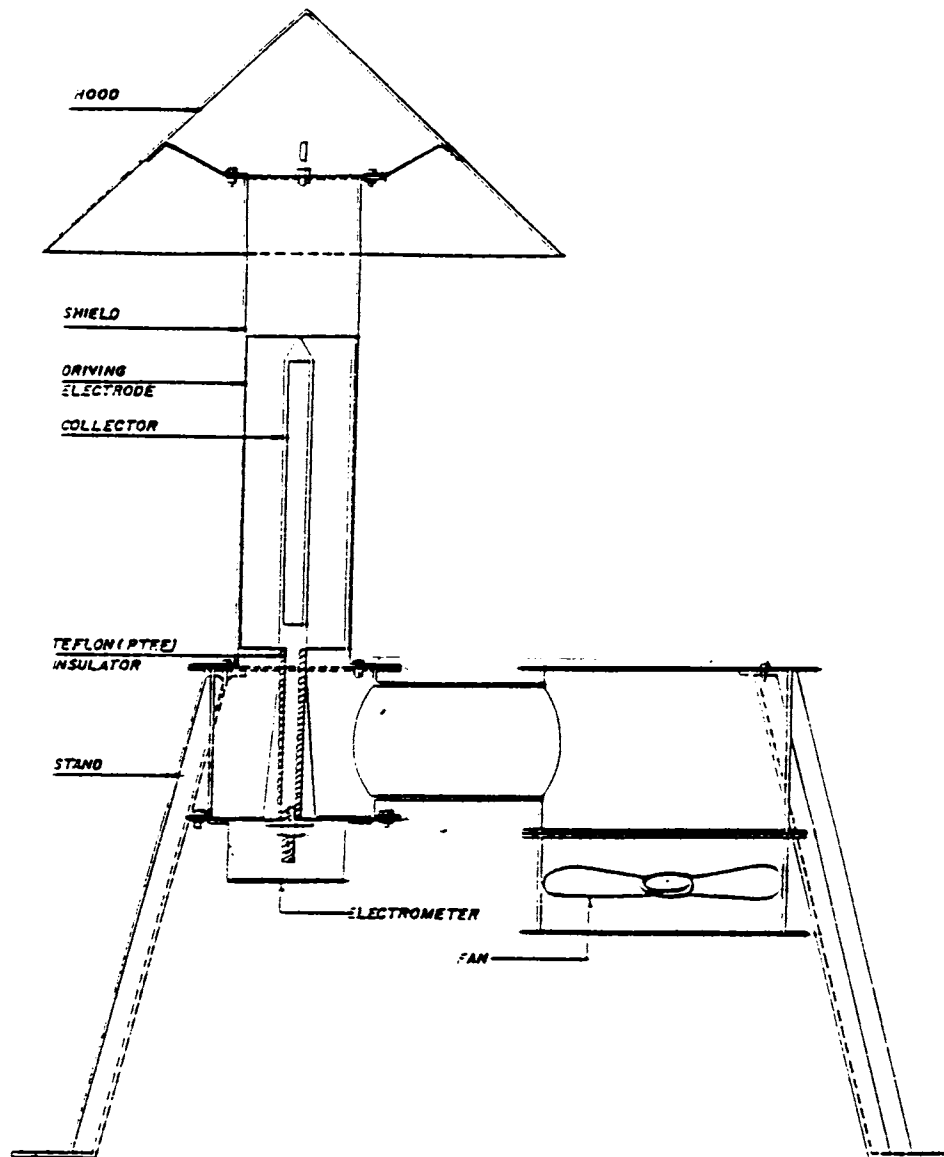


Figure 2.3 Sectional elevation of the Gerdien condenser used for ground-based measurements.

collector so that it can be directly connected to the collector without using long cables. And thirdly, the bottom end of the collector and its PTFE insulator can be protected from dust and dirt. The front end of the electronic circuit is mounted directly beneath the collector. The top of the driving electrode assembly holds a conical hood that prevents rain water from entering the sensor. The entire sensor is made in brass and is chromium plated to protect it from corrosion. It stands on four legs that can be anchored to the ground.

The electronic circuitry of the instrument consists of two parts: the driving voltage generator and the signal conditioner. The former generates suitable voltages at regular time intervals to be fed to the driving electrode. The output current from the Gerdien sensor is converted to voltage and suitably amplified for recording by the latter. A block diagram of the circuitry is shown in Figure 2.4. A discussion of their design considerations and operation are given below, along with the detailed circuit diagrams.

The instrument was designed to measure both positive and negative polar conductivities. This was achieved by alternately giving positive and negative driving voltages. Voltage of each polarity was given for 20 minutes, after which the driving electrode was earthed for 5 minutes. Thus a zero reference was available between every pair of samples. The driving voltages used were ± 4.3 V. This is much lower than the saturation voltage (about 20 V) of the condenser. The voltages were derived from stable regulated sources, and the polarity was selected using relays driven by a clock and suitable control circuitry. Figure 2.5 gives the circuit used for controlling the driving voltage.

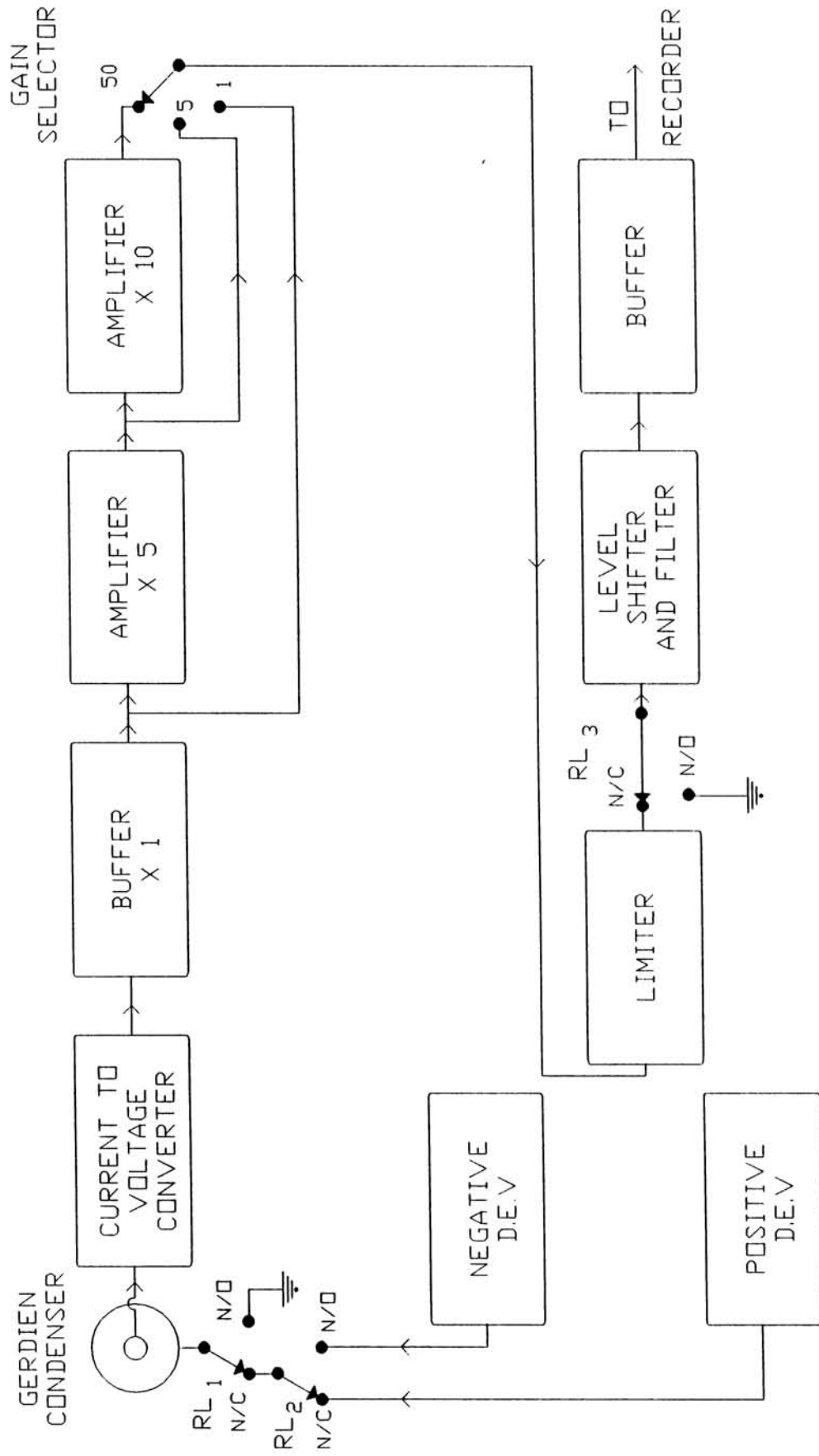


Figure 2.4 Block diagram of the electronic circuit of the Gardien condenser used for ground based measurements.

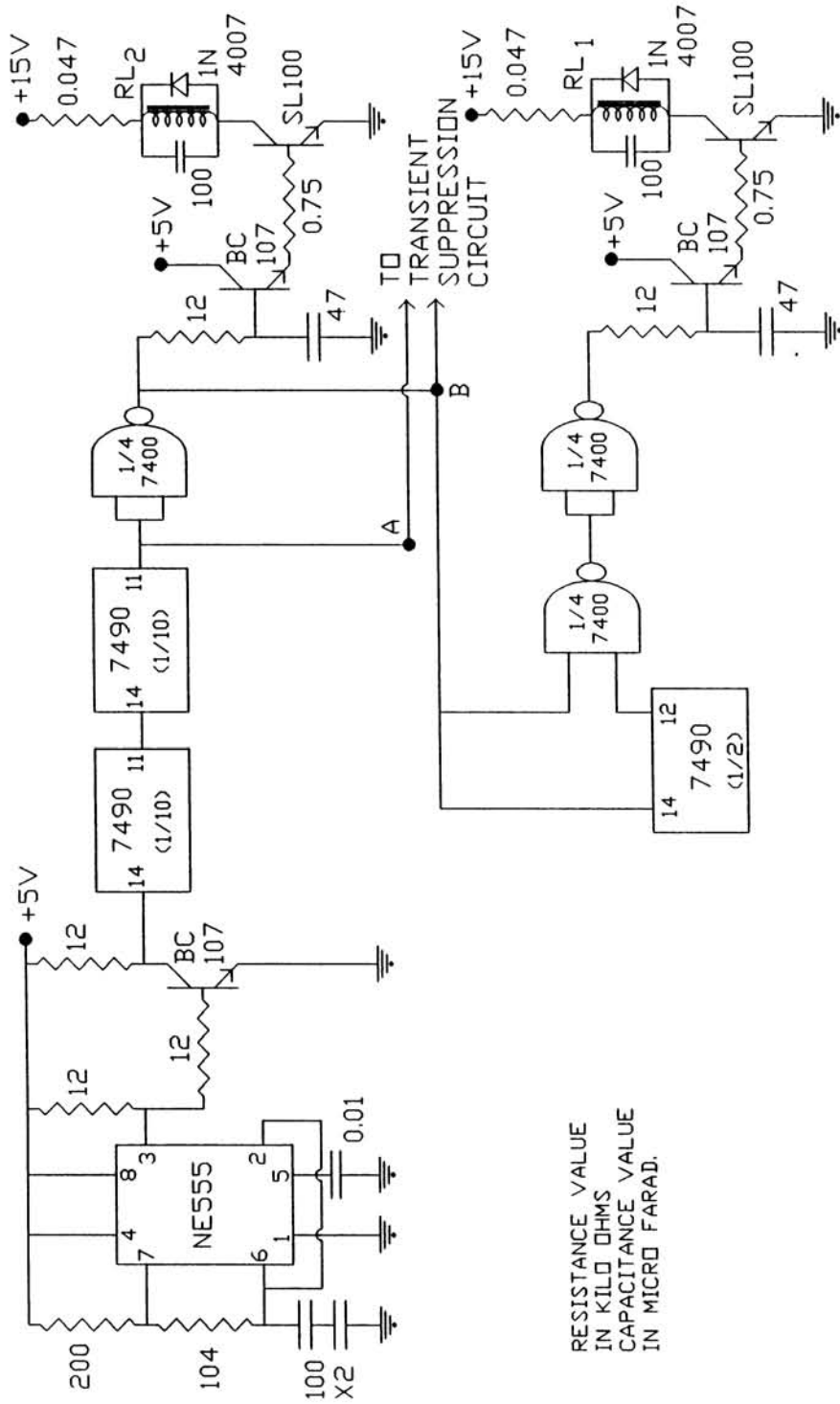


Figure 2.5 The control circuitry used for switching the driving voltage.

The instrument cooling fan used in this instrument was found to deliver a volume flow rate of about 17 m^3 per hour. For this flow rate the collector current obtainable for an ion density of 10^8 ions per cubic metre is of the order of a pico ampere. For measuring such currents, amplifiers with good long-term stability and very low input bias current are needed. This was achieved in the following way. The signal conditioning circuit was designed with a current to voltage converter at the front end, followed by a three stage voltage amplifier. The front end current to voltage converter was built around an AD 515L operational amplifier, which has bias currents as low as 75 fA. A sensitivity of 0.1 V/pA was obtained from this. This was achieved using a Victoreen glass encapsulated 100,000 Megohm resistor in the feedback. The input end of the resistor and the input terminal of AD515L were mounted on PTFE stand-offs to minimise the leakage current. The voltage amplifier had a unity gain buffer at the input, followed by two successive gain stages of x5 and x10. The output of any of these amplifiers could be selected for recording, thus making it possible to adjust the gain level according to the sensitivity required. A 3.3 second filter was used to reduce the noise in the output signal. A level shifter also was provided since the type of recorder used could accept only a unipolar input. Limiter circuits were included in order to confine the output levels between 1 and 5 V, which was the range acceptable to the recorder. The detailed circuit diagram is shown in Figure 2.6. The parts of the circuit that correspond to the blocks given in the block diagram are enclosed in boxes drawn with broken lines.

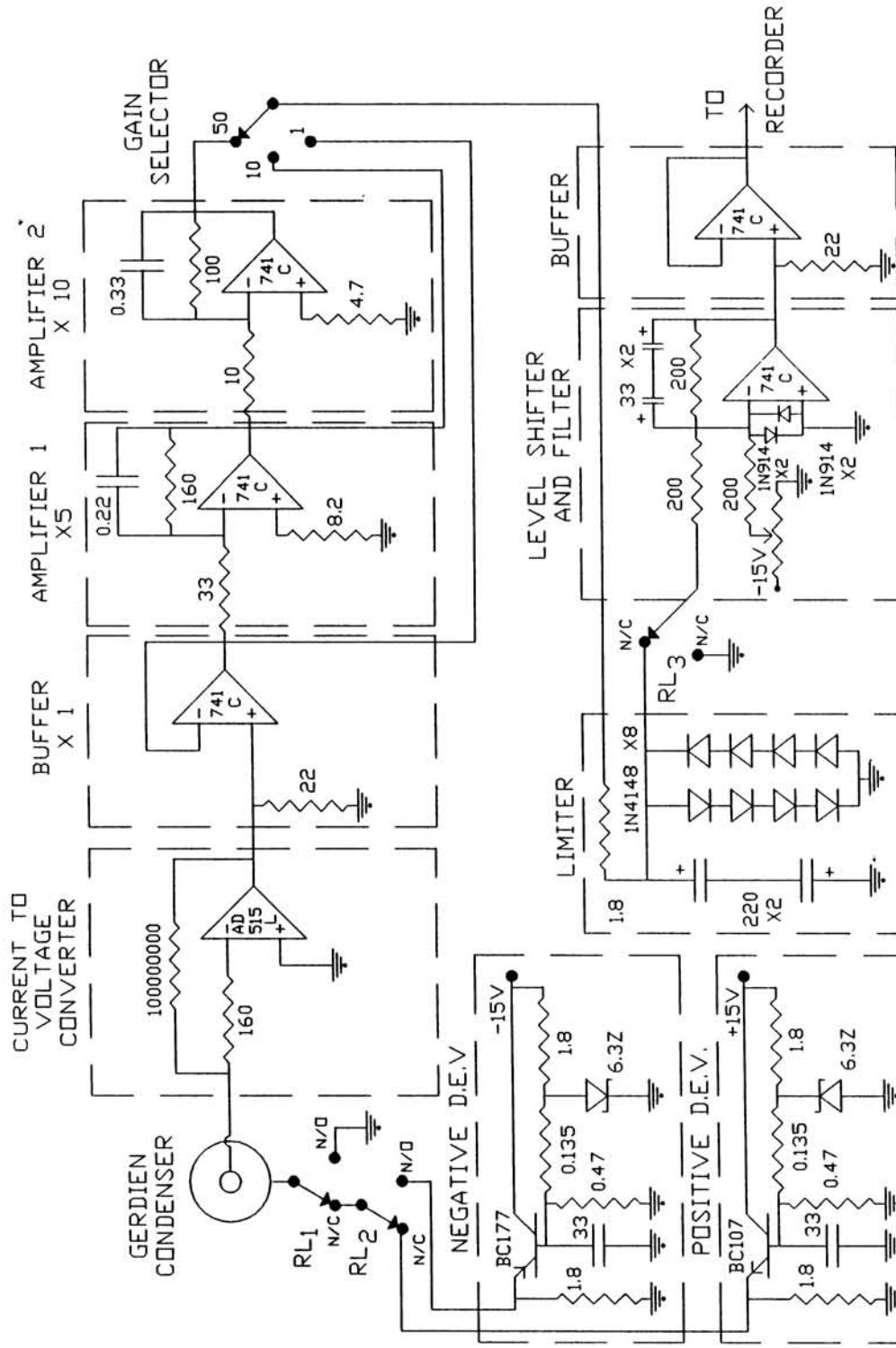


Figure 2.6 Detailed circuit diagram of the electronics of the ground-based Gerdien condenser.

In addition, a circuit was included to suppress the transient signal that accompanies the switching of the driving voltage. These transients are caused by the displacement currents, which are proportional to the rate of change of voltage, that flow through the condenser. The transients were suppressed by disconnecting the recorder input during the switching periods and reconnecting after a delay of about 20 s. The circuit used for this is shown in Figure 2.7.

The entire system was calibrated by giving input at the collector from a Keithley Instruments pico ampere source and recording the output on the strip chart recorder. The output was also measured using a digital voltmeter. A typical calibration curve is shown in Figure 2.8. The non-linearity seen at the extremes is because of limiter circuits that are used to ensure that the recorder is not damaged. The current-voltage characteristic of the condenser is shown in Figure 2.9. The instrument was operated at Trivandrum in the premises of the institution to evaluate its performance. It was run continuously over several days and its performance was found to be satisfactory.

2.3 THE FIELD MILL

The electric field mill is an established technique for measuring the vertical electric field in the atmosphere. It does not have the disadvantages of other probes like the radioactive potential equalizer which modifies the electrical environment through nuclear radiations. However, obtaining the sign of the field from the output of the field mill involves the synchronous detection of its output signal, which is usually not simple. In the present study, a field mill was designed and fabri-

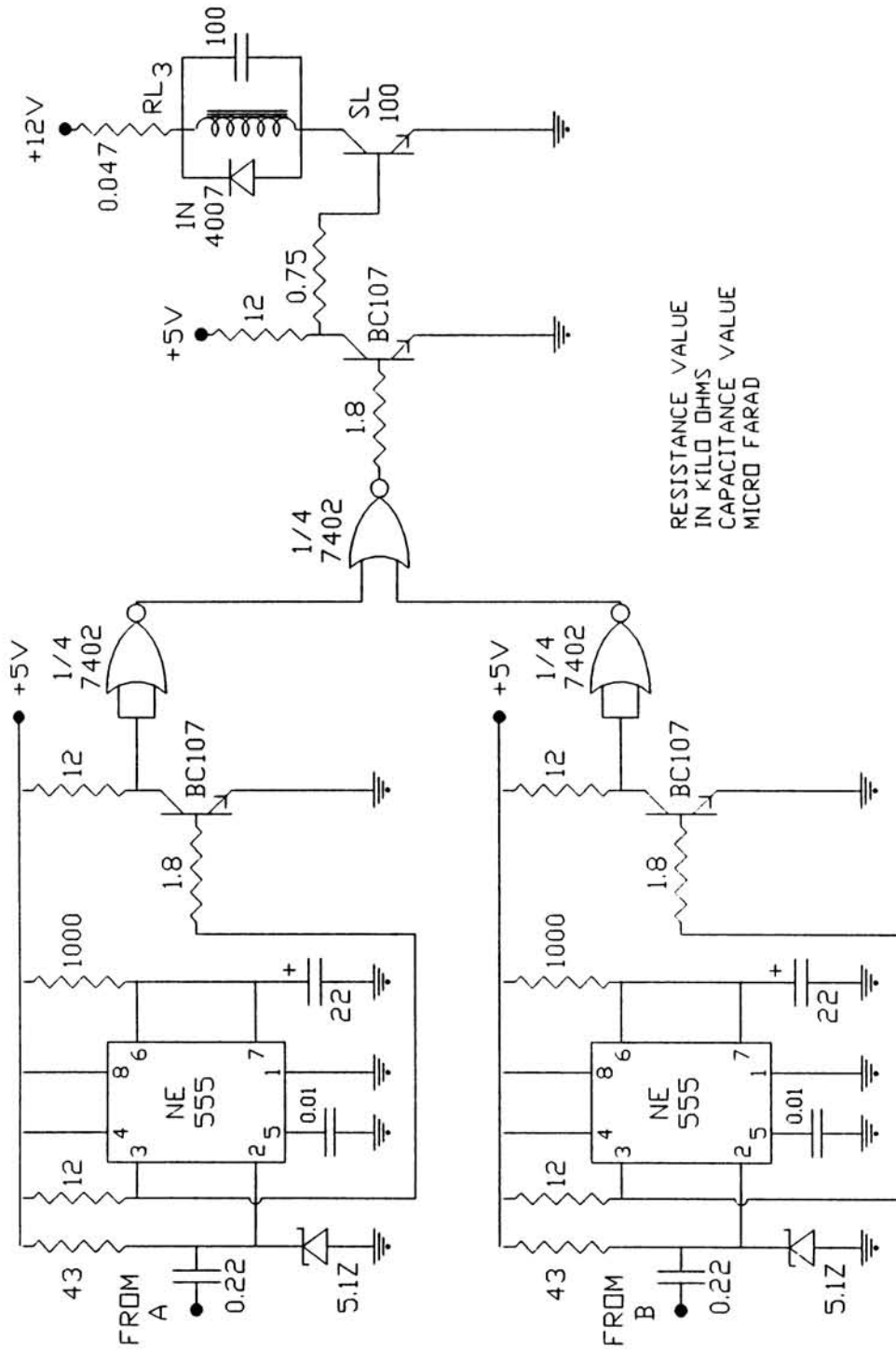


Figure 2.7 The circuitry used for eliminating the transients from the recorded data.

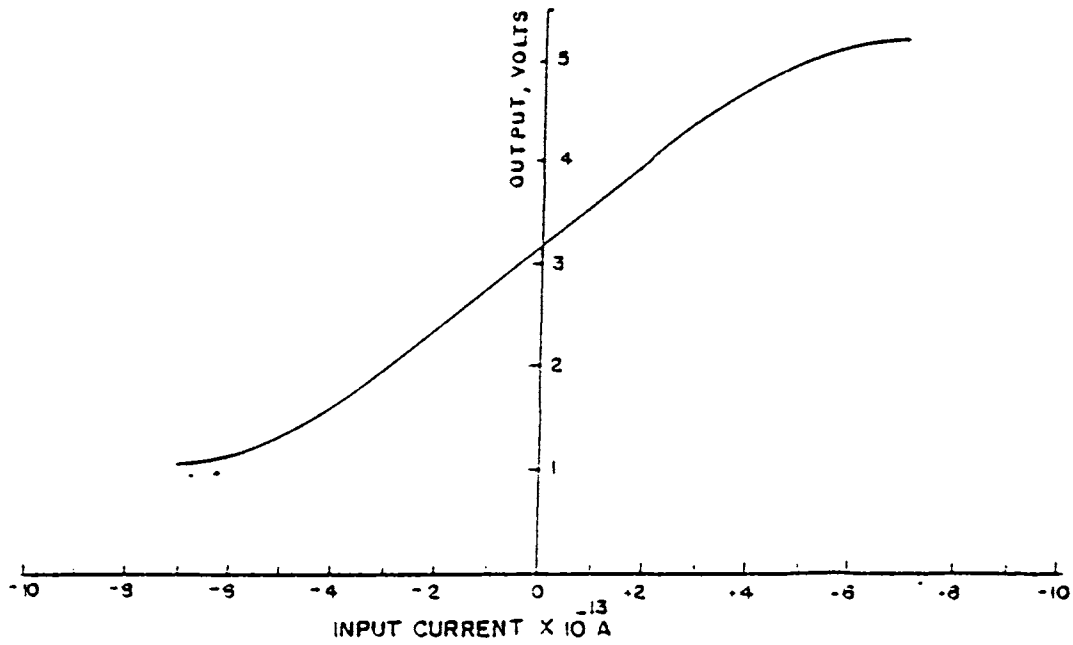


Figure 2.8 Calibration of the Gerdien condenser system.

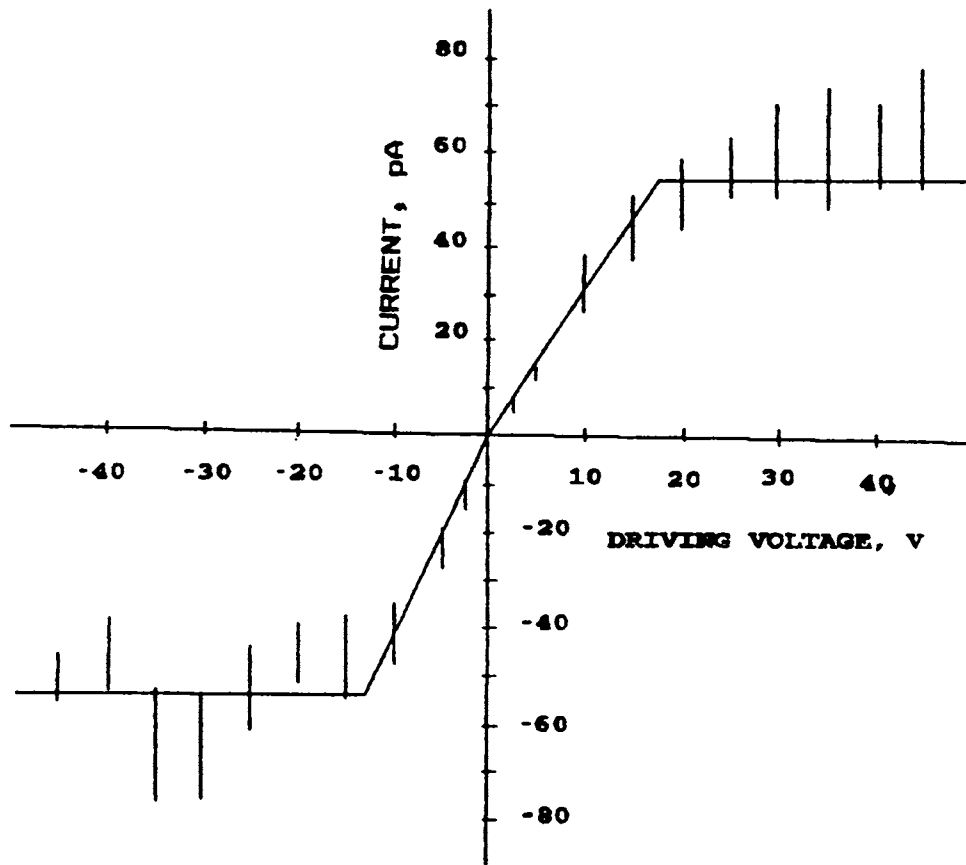


Figure 2.9 Current-voltage characteristic of the Gerdien condenser used in the monitoring stations.

cated and test run for a short duration at one station. Since certain modifications were found to be needed if continuous monitoring was to be carried out, the instrument was dismantled and brought back. The required modifications could not be carried out in time, and hence data are available only for a short duration. In the field mill used in the present study, although the basic design allows for the derivation of the sign of the field, this was not implemented due to certain problems faced in the fabrication of the instrument. Further development of the instrument is being taken up.

2.3.1 Theory

The electric field mill works on the principle that an electric field that terminates on a metal plate that is earthed induces electric charge on it. The surface density of charge, ρ , is given by the expression:

$$\rho = \epsilon_0 E \quad (2.19)$$

where E is the electric field and ϵ_0 is the permittivity of free space. The sign of the charge depends on the direction of the field. A field pointing towards the plate induces a negative charge, and a field in the opposite direction induces a positive charge.

In the field mill, an earthed metal plate is alternately exposed to and shielded from the vertical electric field. When the plate is exposed to the field, a charge is induced on it so that the opposite charge flows to the earth. When the plate is then shielded from the field, the excess charge on the plate gets neutralised by charges that flow from the earth to the plate. Thus, when the plate is alternately exposed and shielded, two currents of opposite polarities flow between the plate and

the ground. The directions of these currents depend on the direction of the electric field, and the magnitude of the currents depends on the magnitude of the field and the exposed area of the plate. In the basic instrument, the plate is alternately exposed to and shielded from the vertical electric field by using two electrically grounded metal plates with alternately open and closed sectors of which one rotates. The instrument normally is mounted at the surface with the collecting plate facing upward. Modifications to this basic design have been attempted. **Johns & Kreielsheimer** (1967), for instance, suggested an end-on field mill, and **Kamra** (1983) designed a spherical field mill that could give simultaneous measurement of all the three components. The agrimeter (for instance, **Kamra & Varshneya**, 1968) is a slightly different type of instrument that works on the same principle. The instrument used in the present study is a normal field mill mounted upside down.

2.3.2 The sensor

The field mill consists of three parallel plates, namely, the stator, the rotor, and the collector. Each of the first two is divided into equal sectors that are alternately closed and open. Each plate may have four six or more sectors, the present design having six. The three plates are mounted one above the other such that by turning the rotor, the open sectors of the two plates can be brought one above the other, thus exposing the corresponding area of the collector. If the rotor is now moved through an angle equal to the angle subtended by each sector, the closed portion of the rotor is brought in line with the open portion of the stator so that the collector is completely shielded from

the external field. When the rotor is continuously rotated, the collector is alternately exposed to and shielded from the field.

The mechanical design of the sensor used in the study is shown in Figure 2.10. Here, a small 6 V dc motor was used to drive the rotor. This motor was adopted since it is compact, easily available for replacement, and avoids bringing lines carrying large voltages close to the instrument. The motor was mounted on the stator with its shaft projecting inside. The rotor was mounted on the shaft with the help of a solid cylindrical shank into which the shaft fits tightly. The rotor was earthed through the shaft of the motor. The collector plate was mounted on PTFE blocks screwed onto the base of the field mill. The front end of the signal conditioning circuit was mounted on the field mill itself. As in the case of the Gerdien condenser, this helped in avoiding a long input cable from the sensor leading to the electronic circuit.

An inverted configuration was adopted in this design, where the field mill is kept inverted so that the field that impinges on the collector plate is due to field lines that curve upward from the sides of the sensor and terminate on the collector. Such a configuration has been used by **Takagi and Iwata** (1980). An optical sensor was designed to sense the position of the rotor in order to synchronously detect the output signal. This part of the instrument could not however be completed and installed due to certain difficulties encountered during implementation.

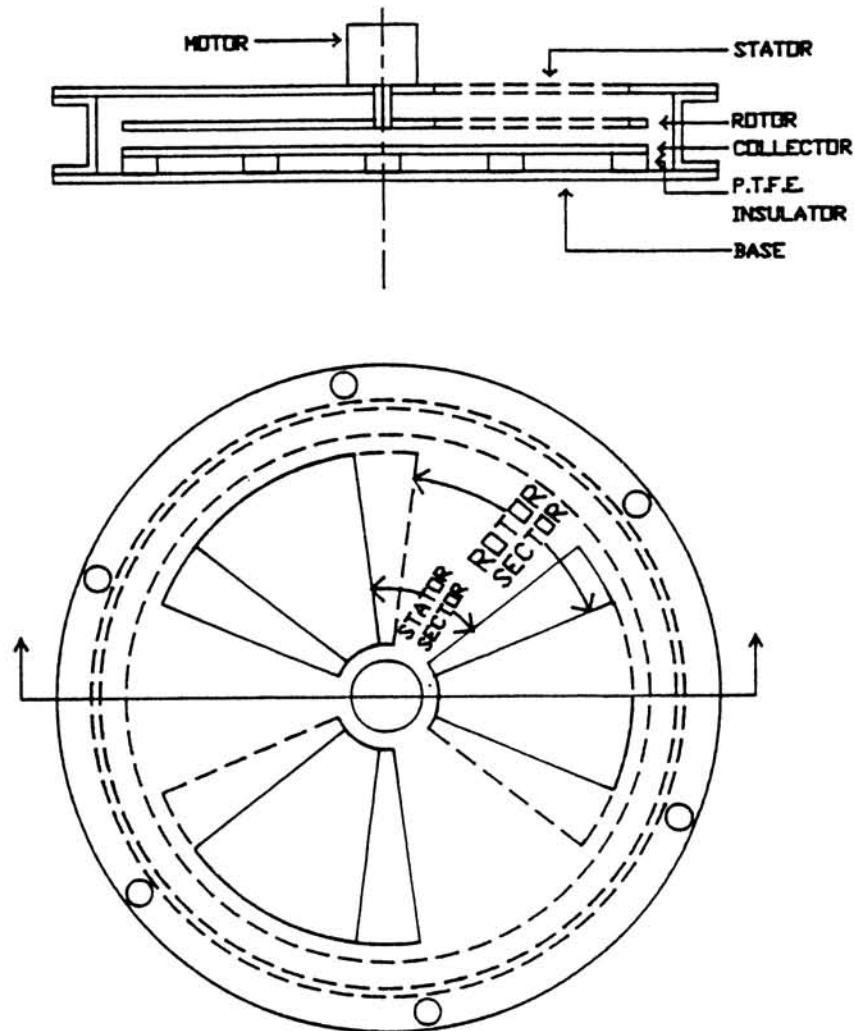


Figure 2.10 Schematic diagram of the field mill sensor.

The instrument was successfully operated only at one site, namely Kottarakara. There, the instrument was mounted on $1\frac{1}{2}$ MS angles fixed on two brick masonry pillars about four feet high and six feet apart.

2.3.3 The electronics

A block diagram of the electronic circuitry used for the electric field mill is shown in Figure 2.11. The output from the collector is fed to a current to voltage converter having a sensitivity of 0.1 V/pA. This

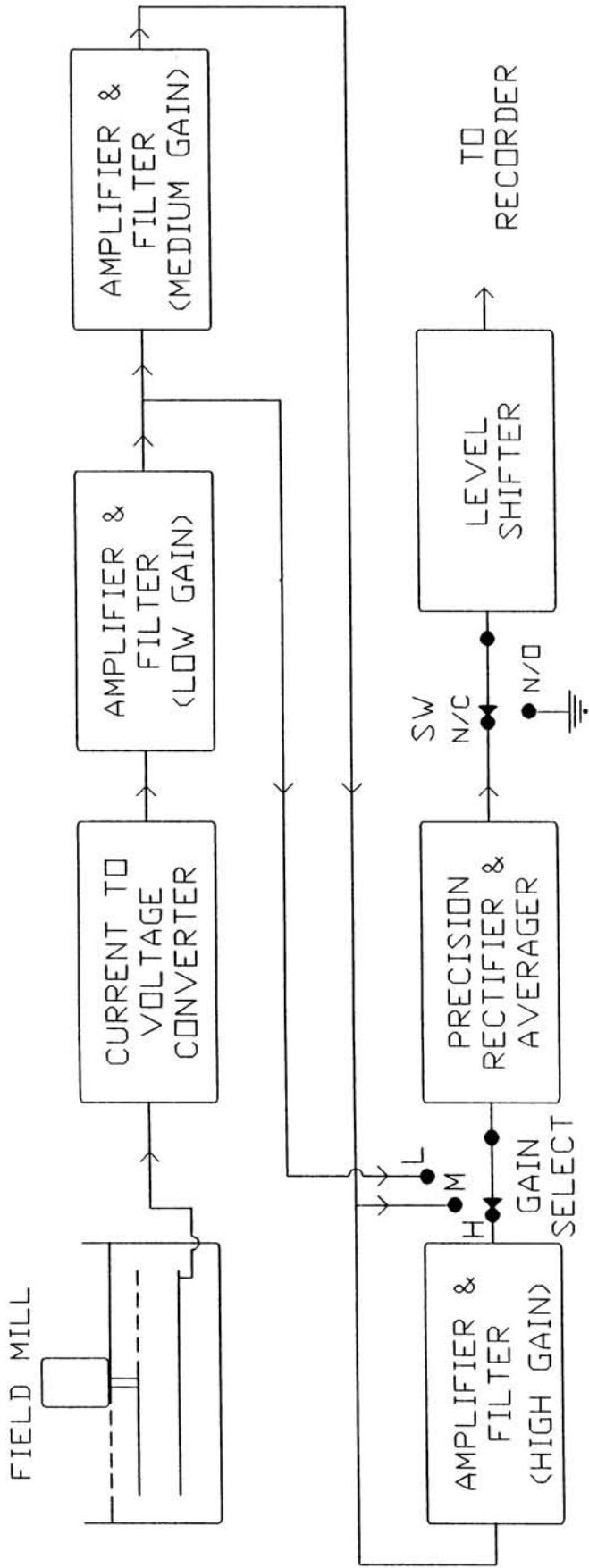


Figure 2.11 Block diagram of the electronic circuitry of the field mill.

stage is similar to the one used for the Gerdien condenser. The output of this stage is amplified and filtered to remove the noise present in the original signal. This noise is mainly due to the wobbling of the rotor and the vibration due to its rotation. The filtered signal is rectified, amplified and again filtered to obtain a dc output. Detailed circuit diagram of the circuitry is shown in Figure 2.12.

A rough calibration of the instrument was done by generating an electric field between two plates kept one metre apart. This calibration is unsatisfactory for making good measurements. The field mill has to be calibrated inside a Faraday cage where the influence of external fields would not be felt. The simple calibration was resorted to since this was only a test run, and also because a suitable Faraday cage was not available. The results from the electric field measurements therefore are used only as a supporting data.

2.4 THE SYSTEM CONSOLE

The major part of the electronic circuits (except for the front end amplifiers), the power supplies, the recorders, etc. were integrated in a console, shown in Figure 2.13. The console was designed to accommodate the electronics associated with up to four sensors, and two dual channel recorders of the panel mounting type. The rack is divided into three parts. The top part holds the two recorders. The electronic circuits are mounted on a sliding rack in the middle part. The front panel of this part has a digital panel meter which can display the voltages at various points in the circuit as selected using a thumb-wheel switch below it. Two push-button switches are provided for

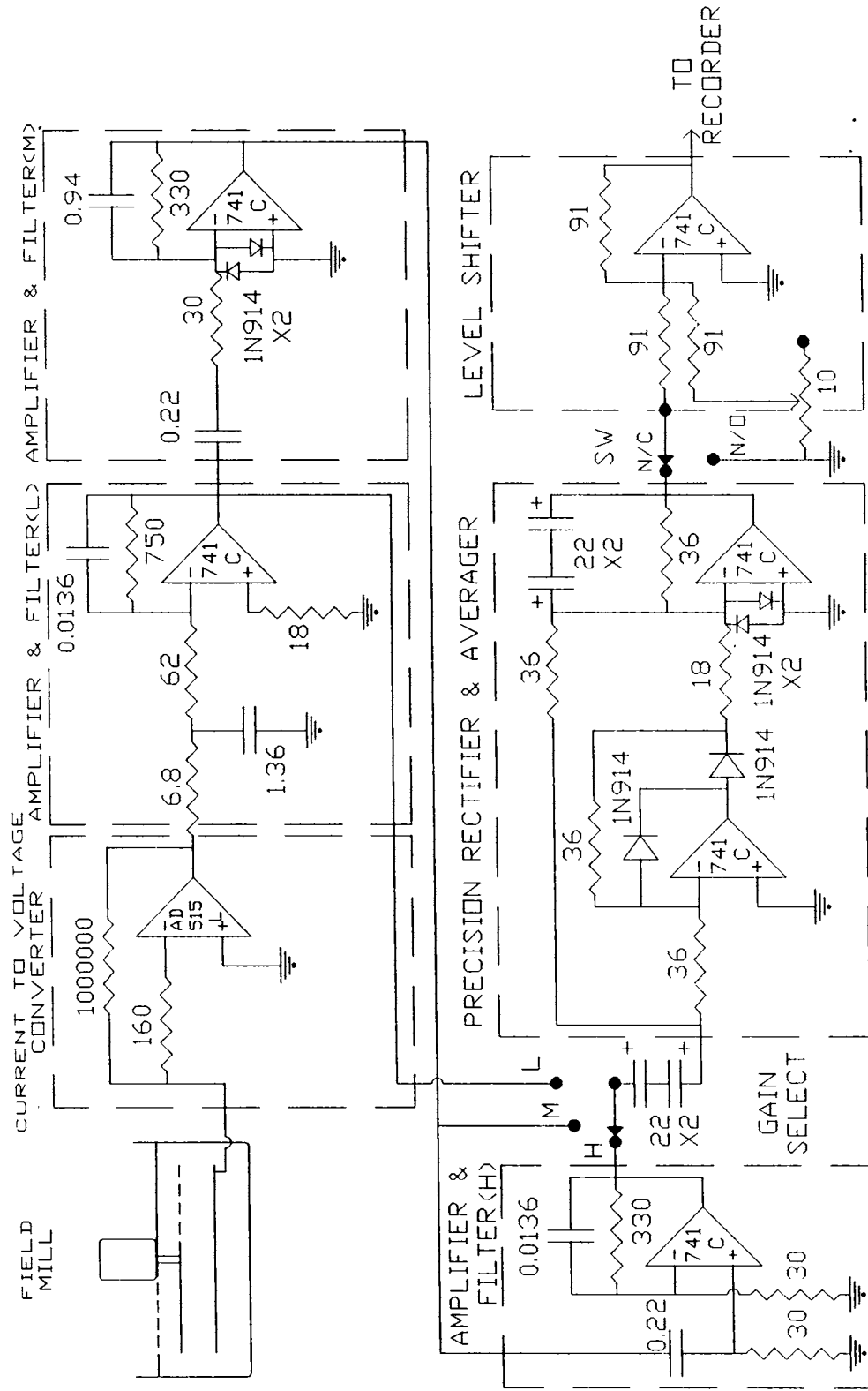


Figure 2.12 Detailed circuit diagram of the electronics of the field mill.

RESISTANCE IN KILO OHMS
CAPACITANCE IN MICRO FARAD

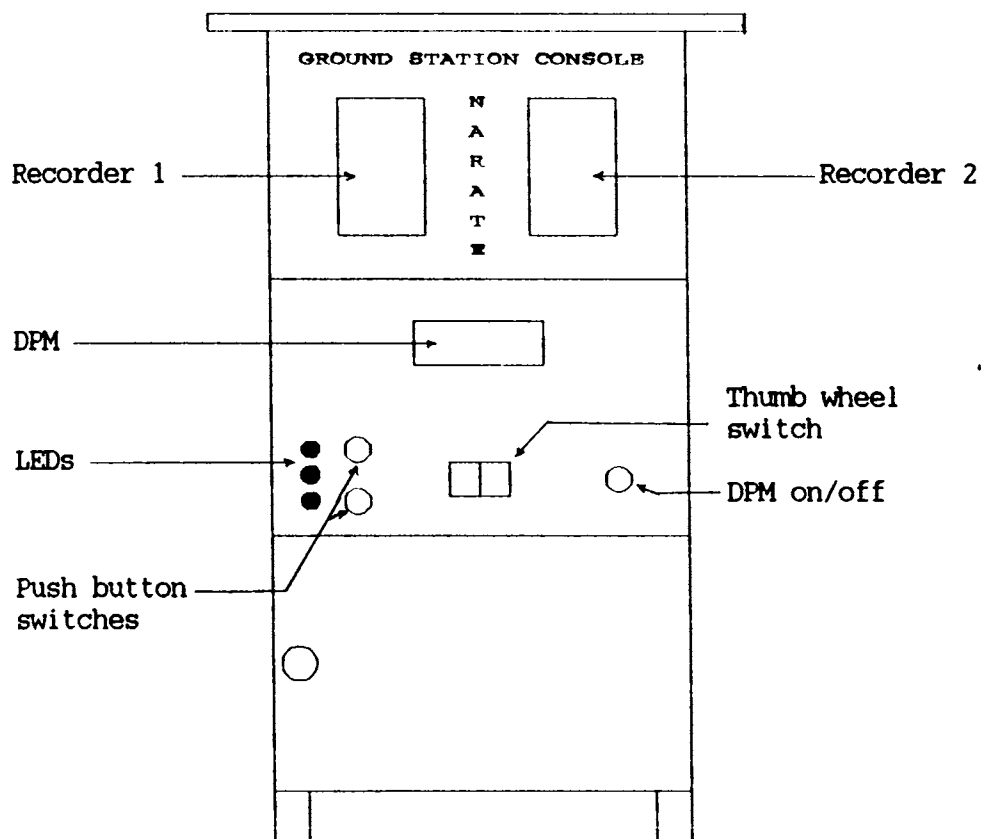


Figure 2.13. Schematic diagram of the ground station console.

button switches are provided for disconnecting the inputs so that the zero levels of their amplifiers can be checked. Three LEDs of different colours display the polarity of the driving voltage of the Gerdien condenser.

CHAPTER III

3. THE EXPERIMENTS

3.1 INTRODUCTION

Much of the work described in this thesis was carried out under a research project financed by the Department of Science and Technology, Government of India. The primary objective of the project was to understand the behaviour of atmospheric electrical parameters over the highly radioactive region along the Kerala coast. However, measurements were carried out at sites with low levels of radioactivity also. In addition, measurements were carried out in the campus of our institution, using the instruments developed for the project. These measurements have helped in determining the effect of some of the meteorological parameters like temperature, rainfall, winds, etc. The results are presented in this thesis. The influence of certain environmental parameters like pollution have not been studied during this investigation.

As part of the study, observations were carried out at different places at the surface. In addition, a few surveys were carried out at the surface and up to an altitude of about 660 m using an aircraft. A brief description of the physiographical and meteorological characteristics of the region where the study was conducted, the sites where observations were made, the kind of environment at each site, data reduction and analysis techniques used, survey routes, etc. is given in this chapter.

3.1.1 The study region

The study described in this thesis was carried out in the south-western region of India, mainly in the state of Kerala, with some measurements extending beyond the southern border into the adjoining state of Tamil Nadu. Kerala is a small state confined to a narrow region between the Western Ghats on the east and the Arabian sea on the west. The physiography of the state is shown in Figure 3.1. The land area of the state can be divided into three regions, namely, the low land consisting of the coastal areas and adjoining lakes and wetlands, the high land consisting of the Western Ghat region, and the midland between them. The state has a high density of population, with the highest densities in the coastal region. Blessed by good rainfall during the more than six months of the year, the state is also densely covered with vegetation.

Since the width of the state is rather small, the Western Ghats have a strong influence on the climate of the state. Being oriented almost perpendicular to the flow of the monsoon winds, the Ghats act as an obstruction to the clouds and thus bring copious rainfall to the state.

In the state, the year may be divided into three main seasons from the climatological point of view. These are: (i) the south-west monsoon season, from June to mid-October, (ii) the north-west monsoon season, from mid-October to February, and (iii) the hot, or summer, season from March to May. The third season is marked by relatively high temperatures and high humidity. The mean maximum temperature

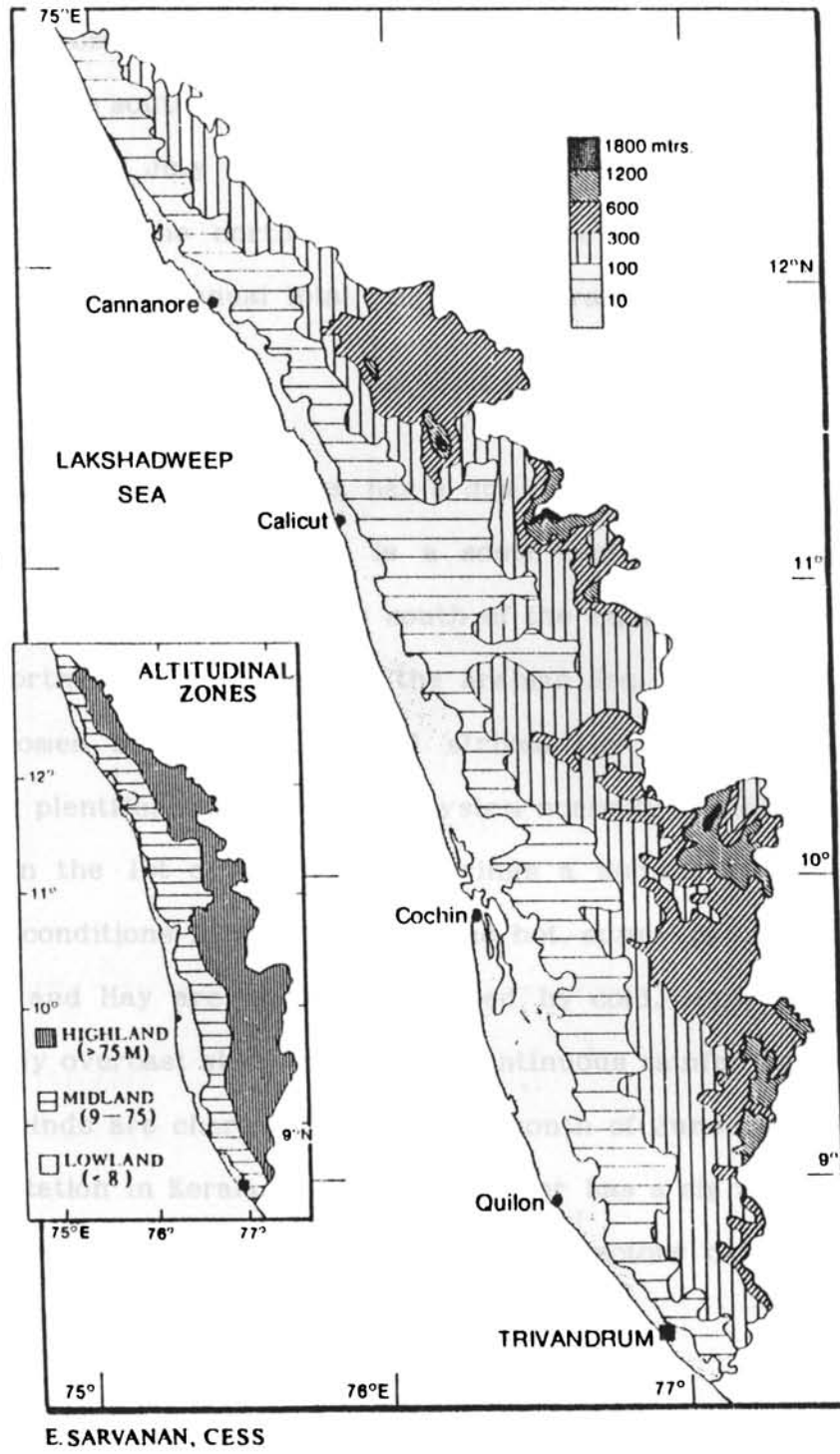
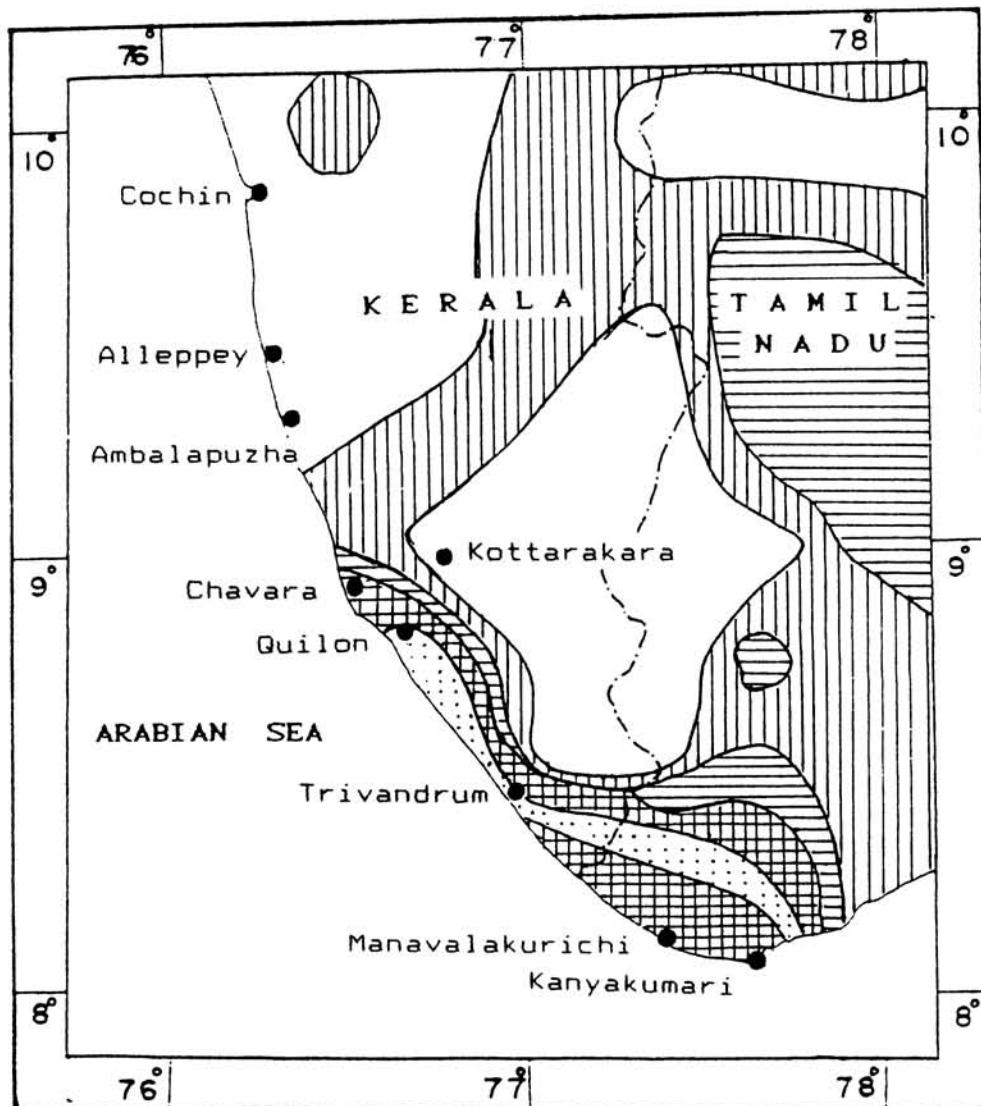


Figure 3.1 Map showing physiography of Kerala State.

is generally the highest in March, around 33⁰ C, and is higher in the northern parts. The diurnal range in temperature is lowest in July and August, and highest in January. The total rainfall received per year increases from about 1800 mm in the south to about 3800 mm in the north. In the southern parts, about half of this is obtained during the months of June, July and August. The fraction increases towards the north. During the north-east monsoon, the southern parts receive around 25% of the annual total rainfall, the fraction decreasing towards the north (*IMD*, 1986).

The monsoon, therefore, has a dominant influence on the climate of this state. The monsoon is a south-easterly wind system that develops over the Indian ocean south of the Equator and crosses over to the northern hemisphere over the Arabian Sea. The wind then turns and becomes south-westerly, and strikes the Indian sub-continent, bringing plentiful rain. The wind system normally reaches the coast of Kerala on the 1st of June. This brings a sudden transition in the weather conditions in this region. The hot, sunny days of the months of April and May are suddenly replaced by cold, rainy days. Almost completely overcast skies, heavy and continuous rainfall and continuous strong winds are characteristic of the month of June, especially for a coastal station in Kerala. Since the weather has a significant influence on atmospheric electrical parameters, these factors have been kept in mind during the interpretation of the results.

One of the unique features in this region of the country is the rich placer deposit of the radioactive mineral monazite along the south western coast of south India. Figure 3.2 shows a map of the region



LEGEND

Terrestrial Radiation, mr/yr.

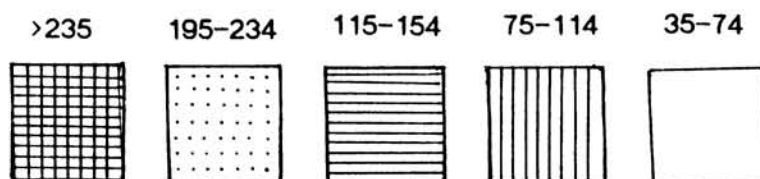


Figure 3.2 Map of the southern part of Kerala State and the adjoining regions of Tamil Nadu showing the distribution of radioactivity, in terms of the intensity of terrestrial radiation.

(adapted from *Sankaran et al.*, 1986) where the terrestrial radiation levels for this region are marked. The region along the coast from around Chavara southwards is seen to have high values. This is due to the high concentration of thorium in the sands in this region. Estimates of the concentration of thorium in the beach sands in the southern part of Kerala (*Prakash, et al.*, 1991) show that it varies from about 200 ppm to more than 2000 ppm, with a mean value of about 550 ppm. The range of average content of thorium in igneous and sedimentary rocks is considered to be 4 to 15 ppm (*Junge*, 1963, p 213). The lowest concentrations of radioactive substances are found in extremely alkaline igneous rocks, and the highest in acidic igneous rocks, with the values for sedimentary rocks somewhere in-between (*Israel*, 1971, p 185). These coastal sands, therefore, contain about 100 times the global average level of radioactivity. This was therefore one region which was selected for the study. Since the deposits are found mainly in the coastal sands, it was decided to make observations at another coastal site that does not have any radioactivity so that effects common to coastal areas could be eliminated. Such a site can be obtained towards the north of Chavara. As explained below, a suitable site was obtained at Ambalapuzha. An inland non-radioactive site also was chosen for observations so that the difference between continental and marine environments could be discerned. The radioactivity levels are lower in the midlands than in the coastal region, but the lowest values are seen in a patch almost straight to the east of Chavara. A site was found at Kottarakara, about 25 km east of Chavara, which falls at one corner of this patch. Apart from these sites, some observations were also carried out in the campus of our institute at Trivandrum.

3.2 MEASUREMENTS AT THE SURFACE

During the present investigation, measurements were carried out at four sites at the surface, and jeep-borne and air-borne surveys were carried out. This section gives a brief description of the sites selected, and the operation and maintenance of the instruments.

3.2.1 Monitoring sites

For monitoring atmospheric electrical parameters at the surface, sites had to be identified where it would be possible to install and run the instruments conveniently. The requirements were that the place should have convenient access so that the equipment could be carried in a vehicle, power should be available for running the instruments, sufficient security should be available for the instruments, and some amount of open space should be present so that the instrument would not have to sit under trees or other vegetation. These conditions are not easily met in a thickly populated and vegetated state like Kerala, especially when the site has to be located within a small specified region, as in the present case.

For the station within the radioactive region, a convenient site was found at Chavara ($8^{\circ} 59' N$, $76^{\circ} 31' E$), a place that has a very high concentration of monazite sands. The site was near a factory of the Indian Rare Earths (IRE) where the sand mined from the region is mechanically separated to extract monazite and other useful minerals. A lighthouse belonging to the Department of Lighthouses and Lightships, Government of India, exists near the factory and close to the seashore,

which can be reached through a muddy jeepable road. The place is well protected, and some open space is available for installing the sensor. A small building was available where the power supply and control and recording instruments could be kept. Power disruption was minimal since the lighthouse had its own generator that would take over within a few minutes in case of power failure. The proximity of the IRE factory did not cause problems because it generated very little pollution. The nearest main road is the National Highway (NH47) about 1 km east of the lighthouse, so that pollution due to automobile exhausts is also small at this site. The coast line is protected by a sea wall that was about 30 m to the west of the place where the sensor was situated. Being so close to the sea created problems during the monsoon season due to excessive corrosion, especially in the sensor.

The second station was established at Ambalapuzha ($9^{\circ} 23' N$, $76^{\circ} 46' E$), in the premises of a building of the Kerala State Fisheries Department. This was situated on the Ambalapuzha beach. The sea was about 100 m from the building. Due to safety reasons, the instrument could not be installed outside. The sensor was kept inside a room in the ground floor of the building, but care was taken to ensure that there was free passage of air through the room at all times by keeping the windows open. The sensor was occasionally kept outside for short durations in order to compare the values obtained outside with those obtained inside. The two sets of values were in good agreement with each other. No significant difference was noticed. The building had the open beach to its west, with fishermen's huts on the eastern and southern sides. A road leading from the Highway about 1 km to the

east terminated in front of the building. A similar building was situated on the opposite side of the road, with more huts behind it.

The third station was located at Kottarakara (9° N, 76° 46' E), about 25 km to the east of Chavara, in the campus of the Kallada Irrigation Project office of the Kerala State Irrigation Department. The sensors (Gerdien condenser and field mill) were kept on the terrace of their dormitory building, and the rest of the system was kept inside one of the rooms. The dormitory is a two-storied building and it stands on the slope of a small hillock close to the town. At this site, the instruments were kept at a height of around 10 m from the ground. Moreover, the site is different from the other two in that it is close to a small town. These factors would affect the conductivity values obtained. This has been kept in mind while interpreting the data.

Measurements were also made at the campus of the Centre for Earth Science Studies (CESS). Here, in addition to conductivity, rainfall also was measured using a self-recording rain gauge certified by the India Meteorological Department. The CESS campus is situated at Akkulam in the outskirts of Trivandrum city. The Centre is situated in its own land of about 18 ha in the Ulloor Panchayat, in a region where population density is low and there is virtually no industrial activity. There is no major highway nearby. The area thus has very little pollution. The sensor was kept on top of a single storied building, and the rest of the system inside. The rain gauge also was kept near the sensor since a suitable open area was not available on the ground. The terrace, however, provided a relatively large open space without any obstructions nearby. This arrangement was more or less sufficient for

the present purpose since the precise value of rainfall was not of much interest, but only its variation. The locations of the monitoring stations are marked in a map in Figure 3.3.

3.2.2 Operation and maintenance

The monitoring stations were manned by technicians trained in their operation and maintenance. Since the data were recorded on chart paper, the technician was required to mark time on the chart twice a day, in the morning and in the evening. He was also required to ensure that the instrument functioned normally. A log book was provided at each station in which the technician was required to note down the values of certain parameters that could be read from the digital panel meter (DPM) on the system console. These included the driving voltage levels and the output voltage levels at different stages in the Gerdien condenser and field mill circuitry, the input voltages to the recorders, and the power supply voltages. This provided a very useful check on the system performance, and also was of considerable help on trouble shooting. Periodic cleaning of the sensor, lubrication of the fan in the sensor, ensuring that the recorder functioned smoothly, noting the periods when power failed, and noting down in the log book his observations about general weather conditions like thunderstorm activity, rainfall, cloudiness, etc. were also part of the duties of the technician. In case of any problem that he was not able to tackle, he was required to immediately inform the investigator. In addition, the investigators visited the stations at periodic intervals to ensure that the instruments were running smoothly.

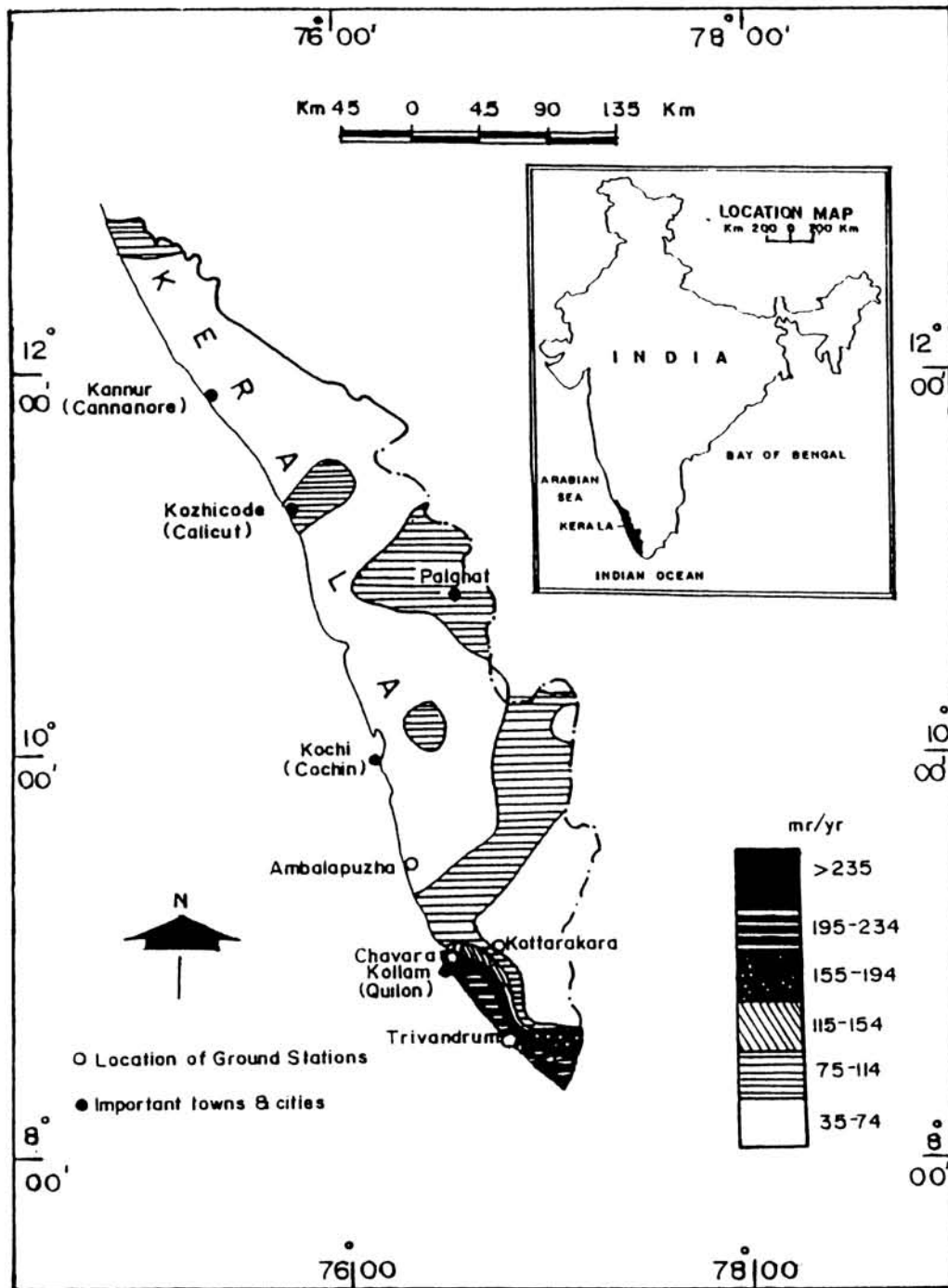


Figure 3.3 Map showing the locations of the monitoring stations.

3.2.3 Data reduction and analysis

The data were recorded on chart paper using a strip chart recorder running at a speed of 20 mm per hour. The chart rolls were brought to Trivandrum every month, along with the log book, by the technician, who also reported on the performance of the station. The log book and the chart record together give a clear picture of the functioning of the station with regard to accuracy and stability. For reducing the data, time marks were put for each hour of the day by interpolating between the time marks put by the technician. While doing this, care was taken to ensure that the intervals are more or less uniform for all hours of the day. If there had been any power failure during night time that the technician had failed to note, then the time interval would not match with the distance on the chart paper. Periods when the time marks and the distance on the chart paper do not match within reasonable limits have been excluded during data reduction. Data have been lost also during periods when the record was noisy due to heavy rain or some other extraneous interference, or during periods when the recorder did not function properly. Data for short durations were lost also when the maintenance of the instrument was being carried out. These are limited to about half an hour on each occasion. Figure 3.4 shows a sample portion from a chart.

The readings were taken for each hour of the day. For a given hour, the readings were taken for the period between half an hour before the time mark and half an hour after. For instance, the output recorded between 0030 hr and 0130 hr was noted as the values for the time 0100 hr. Since the period of the driving voltage waveform was 50.

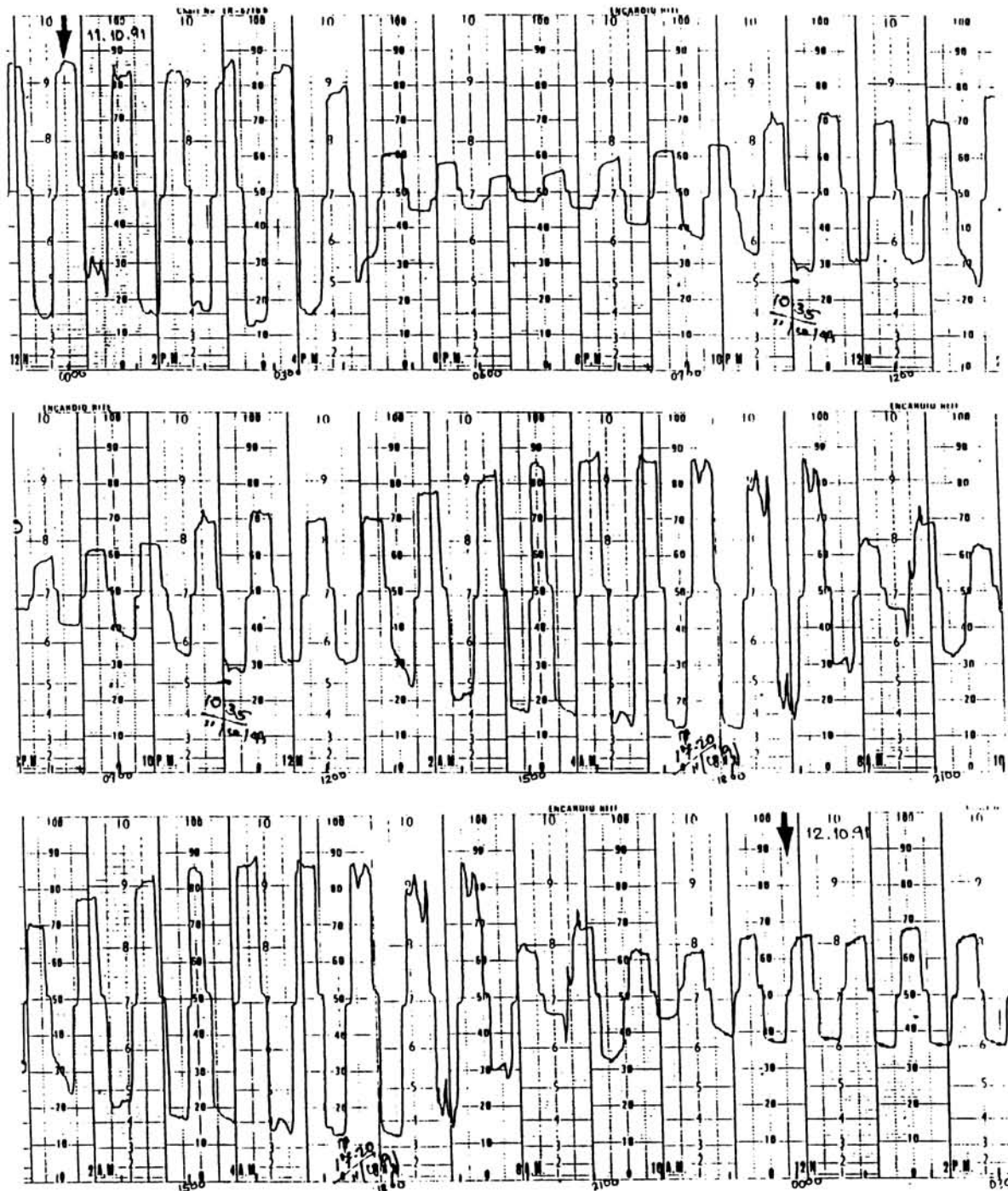


Figure 3.4 Sample portion of a day's record of conductivity.

minutes, normally there would be one positive value and one negative value for each hour of the day. The change over from one voltage to zero, or vice versa, need not coincide with the midway mark between two time marks. Therefore, the output for each polarity of driving voltage was ascribed to the hour in which the larger part of it fell. An average value for the period of the particular driving voltage (about 20 minutes) was noted down as the reading for the corresponding hour. But once in a while, three readings, one of one polarity and two of the other, would be present for one hour. In such cases, for the polarity for which two readings were present, an average was taken.

The readings were converted into conductivity values by multiplying with the proper conversion factor. The conversion factors were determined from the calibration of the system. The polar conductivity values were separately tabulated for each month. From this, the monthly mean for each hour of the day and the daily average of the hourly values were computed. The standard deviation also was determined for each average value. For each polar conductivity, an average value was derived from the daily means for each month.

3.3 JEEP-BORNE AND AIR-BORNE SURVEYS

The data from the monitoring stations at the surface were useful for understanding the temporal variation of the atmospheric electrical parameters and studying the nature of the influence of the radioactive deposits. It was also desired to study the horizontal and vertical extent of the influence. For this, air-borne surveys were carried out over the region of study. A Pushpak trainer aircraft of the Kerala

Aviation Training Centre (KATC), Trivandrum, was used for the purpose. The survey routes were chosen such that they would cover the sites where the monitoring stations were set up. Thus one survey was done from Trivandrum to Alleppey and back along the coast, which went over the sites of the monitoring stations at Chavara and Ambalapuzha. A second survey was carried out from Trivandrum to Kottarakara, from there to Chavara and about one kilometre beyond the coast over the sea, and back along the same route. A third survey went southward from Trivandrum to Manavalakurichy, in Tamil Nadu, and some distance beyond almost up to Kanyakumari, along the coast and back. This was done because this region also has significant deposits of monazite, especially in the areas around Manavalakurichy. Data were recorded on magnetic tapes and later transferred onto chart paper. The details regarding the aerial surveys are given in Chapter 5.

The instrument developed for the aerial surveys was tested in some surveys at ground level where the instrument was carried in a jeep. Of these, only one survey gave good continuous data. The results from these are also presented in Chapter 5.

CHAPTER IV

4 . CONDUCTIVITY VARIATIONS AT THE SURFACE

4.1 INTRODUCTION

Polar conductivities at the surface are known to vary in a rather well defined manner at any given place. The variation pattern at any place is, in fact, often taken as a characteristic of the electrical climatology of the place (Israel, 1971, p 97). Therefore, in the present investigation, for studying the influence of environmental parameters on atmospheric electricity, the first requirement was to form an idea about the normal behaviour of conductivity in this region. As shown in this chapter, conductivity has a more or less similar pattern of variation at all the sites in most of the months when it was monitored (the few exceptions are also discussed and explained below). This is taken to indicate that this region has a uniform electrical climate.

In this chapter, the data from the ground stations are presented and discussed. The salient features of the variation pattern of conductivity in this region are brought out. The influence of the radioactive deposits on the conductivity values at Chavara, and the effect of meteorological variables on them, are demonstrated. Finally, the explanation that is currently accepted for the observed pattern of diurnal variation of polar conductivities is shown to be unsatisfactory, and some suggestions are given for an alternative explanation.

4.2 DIURNAL VARIATION OF POLAR CONDUCTIVITIES

At any station, polar conductivities show a certain regular pattern of variation. As explained in Chapter 1, two types of variation are usually seen - the single oscillation type and the double oscillation type. The variation patterns observed in this study mostly fall into the latter category. This, therefore can be taken to be typical of this region. Figure 4.1 shows the variation pattern of the monthly mean hourly values (λ_{m}), that is the average of the values for each hour of the day for a month, of positive and negative polar conductivities, respectively, for the months of May, June, July, August and September, 1991, for Kottarakara. The pattern can be seen to remain constant for all these months. This period covers one month prior to the onset of the south-west monsoon (May), three months (June, July and August) during which heavy monsoon rainfall is present, and one month (September) when the rainfall is generally low. The fact that the variation pattern has remained virtually constant over such varying weather conditions indicates that the pattern is characteristic to this region.

Figure 4.2 shows the diurnal variation of λ_{m}^{+} and λ_{m}^{-} for five months from June 1991 for Ambalapuzha. The variation pattern is the same as for Kottarakara. Chavara also shows a similar pattern in June, as discussed later. These three stations are widely separated, and are situated in different environments. The fact that all of them show the same type of variation indicates that the pattern is typical of this region. The results from Chavara will be discussed later.

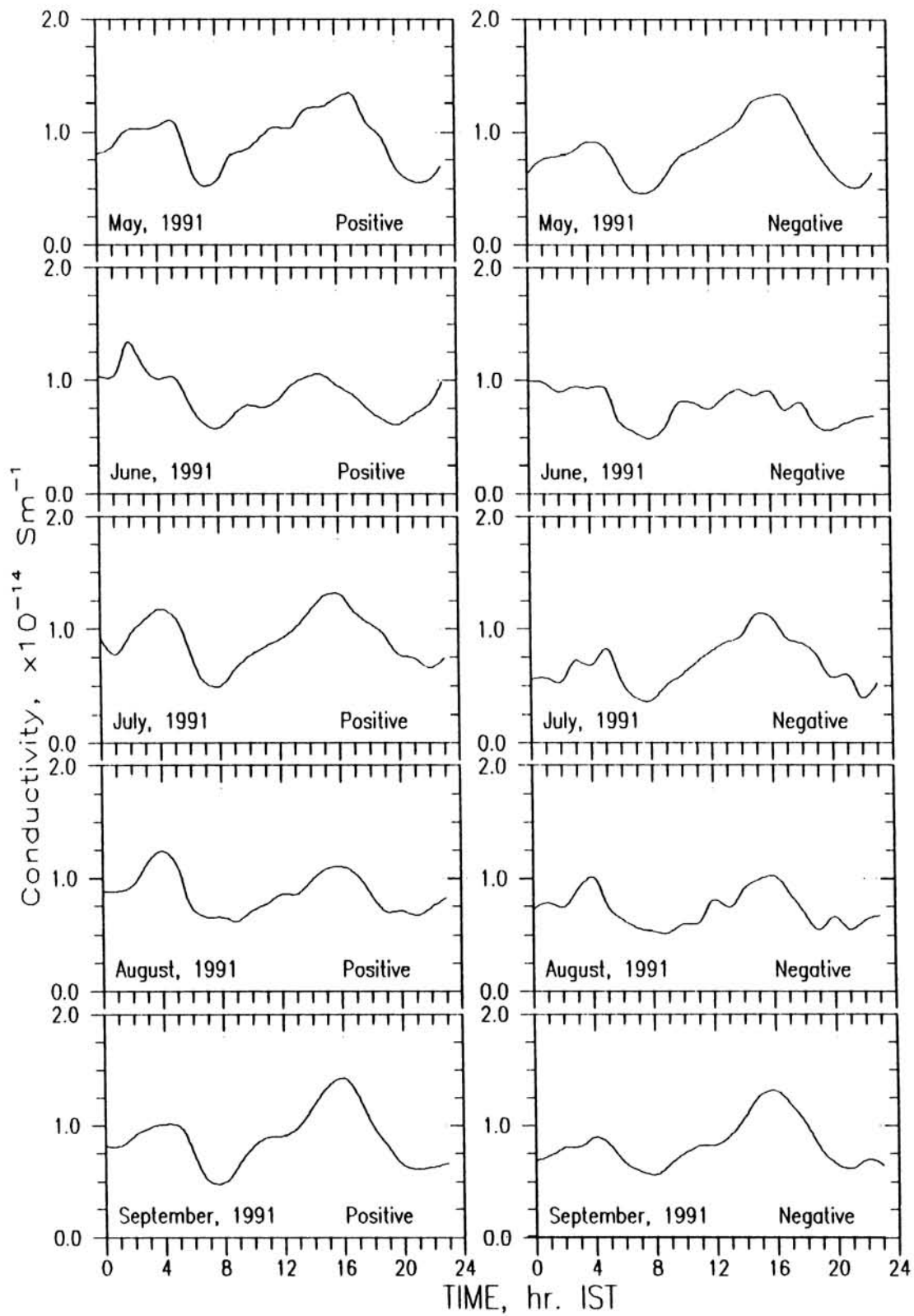


Figure 4.1 Diurnal variation of conductivity at Kottarakara for the months of May, June, July, August and September, 1991.

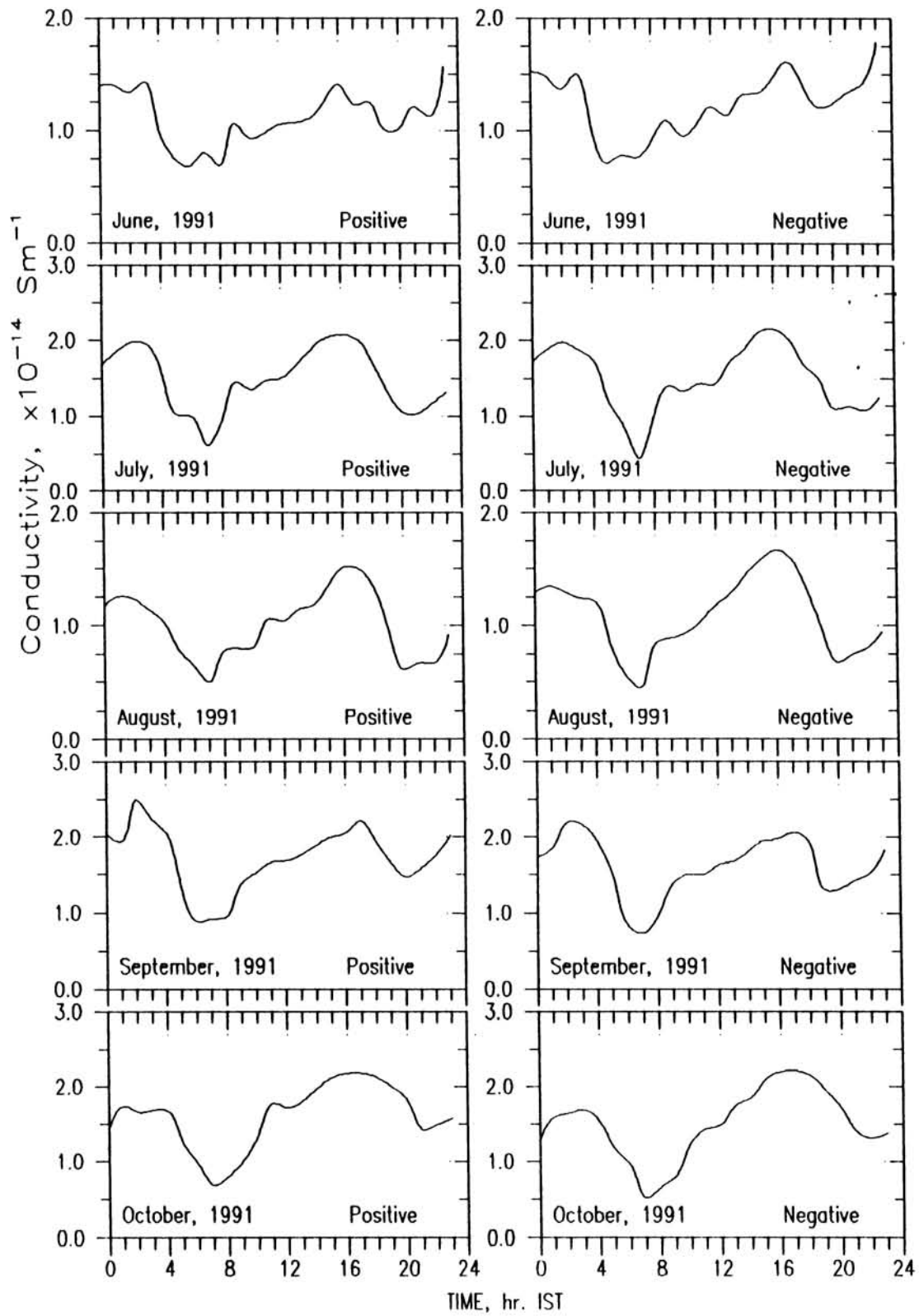


Figure 4.2 Diurnal variation of conductivity at Ambalapuzha for the months of June, July, August, September and October 1991.

The reason for this kind of diurnal variation is usually explained as given below. This explanation largely follows **Kamra** (1969, b) and **Retalis & Zervos** (1976). During night time, the atmosphere is relatively calm with low winds and hardly any convective motion. The radon exhaled from the soil therefore accumulates near the ground and causes an increase in ionization, thus increasing conductivity. Early in the morning, due to human activity and also due to the onset of convection resulting from increase in atmospheric temperature in the morning, aerosols are pushed into the atmosphere. This causes a conversion of small ions into large ions through attachment, thus virtually preventing them from contributing to conductivity, and an increase in the destruction of small ions through recombination with large ions of the opposite polarity. The onset of circulation also removes radon from near the ground to higher altitude regions. These contribute to the observed decrease in conductivity around 0600 to 0800 hrs in the morning.

Once the temperature increases and convection builds up, the aerosols are pumped higher into the atmosphere so that their concentration near the ground decreases. Consequently, a smaller fraction of the small ions only is lost due to attachment to aerosols, and the conductivity increases. Convection becomes maximum in the afternoon, thus giving rise to the maximum in conductivity around 1600 to 1700 hrs. In the evening, with decreasing ground temperatures, the aerosols that had been pushed to higher altitudes begin to settle down and a greater fraction of small ions are lost through attachment. Conductivity therefore again decreases and reaches a minimum around 2000 to 2300 hrs. Finally, after nightfall, the aerosols settle down, and the conductivity gets back to its normal night time high values. The

concentration of small ions is known to be smaller for higher aerosol concentrations (for instance, Mani & Huddar, 1975). Retalis (1983) found that the large ion concentration has a double oscillation type of diurnal variation. The double oscillation type of behaviour of polar conductivities is thus ascribed to the conversion of small ions into large ions by attachment to aerosols. This hypothesis is more closely examined at the end of this chapter, and some suggestions are made based on the observations during the present investigation and reported measurements from elsewhere.

4.3 EFFECT OF SURFACE RADIOACTIVITY ON CONDUCTIVITIES

Ionization near the earth's surface is mainly due to nuclear radiations from radioactive species in the air and in the soil. The former are released into the air from the soil where they are produced by radioactivity. In a region where the soil contains high concentrations of radioactive substances, therefore, the conductivity of air should be correspondingly higher. In the present study, one of the stations where conductivity was monitored, namely Chavara, has a high concentration of the radioactive mineral monazite. The conductivity at this station is therefore much higher than that at the other stations. The monthly mean values of positive and negative polar conductivities at the three stations are given in Table 4.1. The values for Chavara are much higher than those for the other two stations. In June, for instance, the positive conductivity at Chavara is about 6 times higher than that at Ambalapuzha. In May, it is about 11 times that at Kottarakara. The observed conductivities at Ambalapuzha and Kottarakara are comparable, although the values for Kottarakara are slightly lower. It has to be

Month	Chavara		Ambipzha		Kttrkra	
	+ve	-ve	+ve	-ve	+ve	-ve
Mar	8.59	8.56				
Apr	12.06	10.09				
May	10.51	9.28			0.91	0.88
Jun	7.09	7.23	1.13	1.26	0.88	0.81
Jul			1.55	1.58	0.93	0.81
Aug			1.07	1.09	0.87	0.73
Sep			1.88	1.61	0.88	0.82
Oct			1.66	1.55		

Table 4.1. Monthly mean values of conductivity at the three stations. remembered that the measurements at Kottarakara were made at a higher altitude from the ground than at Ambalapuzha, and that the site was located near a town, so that the values would be lower. The ratio of Chavara and Kottarakara values is therefore higher.

In order to test the assumption that the high values at Chavara are due to radioactivity, spot measurements of the γ -radiation level were taken at Chavara, Kottarakara and Ambalapuzha using a portable scintillometer. At the last two places, the levels were too low for reading clearly. However, it was found that the ratio between the levels at Chavara and the other places was at least 40. This is in broad agreement with the observed conductivities, as discussed below. Conductivity, λ^{\dagger} , of air due to ions of one polarity alone is the product of the concentration, n^{\dagger} , and mobility, μ^{\dagger} , of that polarity of ions and the charge on the ion. Since virtually all the small ions in the

atmosphere are singly charged, the conductivity can be written as $\lambda^{\pm} = n^{\pm} e \mu^{\pm}$, where e is the elementary charge. The ion density, in the absence of aerosols, is given by the equation $n^{\pm} = (q / \alpha)^{\frac{1}{2}}$, which is the same as equation 1.3. Assuming that the recombination coefficient, α , is the same at all the above places, then ion density, and hence conductivity, should be proportional to the square root of ion pair production rate, q . The fact that the γ - radiation level at Chavara was about 40 times that at the other two sites would indicate that the ion pair production rate there also would be correspondingly higher. This is in good agreement with the observed ratio in conductivities. This shows that the measured conductivities are in broad agreement with the radioactivity levels.

An interesting feature is seen in the behaviour of the monthly mean values, and of the percentage variation of conductivity values over the mean, at Chavara. The monthly mean positive polar conductivity, λ_{pm}^{+} , ie. the average of the daily mean values over a month, is the highest for April, followed by May, March and June in that order. The variation in λ_{pm}^{-} is also similar. The percentage variance of the hourly means, that is the variance expressed as a percentage of the mean, of λ_{h}^{+} and λ_{h}^{-} also follow a similar pattern. This could be a reflection of the seasonal variation of the exhalation rate of radon, as mentioned earlier, coupled with the effect of meteorological parameters. The mean maximum temperatures for these months recorded at India Meteorological Department's observatory at a similar coastal station (Alleppey) about 60 km north of Chavara are the highest in April, followed by March, May and June. The monthly mean temperatures, the monthly mean polar conductivities and the percentage variances of the monthly mean hourly

values are presented in Table 4.2. Except for the monsoon month of June, the other three months show a linear relationship between the mean maximum temperature and the percentage variance of polar conductivities. The percentage variances are plotted against temperature in Figure 4.3. Another point that may be noted from the table and the figure is that the variability in negative polar conductivity is higher than that of positive. The rate of change with temperature also

Month	Mean max Temp.	Conductivity		% Variance	
		+ve	-ve	+ve	-ve
March	33.71	8.59	8.56	47.1	61.1
April	33.83	12.06	10.09	61.9	86.1
May	33.38	10.51	9.28	21.9	25.5
June	29.62	7.09	7.23	17.5	16.0

Table 4.2 Monthly mean maximum temperatures (in °C) at Alleppey; monthly mean conductivity (in 10^{-14} Sm^{-1}) and percentage variances of monthly mean hourly values of polar conductivities at Chavara.

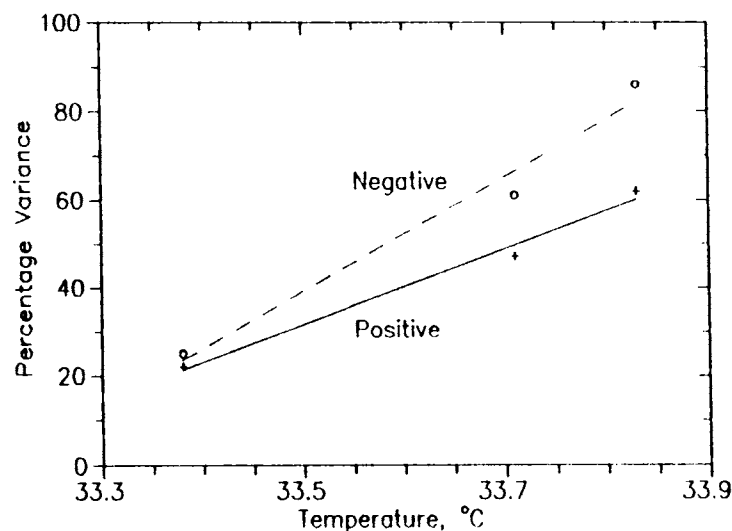


Figure 4.3 Percentage variances of the monthly mean hourly values of polar conductivities at Chavara plotted against monthly mean temperatures for Alleppey.

appears to be higher for negative values. This is probably due to the influence of aerosols. Since negative ions have a larger attachment coefficient to aerosols, changes in aerosol concentration can affect them more than positive ions.

In spite of the limited extent of data, the observed relationship could be real. This behaviour is possibly due to the dependence of radon exhalation rate on soil temperature, and that of atmospheric transport of the gas on turbulence, which again depends on temperature. Higher soil temperatures induce higher exhalation of radon from the soil so that night time values of conductivity would be higher. On the other hand, higher air temperatures during day time increase the transport of the gas from the vicinity of the surface, so that day time values of conductivity would be lower. Another factor that could contribute to this is the change in aerosol concentration. The variation over a day would therefore be larger for a warmer day. But this relationship is not seen when each day's data are taken. This is possibly because of the influence of other random factors like wind, rain, etc., which would average out when a monthly mean is taken. Also, this dependence may be seen only at a highly radioactive site like Chavara. Similar relationship is not seen for the Ambalapuzha data. There, the variance is found to be more or less the same for the months of July, September and October, but is somewhat lower for June and August.

4.4 DIURNAL VARIATION OF CONDUCTIVITY AT A RADIOACTIVE SITE

It was shown in Section 4.2 that the diurnal variation pattern of polar conductivities in the region where this study was carried out is of the double oscillation type. The results from Chavara were not presented there because they showed a behaviour that was different from that of the other stations. In this section, the diurnal variation patterns seen at Chavara during the four months from March to June are presented and an explanation is suggested for the observed departure from 'normal' behaviour.

The diurnal variation pattern of conductivity is generally understood to remain more or less the same in all seasons. Retalis and Zervos (1976) for example, present the diurnal variation patterns for Athens, Greece, for all the months, averaged for a period of 4 years. The difference between seasons is seen to be minimal. The pattern of variation seen at Pune (Dhanorkar, 1992) also remains constant throughout the year, with low values during day time and high values at night, although the amplitude of variation is much larger during the winter months. This is the case at Kottarakara and Ambalapuzha, at least for the five months for which data have been presented. Israel (1971) states that 'since the nature of the trend at the individual stations displays a low variability throughout the year, the diurnal variation of the conductivity at one station apparently constitutes a certain characteristic for the local "atmospheric electric climate".'(vol. 1, p 97). Chavara is one station for which this is not true. The most striking feature of the behaviour of polar conductivities at Chavara is

the significant difference in the pattern of diurnal variation between the pre-monsoon months and a monsoon month.

The pattern is more or less similar for the first three months for which data are presented in Figure 4.4. The values are high during night time. There is a rather sharp drop early in the morning reaching a minimum around 0700 hrs IST. The behaviour after that is slightly different for each month. In March the conductivities recover as rapidly as they fall, and reach a sharp peak around 0900 hrs. They remain low almost throughout the rest of the day, and recover only by nightfall. In April, the 9 O'clock peak is not as sharply defined as in March, and the profile almost resembles the trough of a sinusoidal variation. The daytime trough is less marked in the profile for May, and the variation in conductivity is rather small for this month, except for the sharp early morning drop.

The situation is quite different in June. For this month, the curve is similar to the diurnal variation pattern for the other two stations, and also those reported by **Retalis & Zervos (1976)**. Conductivity is large during night time. It starts decreasing around 0400 to 0500 hrs and falls rapidly to a minimum around 0700 hrs IST. A slow increase follows, leading to a broad maximum around 1400 to 1700 hrs. A secondary minimum around 2000 to 2100 hrs is also seen. The day time variation is almost the mirror image of what is seen in the other months.

A qualitative explanation for the observed behaviour may be as follows: The dominant winds at the site, a coastal one, will be the land

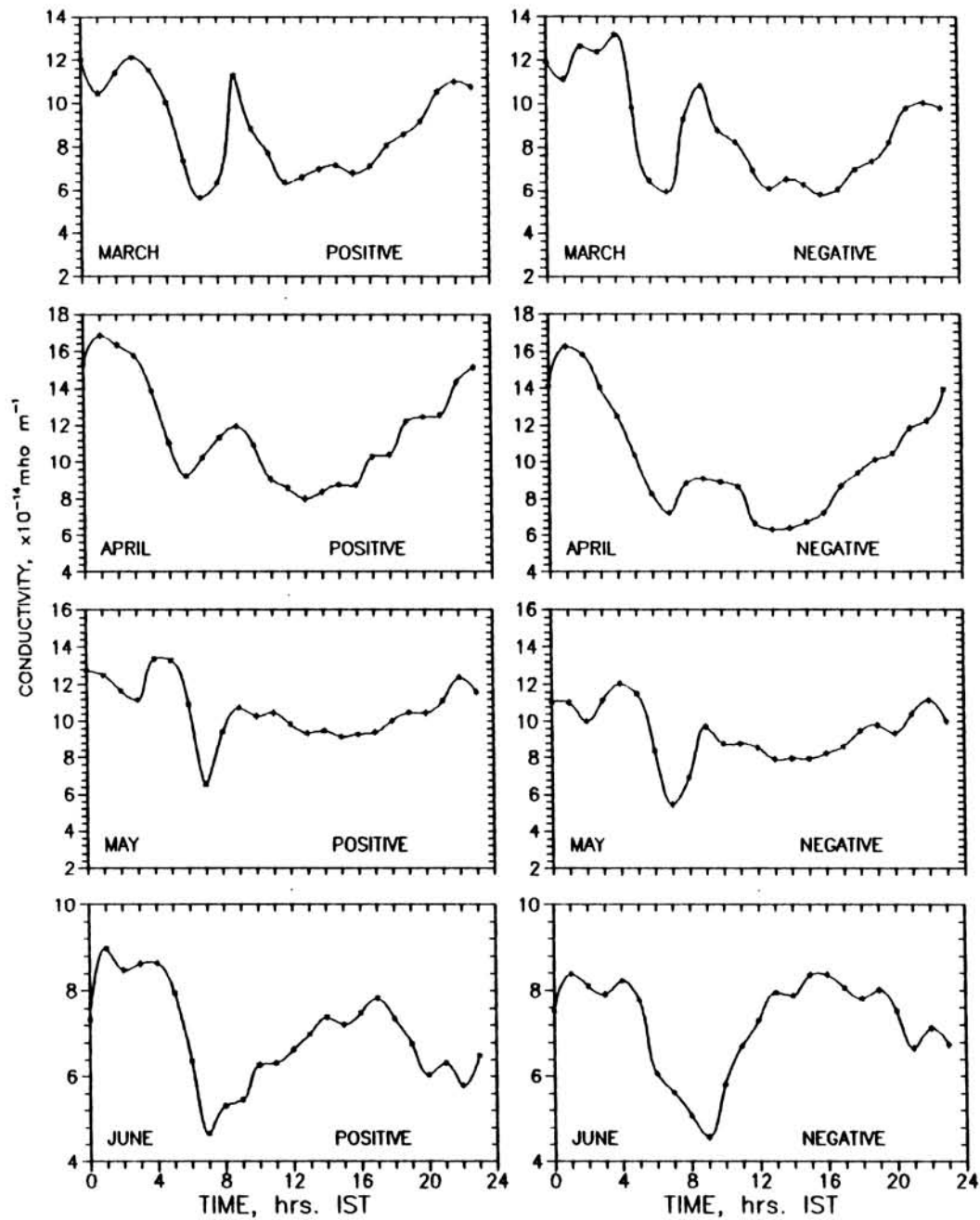


Figure 4.4 Monthly mean diurnal variation of polar conductivities at Chavara for the months of March, April, May and June, 1991.

and sea breezes during the months from March to May. The sea breeze would bring in fresh air from over the sea, and carry away part of the radon released from the soil near the instrument. This would explain the low values observed during day time in these months. The sharp drop in the morning is often attributed to the destruction of small ions through attachment to aerosols and recombination with large ions of opposite polarity. The rapid increase in conductivity after the minimum around 0700 hrs must be due to the relative calm between the subsidence of the land breeze and the onset of the sea breeze, when radon exhaled from the soil remains in the same locality.

At night, the sea breeze subsides about two hours after sunset, and the land breeze begins to pick up. Land breeze is generally a weaker phenomenon compared to sea breeze. Since the monazite deposit extends somewhat into the land region, the land breeze, unlike the sea breeze, would bring along with it the radon released from the soil. During night time generally the vertical circulation is also inhibited. All these factors contribute to an increase in the concentration of radon, and therefore in conductivity, near the surface.

In June, with the onset of the southwest monsoon, the local wind systems are overridden by the large scale winds of the monsoon. These winds blow almost continuously from the sea, so that variations over a day are relatively small. The diurnal profile in June therefore agrees with that observed at other sites in this region.

4.5 EFFECT OF RAINFALL ON CONDUCTIVITY

Conductivity can be influenced by several environmental and meteorological factors. One of them is rainfall. Most of the rainfall obtained in this state is from the two monsoons. During this period, rain is widespread and continuous. The clouds seen most often are stratus and stratocumulus. Most parts of the state also obtain a small amount of rainfall during one or two months before the onset of the south-west monsoon. These are isolated intermittent spells of rain due mostly to thunderstorms, and are often obtained in the evenings. The general weather conditions will therefore be different in this period from that during the monsoons. The effect on atmospheric electrical conductivity also could hence be expected to be different.

4.5.1 Effect of pre-monsoon rainfall

Polar conductivities were measured in the institute campus during the period from April to June 1993. Rainfall also was measured simultaneously using a self-recording rain gauge (SRRG). Comparison of these two sets of data shows an interesting relationship. The results for the pre-monsoon months are presented here.

The daily mean positive polar conductivity for the months of April and May is plotted against day number in Figure 4.5. This shows large fluctuations. The daily rainfall is also plotted in the same figure. It can be seen that conductivity starts decreasing after a rain. A large decrease is seen especially after a heavy rainfall of 29.4 mm, which fell within 15 minutes on 25.4.93. Conductivity tries to recover during days

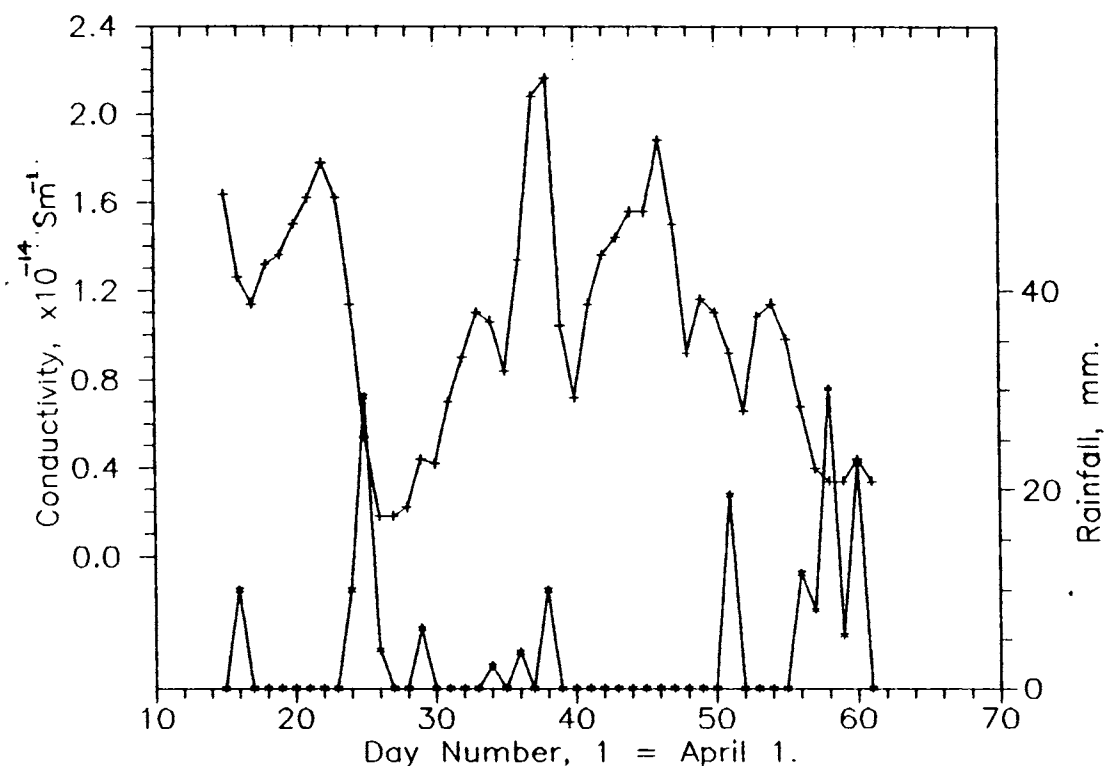


Figure 4.5 Daily mean positive polar conductivity at Trivandrum for April and May, 1993, and the daily rainfall.

of dry weather. The reduction in conductivity associated with rainfall may be due to the suppression of radon exhalation. Increased humidity could be a contributing factor. But in a hot month like April, the high humidity caused by the thundershower may not persist for long.

4.5.2 Effect of monsoon rainfall

The period over which conductivity data are available at the radioactive site (Chavara) and the inland site (Kottarakara) covers one month prior to the onset of the monsoon and one month after the onset. The behaviour of conductivity has been found to be different during these two periods. The change is striking at Chavara, where the positive polar conductivity showed a significant reduction after the onset of the monsoon. The average values of positive polar conductivity

for the months of May and June are 10.51, and 7.09, in units of 10^{-14} S m^{-1} (see Table 4.1). The variation in the daily means of positive polar conductivity during these two months is shown in the graph in Figure 4.6. The sharp reduction after June 1st is clearly seen. The decrease in conductivity is more or less uniform for the entire length of the day. The data obtained from Trivandrum also show similar reduction with the onset of the monsoon. The daily mean values for May and June for Trivandrum are presented in Figure 4.7. The rainfall during this period, measured alongside with an SRRG, is also shown in the figure.

The reduction is probably due to two reasons: one, the suppression of exhalation of thoron (Rn^{220}) gas from the soil by the rain water,

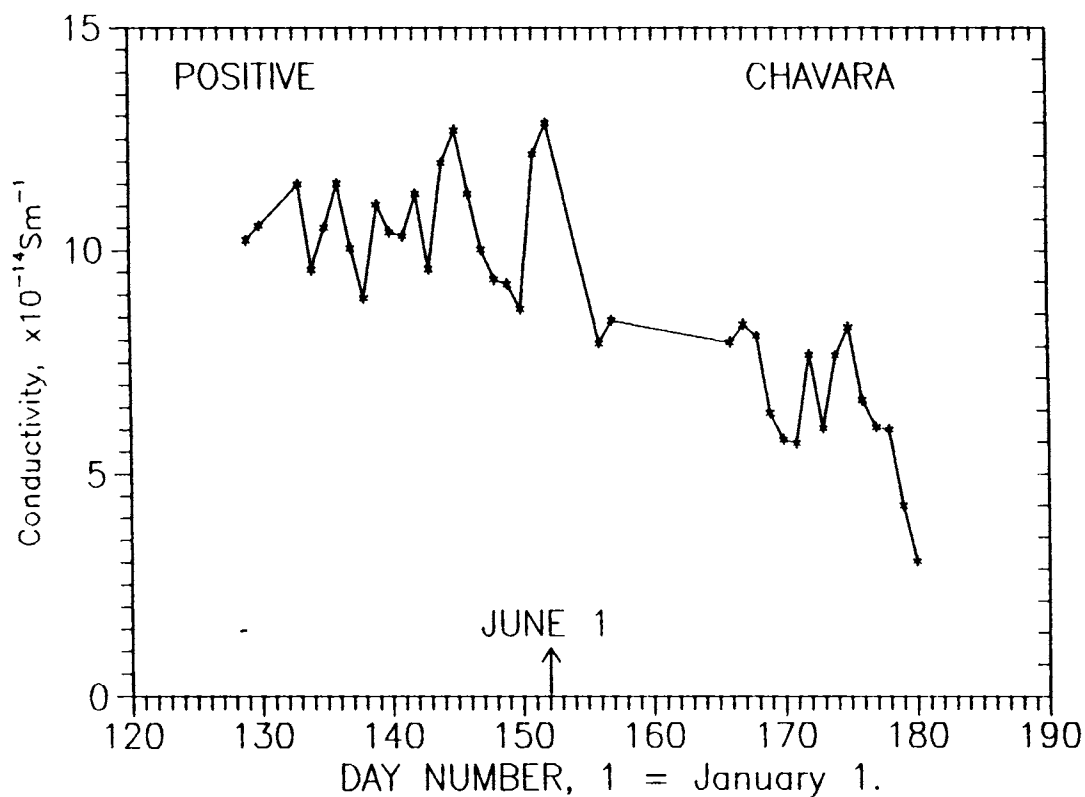


Figure 4.6 Variation of daily mean positive polar conductivity at Chavara during May and June, 1991.

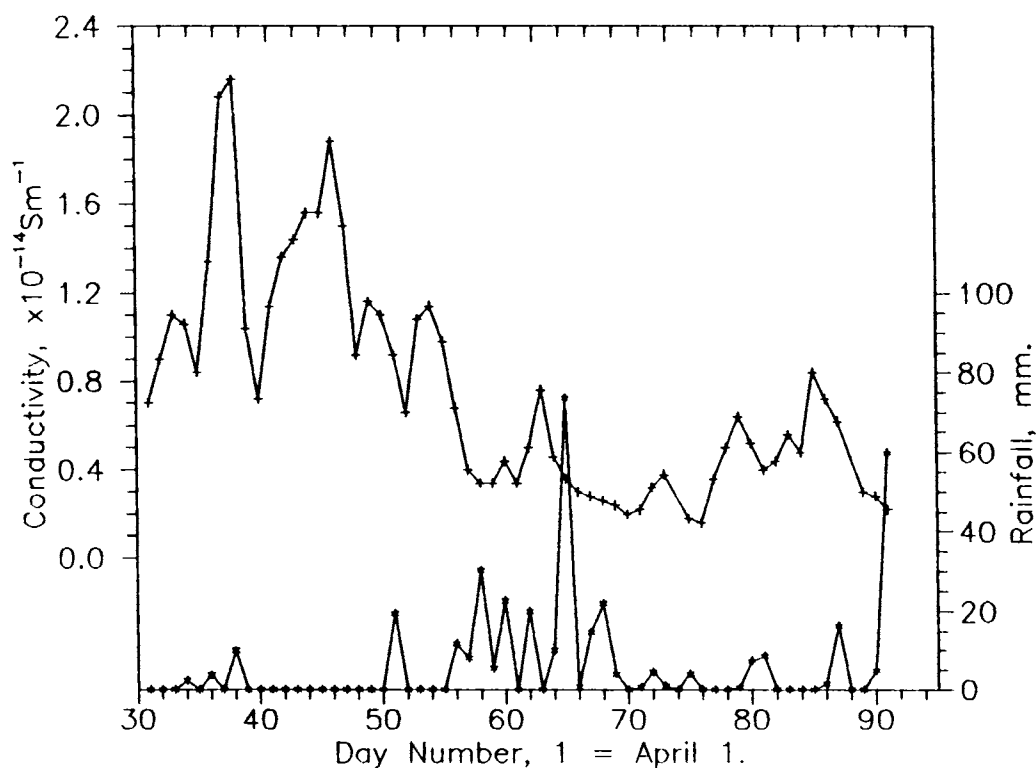


Figure 4.7 Variation of daily mean conductivity at Trivandrum during May and June, 1993. The daily rainfall is also shown.

and two, the prevalence of strong monsoon winds that blow almost throughout the day from the sea, as mentioned earlier. It is known that rain fall can cause large reductions in exhalation rate (Junge, 1963). Another possible factor could be the higher humidity leading to a larger fraction of ions becoming heavier through attachment. However, the data from Kottarakara does not show any significant reduction, the average values for the months of May and June 1991 being 0.91 and 0.88 ($\times 10^{-14} \text{ S m}^{-1}$). This could mean that the increase in humidity may not have contributed significantly to the reduction in conductivity. For the station at Ambalapuzha, data for the month of May are not available since the station was established only in June.

Another effect of the onset of monsoon is a change in the ratio of polar conductivities. The ratio of the monthly mean of the positive

polar conductivity to that of the negative polar conductivity was greater than unity for the pre-monsoon month of May at Chavara. In June, after the onset of monsoon it became less than unity. The ratio of the monthly mean hourly values of the polar conductivities shows a consistent decrease from May to June, but the ratio is not less than unity for every hour of the day. Figure 4.8 shows the monthly mean diurnal variation in the ratio of polar conductivities for the months of May and June for Chavara. The ratio for June for this station is seen to be always below unity. The reason for the observed increase in the ratio of polar conductivities could be the so-called *Lenard effect*, the ejection of negative charges when rain drops hit the ground and break up. A second possible reason is the reversal of the sign of the space

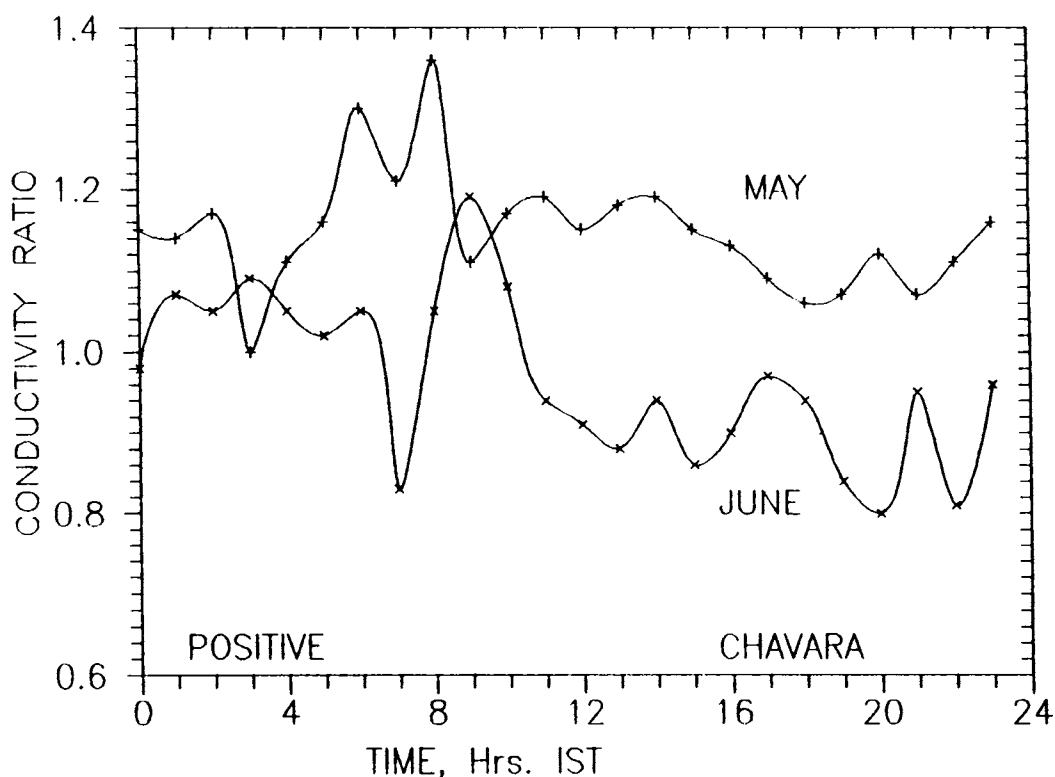


Figure 4.8 Monthly mean diurnal variation in the ratio of polar conductivities at Chavara for May and June, 1991.

charge near the ground during periods when electrically charged clouds are present overhead. Large negative potential gradients have been observed under monsoon clouds (Kamra & Sathe, 1983).

4.6 DIFFERENCE BETWEEN COASTAL AND INLAND SITES

The behaviour of polar conductivities may be expected to be different at a coastal site from that at an inland site. Several factors may contribute to this difference. The weather conditions at the coast is different from inland. Apart from the moderating influence of the sea on temperature, the higher humidity and the effect of sea and land breezes are also important. Another factor that is important is the space charge generated by surf (Muir, 1977). The breaking sea waves are known to release positive space charge into the atmosphere. In the present study, however, striking differences have not been observed between the behaviour of polar conductivities at Ambalapuzha and Kottarakara.

The polar conductivities at Ambalapuzha are slightly higher than those obtained at Kottarakara. One of the reasons for this difference is possibly the fact that the measurements at Kottarakara were made at a higher altitude from the ground. However, the influence of marine air is also one possible reason since conductivities are known to be slightly higher over the sea compared to the average values over land. An interesting observation is that the amplitude of the monthly mean diurnal variation of polar conductivities is the maximum at Ambalapuzha. This appears to be a genuine effect of the proximity to the sea. In marine air, the amplitude is small (Israel, 1971, p 97). But at a coastal

station like Ambalapuzha, where the influence of marine and continental air may be felt alternately, this could lead to a larger amplitude of variation, compared to an inland site where the effect of marine air is not felt. The diurnal variation patterns at these two sites do not show any other difference. The effect of surf-generated space charge also is not seen at either Ambalapuzha or Chavara. This could be because the sea is rather shallow with a small slope at both these places, as along much of the Kerala coast.

4.7 DIURNAL VARIATION OF CONDUCTIVITY - TOWARDS AN ALTERNATIVE EXPLANATION

4.7.1 Need for an alternative explanation

As described earlier, the diurnal variation of conductivity shows a double oscillation pattern in this region, except at Chavara in the pre-monsoon months. The generally accepted explanation for this behaviour also was given in an earlier section. However, one of the intriguing features of the pattern is the sharp decrease seen in the morning, which is usually attributed to the destruction of small ions through attachment to aerosols and recombination with large ions of opposite polarity. As per the hypothesis, the variation seen in conductivity over the period of a day is mainly due to the variation in aerosol concentration. In the morning, the concentration of aerosols increases as the atmospheric temperature increases, and consequently conductivity decreases. Kamra (1969 a), for instance, found that there was rather good agreement between the time at which atmospheric temperature started increasing and the time at which the vertical

electric field started increasing. The variation during daytime is also attributed to the variation in aerosol concentration near the ground due to changes in the strength of the convective motion of air. **Retalis** (1983) found a double oscillation type of variation in the large ion concentration at Athens. This is in agreement with the observed conductivity variation. The explanation therefore appears to be well supported by observations.

A closer inspection, however, would reveal some limitations of this hypothesis. One drawback of this hypothesis is that some stations show a single oscillation type of diurnal variation. For instance, of the data from five stations shown by **Israel** (1971, p 98), two, namely, Watheroo and Davos, show single oscillation type of behaviour. If the above hypothesis is to be accepted, then one would expect all stations to show the double oscillation type of variation. Another difficulty is that the morning decrease often starts very early, around 0400 hrs. This is too early in the morning for either human activity or sunrise to affect conductivity. Also, in the present study, it is seen that the morning decrease is seen in all the months in all the stations. Even at Chavara, during the pre-monsoon months when the pattern is on the whole different from the normal pattern for this region, the early morning decrease is consistently seen. Moreover, in June, when continuous and heavy rainfall is present, the explanation for the decrease seen in the morning does not appear to be satisfactory. The phenomenon therefore appears to be independent of the season, weather, etc.

The diurnal variation patterns at Athens for the different months obtained by **Retalis & Zervos** (1976) are shown in Figure 4.9. Here

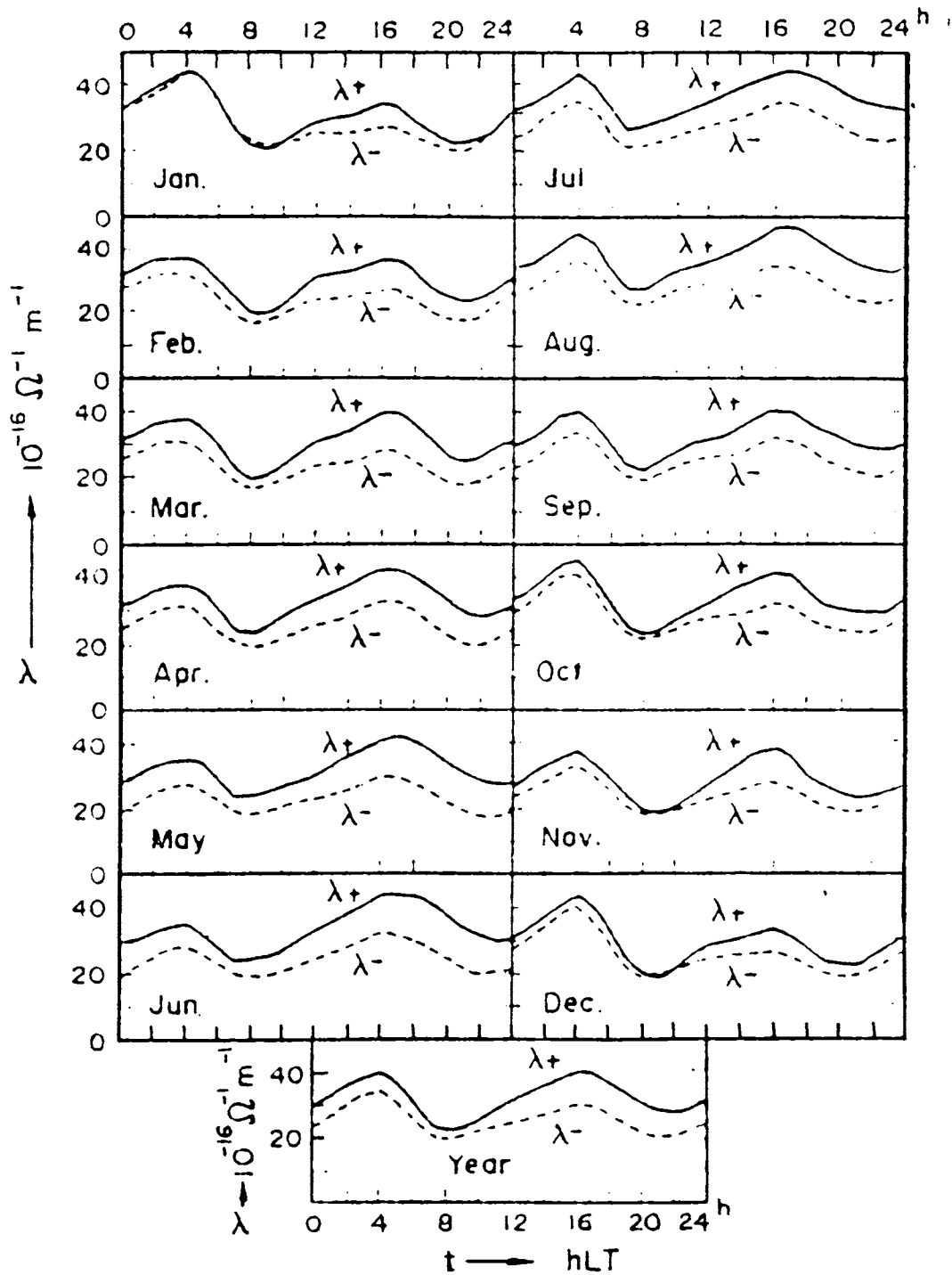


Figure 4.9 Diurnal variation of positive and negative polar conductivities at Athens for each month and for the year (from Retalis & Zervos, 1976).

the morning decrease is seen to be a regular phenomenon. They mention that the morning minimum and the afternoon maximum present a time shift according to the time of the year - the morning minimum occurring earlier in summer, and the afternoon maximum and the evening minimum occurring later in summer. However, they later mention that the morning minimum usually occurs between 0700 and 0900 hrs. The spread in time appears to be small for a station like Athens, where the time of sunrise varies by about four hours over a year. Considering all these factors, it appears that an alternative hypothesis is needed to completely explain the diurnal variation of conductivity.

4.7.2 Harmonic analysis of conductivity

In order to obtain a better understanding of the variation pattern of conductivity, the mean hourly values were subjected to harmonic analysis. In the case of Chavara, the first three months (ie. March, April and May) and June show different types of diurnal variation. Only June has a pattern that is similar to that of the other stations. The second harmonic of the mean hourly values for this month are shown in Figure 4.10. In the case of the other stations, the second harmonics shown are for the average data for all the months. In spite of the relatively small extent of the data, all the curves show a similar behaviour, the morning crest falling around 0400 hr. The phase of the second harmonics may be affected by random influences on conductivity. This influence will be limited if data for a longer period is studied.

Retalis & Zervos (1976) have presented the results of harmonic analysis of conductivity data for the period 1968-72, averaged for each

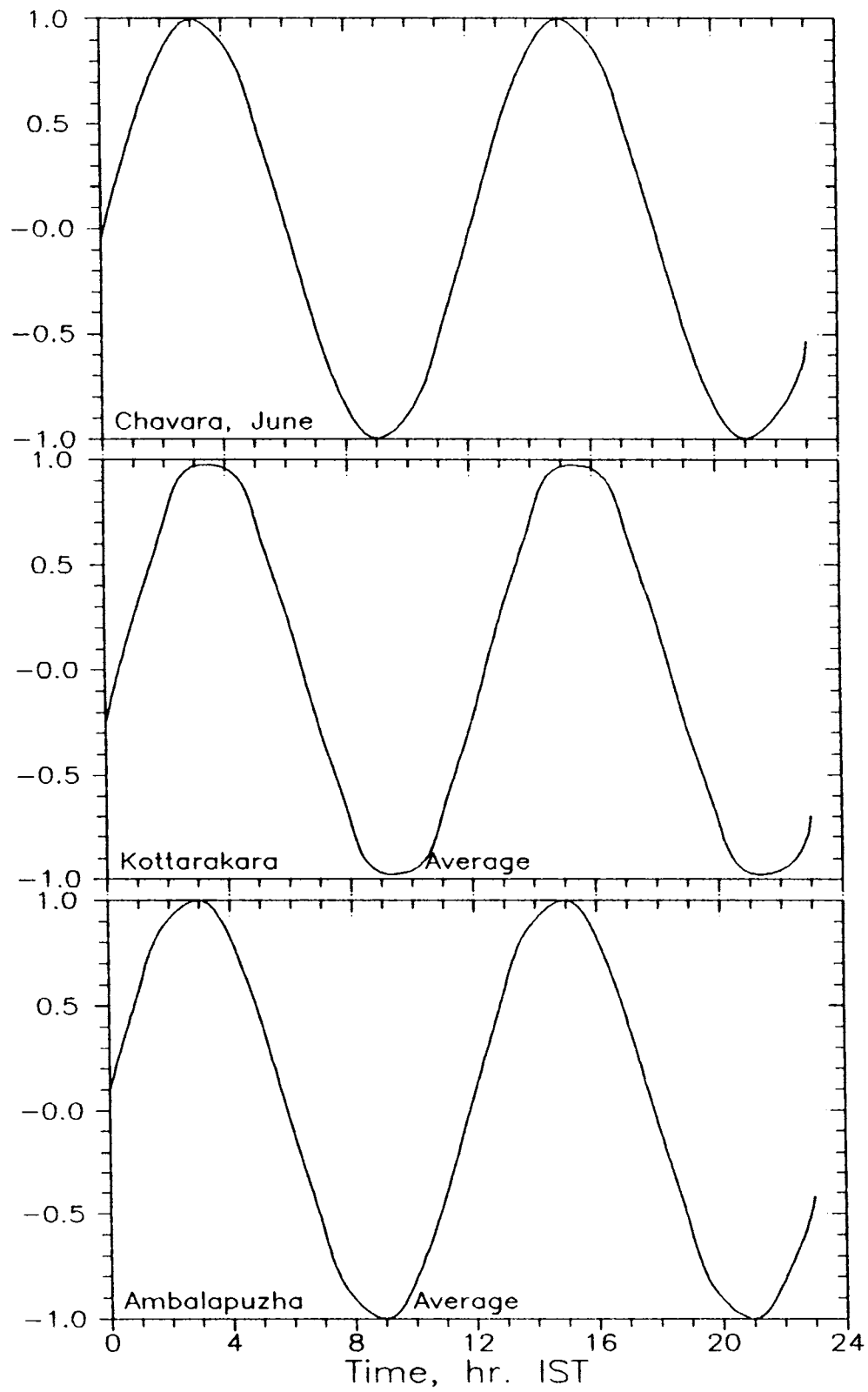


Figure 4.10 Second harmonics of the mean hourly values for the three stations.

month. The second harmonics of the data for all months are shown in Figure 4.11. Their behaviour is similar to that obtained in the present investigation. They show a maximum around 0400 hrs and a minimum around 1000 hrs. As mentioned earlier, the sunrise time at Athens varies widely over the year. If the observed diurnal variation pattern is mainly determined by sunrise and human activity, one would have expected some significant change from month to month. The phase angles of the second harmonic of positive conductivity given by them shows a variation from a high of 343° in February to a low of 315° in June for all weather, and from 313° in June to 342° in December for fine weather. This represents a variation of about ± 1 hour, which is the time resolution of their data, over the year.

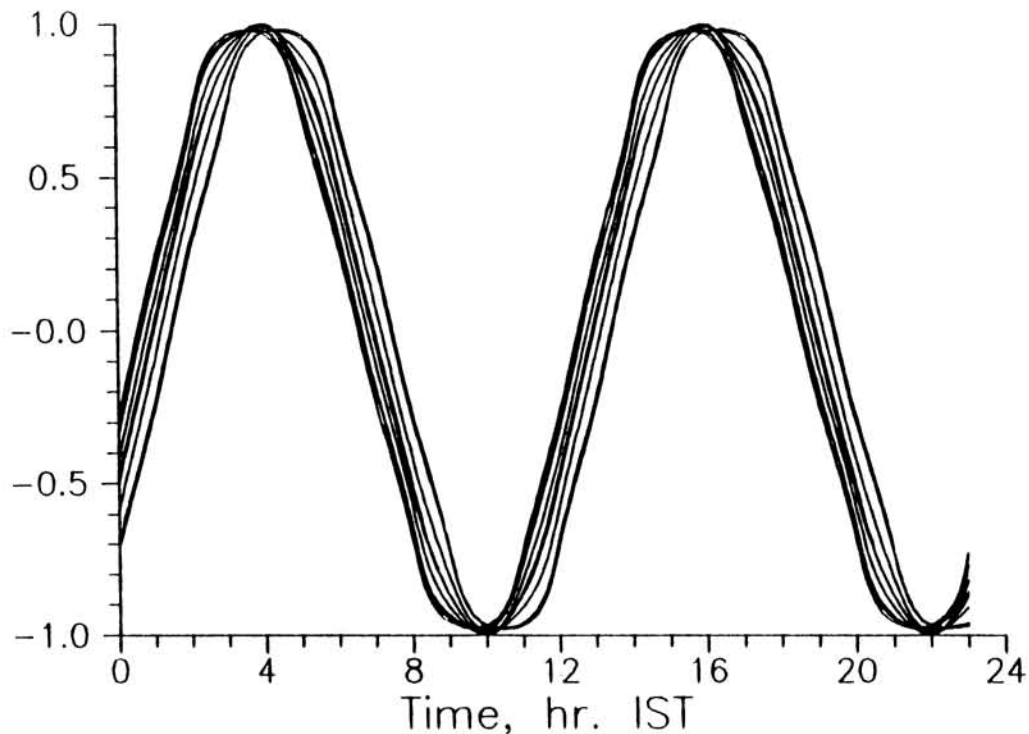


Figure 4.11 The second harmonics of the monthly mean diurnal variation of positive polar conductivity at Athens for every month of the year (computed using figures given in Retalis & Zervos, 1976).

4.7.3 Towards an alternative explanation

From the discussion given above, the limitations of the present explanation are clear. While the role of aerosols and the effect of sunrise cannot be totally ruled out, it appears to be necessary to look for additional mechanisms that may be influencing the behaviour of conductivity over a day. In this context, one factor that emerges as important is the relatively small variation in the time at which the morning maximum and minimum occur. As seen in the present study, the conductivity starts decreasing around 0400 hrs irrespective of the season, weather, location, etc. The explanation, therefore, has to be sought in some phenomenon that shows a constant behaviour in all seasons, and is independent of the weather conditions.

One such phenomenon is the semi-diurnal variation in atmospheric pressure that is seen predominantly in the tropics. This is a well known, but poorly understood phenomenon, which is independent of the seasons, weather conditions, and other effects. In the tropics, atmospheric pressure goes through a well defined semi-diurnal oscillation that has a minimum at 0400 hrs and a maximum at 1000 hrs. A mean profile is shown in Figure 4.12 (Nieuwolt, 1977). The amplitude of this variation is highest in the tropics, around 3 to 4 mb, and decreases towards higher latitudes. The reason for this behaviour has not been successfully explained. But we see that the conductivity variation is almost the inverse of that of pressure. In particular, the conductivity maximum around 0400 hr almost coincides with the pressure minimum. Figure 4.13 shows the second harmonic of a typical day's pressure variation at Trivandrum along with the second harmonic for Kottarakara.

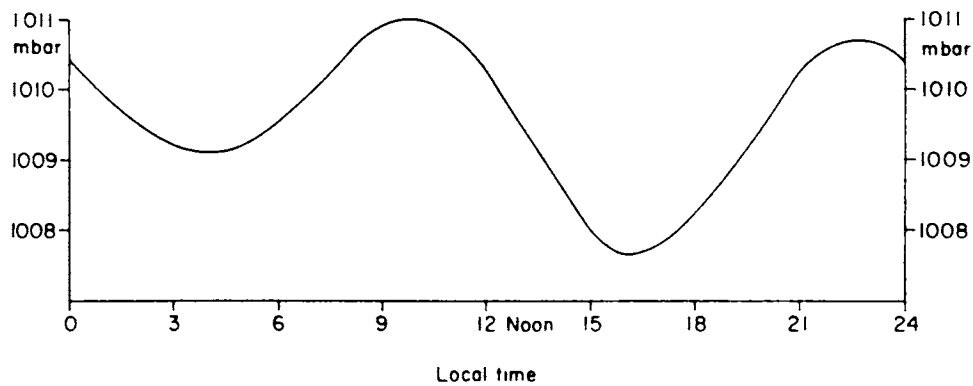


Figure 4.12 Diurnal behaviour of atmospheric pressure in the tropics (from Nieuwolt, 1977).

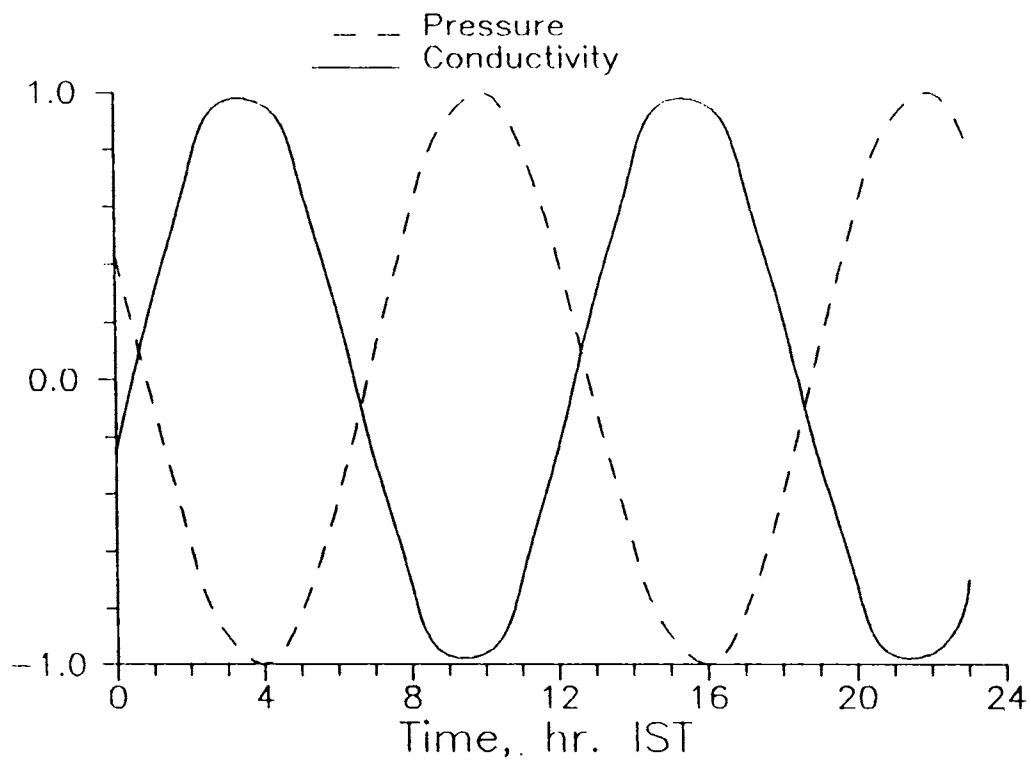


Figure 4.13 Second harmonic of a typical day's pressure variation at Trivandrum and that of the mean value for Kottarakara for all the months.

Atmospheric pressure can influence conductivity through its effect on ion mobility. The mobility, μ_0 , at STP and that at pressure p and temperature T are related by the expression $\mu = \mu_0 \cdot (p_0/p) \cdot (T/T_0)$. A decrease in pressure would, therefore result in an increase in conductivity. This, however, cannot explain the observed diurnal behaviour of conductivity, since the variation in pressure at the surface is very small, as mentioned earlier. The causal link, therefore, has to be found in some other process. One such possibility is the influence of atmospheric pressure on radon exhalation. An increase in atmospheric pressure would tend to reduce radon exhalation from the soil, and consequently reduce the ionization and conductivity. To what extent this may be effective in producing the observed variation depends on the extent of the influence of pressure on radon exhalation. The strong influence of isolated rainfall on conductivity, presented earlier, shows that reduction in radon exhalation can significantly affect conductivity.

It thus appears that the present explanation for the daily variation of conductivity may not be complete. Factors other than the variation in the concentration of aerosols may have to be taken into consideration. Aerosols do influence small ion concentration and therefore their effect on conductivity cannot be ignored. However, some aspects of the behaviour of conductivity over a day, especially the reduction that starts early in the morning, is not satisfactorily explained by the influence of aerosols alone. What is attempted here is only to present a new relationship that has been observed. Conductivity is most certainly controlled by a combination of factors, and a simplistic explanation based on one of them alone may miss some of the

important aspects. The difference in the phase of the second harmonic for the months of March, April and May at Chavara, for instance, must be due to the dominating influence of another factor, the wind, for instance. A complete understanding can emerge only after the question is closely examined in a comprehensive study.

CHAPTER V

5. SPACIAL VARIATION OF CONDUCTIVITY

5.1. INTRODUCTION

The measurement of atmospheric electrical conductivities at various altitudes above the surface is important for obtaining a clear understanding of the electrical processes in the atmosphere. Instruments carried on rockets, balloons and aircrafts are used for this purpose. Each carrier works well in a particular region of the atmosphere, and has its own advantages and disadvantages. Rockets are useful when measurements above fifty kilometres are desired. Balloon-borne instruments usually give good data from about two to three kilometres up to around 35 km. The region between around 35 km and about 50 km is difficult to access. One method is to use parachute-borne instruments deployed from rockets, although this has limitations. Most of the balloon-borne experiments carried out so far have not given good data below about 2 km. This is the region where aircraft-borne measurements are very useful. This also happens to be a very interesting region since the effects of radioactive minerals in the soil are felt up to about two to three kilometres. Of the three platforms mentioned above, aircraft also happens to be the cheapest. Moreover, instruments can be carried in an aircraft over virtually any terrain, whereas special facilities are required for launching rockets or high altitude balloons.

Aircraft-borne instruments have been used by **Gish & Wait** (1950), **Callahan et al.** (1951), **Kraakevik** (1958), **Paltridge** (1966), and others for measuring electrical polar conductivities in the troposphere and the stratosphere. **Gish & Wait** (1950) found that electrostatic charge accumulates on the aircraft and affects the measured values. They also found that if the charge on the aircraft was positive, then it affected only the positive conductivity values and not the negative ones, and *vice versa*. **Coroniti et al.** (1952) investigated this phenomenon using both laboratory experiments and aircraft flights. They concluded that the effect is negligible under fair weather conditions.

In this chapter, the aircraft payload used for the present investigation is described, and the results obtained are presented and discussed. Before the air-borne measurements were carried out, the instrument was tested by carrying out a few test surveys at ground level with the instrument mounted on a jeep. Of these, only one gave continuous data. The results of this measurement are also presented.

5.2 PAYLOAD DETAILS

The Gerdien condenser aircraft payload consists of a sensor, the electronic circuitry for generating the driving voltage and for processing the output signal from the sensor, the system for recording the signal, and the power supply units for all these. The aircraft used for the surveys was a Pushpak trainer aircraft of the Kerala Aviation Training Centre (KATC), Trivandrum. The payload was designed with the capabilities and limitations of the aircraft in mind. These sub-systems are discussed separately below.

5.2.1 Design of the sensor

The sensor developed for the present study, along with the clamp for mounting it, is shown in Figure 5.1. The driving electrode is 300 mm long and 60 mm in diameter. This is fixed inside a tube having a slightly larger diameter (65 mm) with two layers of Milnex insulating sheet in-between. The tube diameters are such that the driving electrode with the two layers of Milnex sheet over it fits tightly into the outer tube. The inner tube acts as the driving electrode and the outer one is electrically grounded and acts as a shield. The shield is slightly extended beyond the driving electrode at either end. The extensions act as guard rings and reduce the fringing of the applied field. The collector is a copper wire 0.6 mm in diameter. This is mounted at the axis of the tubes using two PTFE insulators at the ends. The PTFE pieces are held in place by 4 mm chromium plated mild steel bolts that run across the tube at either end. The driving electrode and the outer tube are fabricated in brass and chromium plated, and the collector wire is tin coated. The capacitance of the sensor is about 1.3 pF. The sensor was mounted with aircraft quality bolts and nuts onto a strut of the aircraft using a clamp. Neoprene rubber padding was provided between the clamp and the strut.

5.2.2 Design of the electronics

A block diagram of the aircraft payload is given in Figure 5.2. The electronic circuitry for the instrument consists of two parts - the signal conditioning circuits, and the fm modulator and associated circuits used for recording the data on tape.

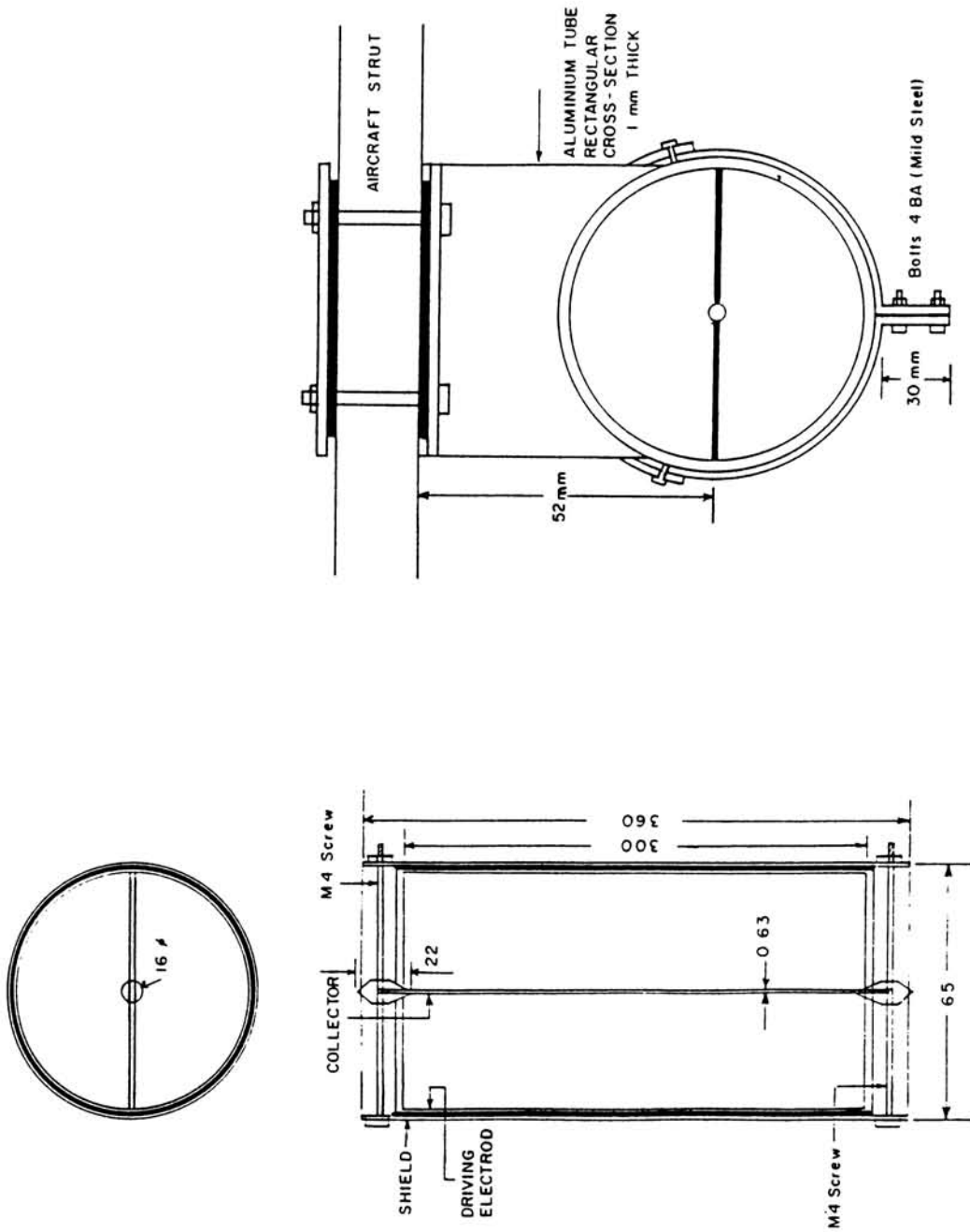


Figure 5.1 The sensor used for aircraft measurements, along with the clamp for mounting it on the aircraft.

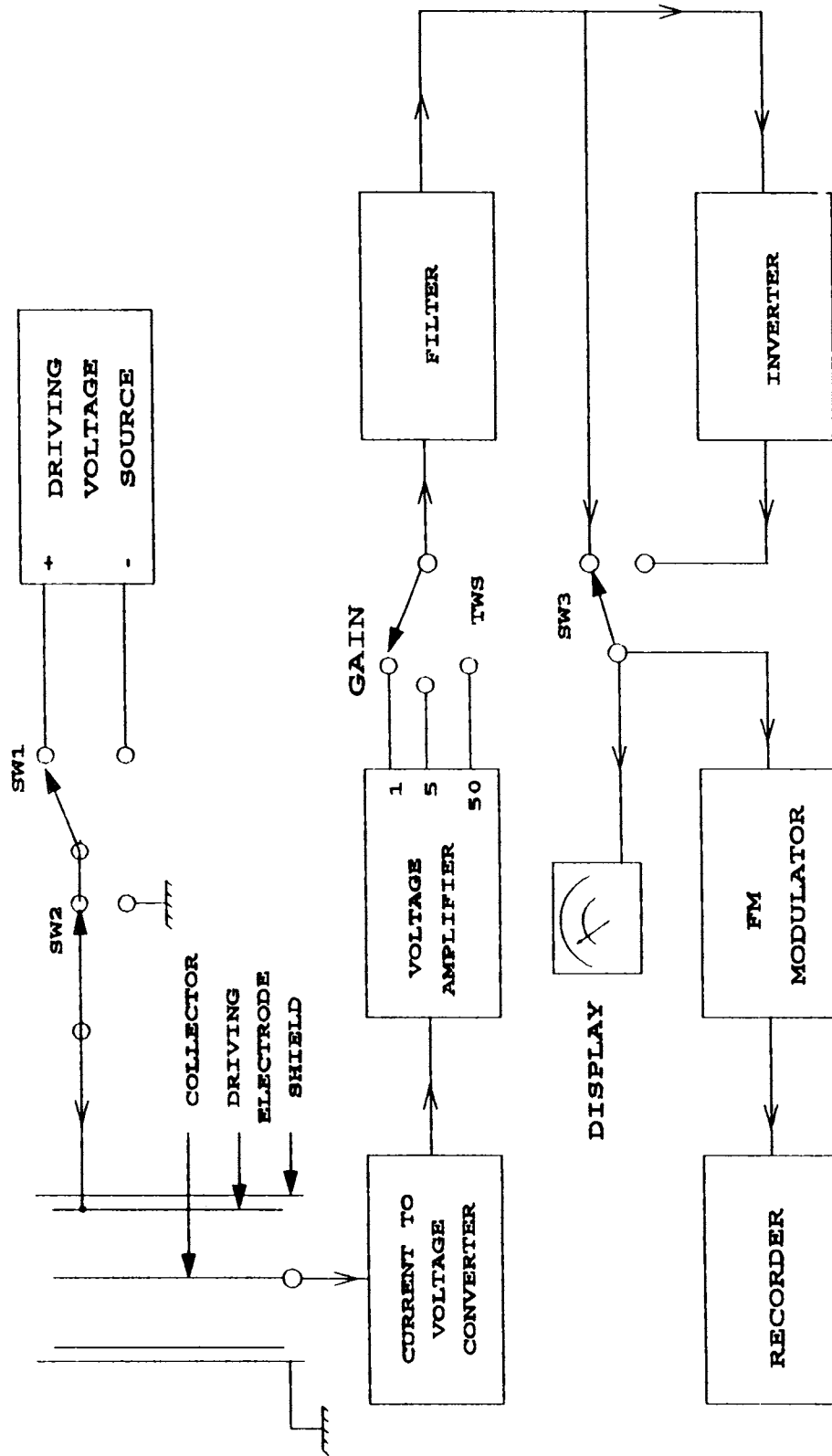
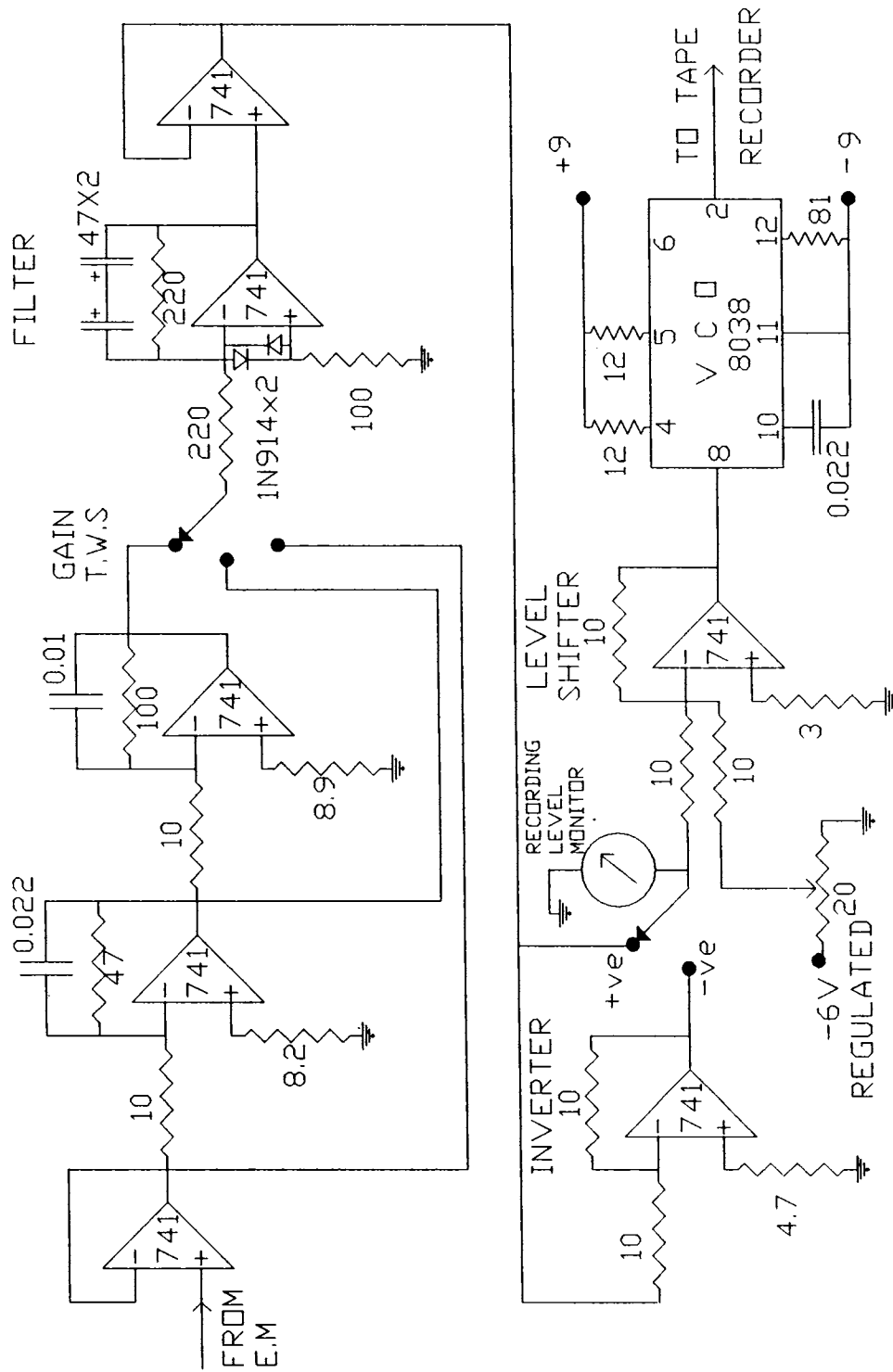


Figure 5.2 Block diagram of the measurement system for aerial survey.

The circuit diagram of the system is given in Figure 5.3. The saturation voltage of the sensor for an aircraft cruising speed of 80 kmph and for the type of ions normally encountered during the flight is about 800 volts. Therefore the driving voltage used was of the order of 200 volts. This was obtained from a bank of 9V dry batteries. Positive or negative driving voltage could be selected using a DPDT switch (SW1 in Figure 5.3). The reference level of the measurement system was obtained by grounding the driving electrode through the switch (SW2) at definite intervals. An alternative for the battery bank is a dc-dc converter run on batteries. In this case, care has to be taken to see that the inverter output is filtered properly since any ripple in the driving voltage would cause a large noise in the signal. Care has also to be taken to see that the inverter does not contribute electrical noise to the rest of the electronics.

The current range from the sensor for the conductivities normally expected in the region of measurement is from about 0.1 to 5 pA. The current was converted to voltage using a current to voltage converter (CVC) with a sensitivity of 0.1 V per pA, built around an Analog Devices AD515L operational amplifier. The output of the CVC was fed to a signal conditioner having three gain stages of x1, x5 and x10 respectively. Thus the total circuit had a sensitivity of 5 V per pA. This is sufficient for the kind of currents expected from the sensor. This part of the circuitry is essentially similar to the one used in the ground-based instrument. Output from all the three stages were available, and the appropriate one was selected for recording by the operator on board using a thumb-wheel switch (TWS). The inverter shown in Figure



RESISTOR VALUE
IN KILO OHMS.
CAPACITANCE VALUE
IN MICRO FARAD.

Figure 5.3 Circuit diagram of the electronic circuitry used in the aircraft payload.

5.3 was used to maintain positive the polarity of the signal at the input to the modulator.

The output from the signal conditioning circuits was fed to a positive input fm modulator built around an 8038 which gave frequency output in the range from about 300 Hz to about 2500 Hz. Whenever the driving voltage polarity or the gain stage was changed, the proper polarity signal for the modulator was provided using the inverter and the switch SW 3 shown in Figure 5.3. The modulated signal was recorded on good quality C90 cassettes during flight. In order to facilitate the selection of the proper gain stage during flight, the modulator input was monitored on an analog meter. This also gave an indication that the system was functioning properly up to that point.

Complete calibration of the system was done before and after each flight by giving known currents from a pico ampere source (Keithley Instruments) to the collector of the sensor and recording the output on the cassette used for the flight. The cassette was played back through an fm demodulator and the data transferred to paper chart after the flight. Calibration of the entire system, from the sensor to the demodulator and the paper chart recorder, was taken and it shows very good linearity. Typical calibration curves are shown in Figure 5.4.

The sensor was mounted onto a strut of the aircraft using a simple clamp. The clamp also had provision to holds the current to voltage converter inside it. This eliminated the problems that a long cable running from the sensor to the amplifier could create. The total weight of the sensor with the clamp is about 1.7 kg.

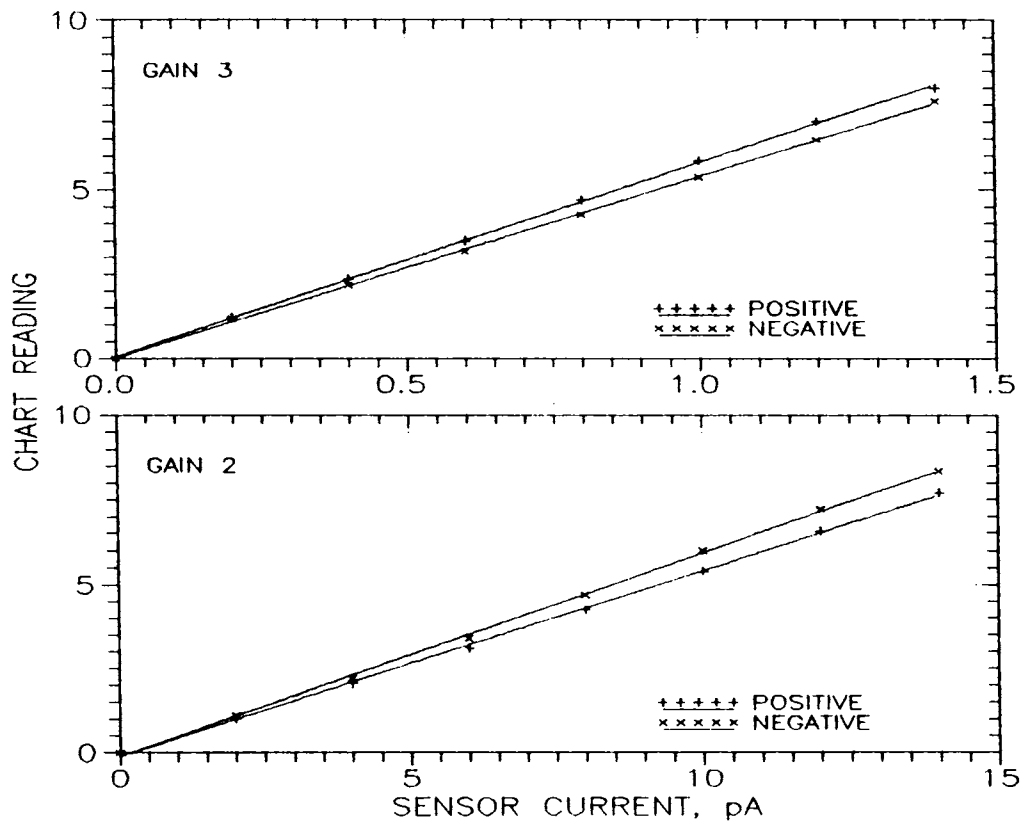


Figure 5.4 Calibration curves of the complete aerial survey system for the two gain stages which were used in the surveys.

5.3 GROUND SURVEYS

In order to test the instrument designed and fabricated for the aerial surveys, the sensor was mounted on a Maruti Gypsy, and a few surveys carried out. Due to the fact that these measurements were during the development of the instrument, data are available only over part of the distance covered, except in the case of a survey from Trivandrum to Manavalakkurichi. Some interesting results that have come out of these measurements are presented here.

Figure 5.5 gives the results from the survey from Trivandrum to Manavalakkurichi. In this survey, positive polar conductivity was measured during the onward journey and negative during the return journey. The vehicle maintained a more or less constant speed of about 60 kmph. At places where the vehicle had to slow down, the data have been rejected. The polar conductivities are large from around Karingal onwards up to the Kadayapatnam beach at Manavalakkurichy.

Another survey was conducted from Trivandrum up to and beyond Chavara. However, data were obtained only at intervals. This also

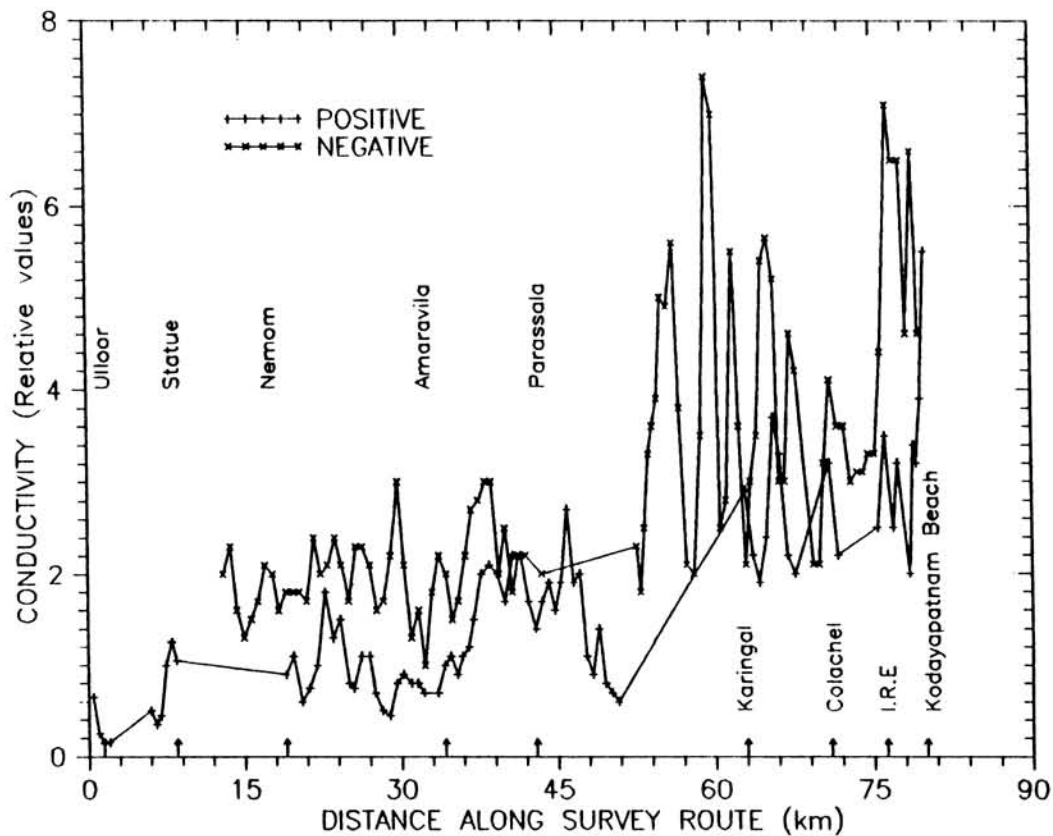


Figure 5.5 Polar conductivity data from jeep-borne survey between Trivandrum and Manavalakkurichy.

showed a peak at Chavara, falling off rapidly towards the north and the south.

In one test run along the MC Road from Trivandrum to Kottarakara, it was observed that conductivity values were high around a granite quarry near a place called Venjammoodu. Figure 5.6 shows the portion of the chart corresponding to the location. The high values are probably due to the release of nuclear radiations and radon from the freshly exposed faces of the rock. Radioactive nuclei present in the freshly exposed surfaces of the rock, including that of small particles of rock released into the air, would provide an abundant source of radiation. Also, since the permeability of the rock is low, radon produced by the decay of radioactive nuclei in the rock would be locked up inside. When the rock is broken, whatever radon remains is released, adding to the ionization in the air.

5.4 RESULTS OF AERIAL SURVEYS

In order to investigate the extent of the influence of radioactivity on electrical conductivities, three surveys were conducted. Aerial surveys in both north-south and east-west directions, covering the regions having radioactive deposits, including a short distance into the sea were done. Initially, a test flight was conducted which was useful for understanding the problems and intricacies involved in such experiments. Three more successful flights were carried out, which helped to validate the technique and to demonstrate its utility in atmospheric electrical investigations. The flights were from Trivandrum to Kanyakumari and back, Trivandrum to Alleppey and back, and

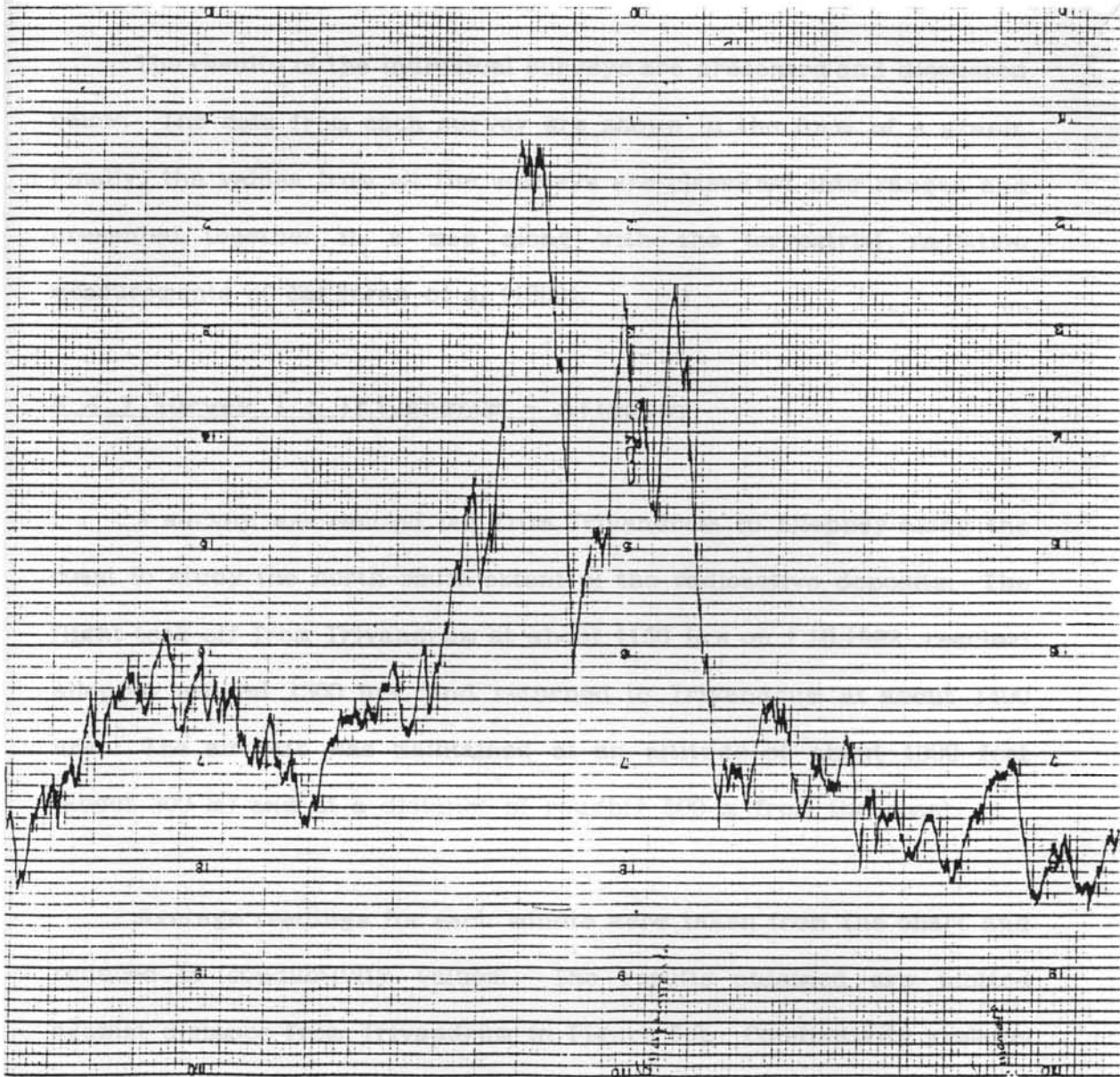


Figure 5.6 Portion of the chart showing enhancement in conductivity near a quarry.

Trivandrum to Kottarakara to Chavara and back. The flight paths of these surveys are shown in Figure 5.7.

The results of the individual surveys are presented and discussed below. The data from each survey are shown in the form of a graph. Finally, the values from all the surveys are classified into ranges and presented together in a map along with the terrestrial radiation measurements of **Sankaran *et al*** (1986).

5.4.1 Survey 1 : Trivandrum - Alleppey

A survey was carried out from Trivandrum to Alleppey along the coast to study the north-south extent of the radioactive deposits. The flight took off from Trivandrum at about 1150 hrs on 1.10.1992, reached Alleppey around 1300 hrs, and returned to Trivandrum at about 1400 hrs. The aircraft was maintained at an altitude of about 1000 feet (about 300 m) and at a distance of roughly 500 m from the coast.

Average readings for each minute were taken from the chart and reduced to conductivity values. The results obtained are plotted against distance from Trivandrum in Figure 5.8. Conductivity remains at about the same value up to a distance of about 45 km from Trivandrum. It is slightly higher there onwards up to about 10 km before Chavara. From here, conductivity increases rapidly, goes through a maximum at Chavara and then decreases. The region north of Chavara shows relatively lower conductivity compared to the southward portion. This is because the deposits of monazite sands are not found to the north of Chavara.

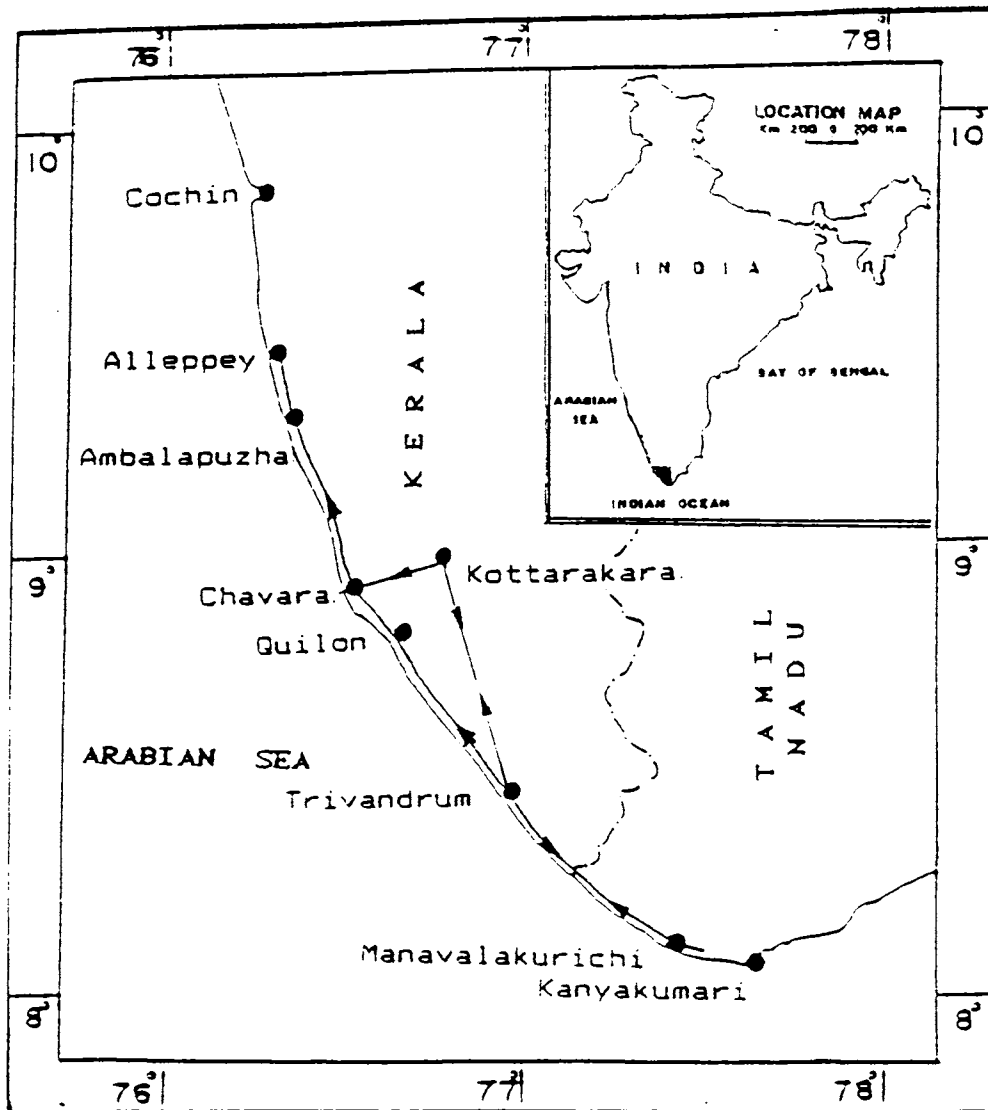


Figure 5.7 Map of the region showing the routes along which aerial surveys of polar conductivities were carried out. A location map of the region is given in the inset.

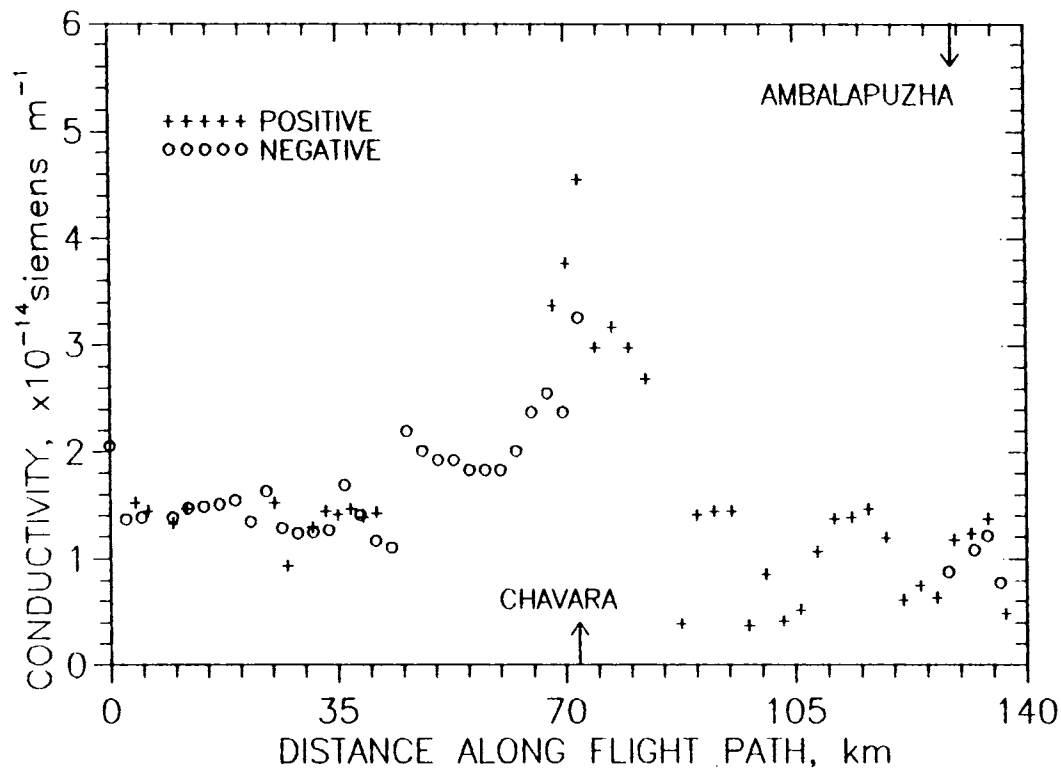


Figure 5.8 Conductivity variation along the coast from Trivandrum to Alleppey.

An interesting observation is the fluctuations seen between Chavara and Alleppey. The data show large fluctuations covering spatial distances from around one kilometre to several kilometres. A sample portion of the chart that shows these fluctuations is given in Figure 5.9. This can be caused by isolated convection cells that bring up air from near the ground which would have a much higher conductivity than the ambient air. These convection cells could be formed by the presence of large and small water bodies. The land regions between these water bodies would support convective motion whereas the water bodies would not. The region between Chavara and Alleppey has many water bodies, and rains a few days prior to the flight had created isolated water bodies in the coastal region.

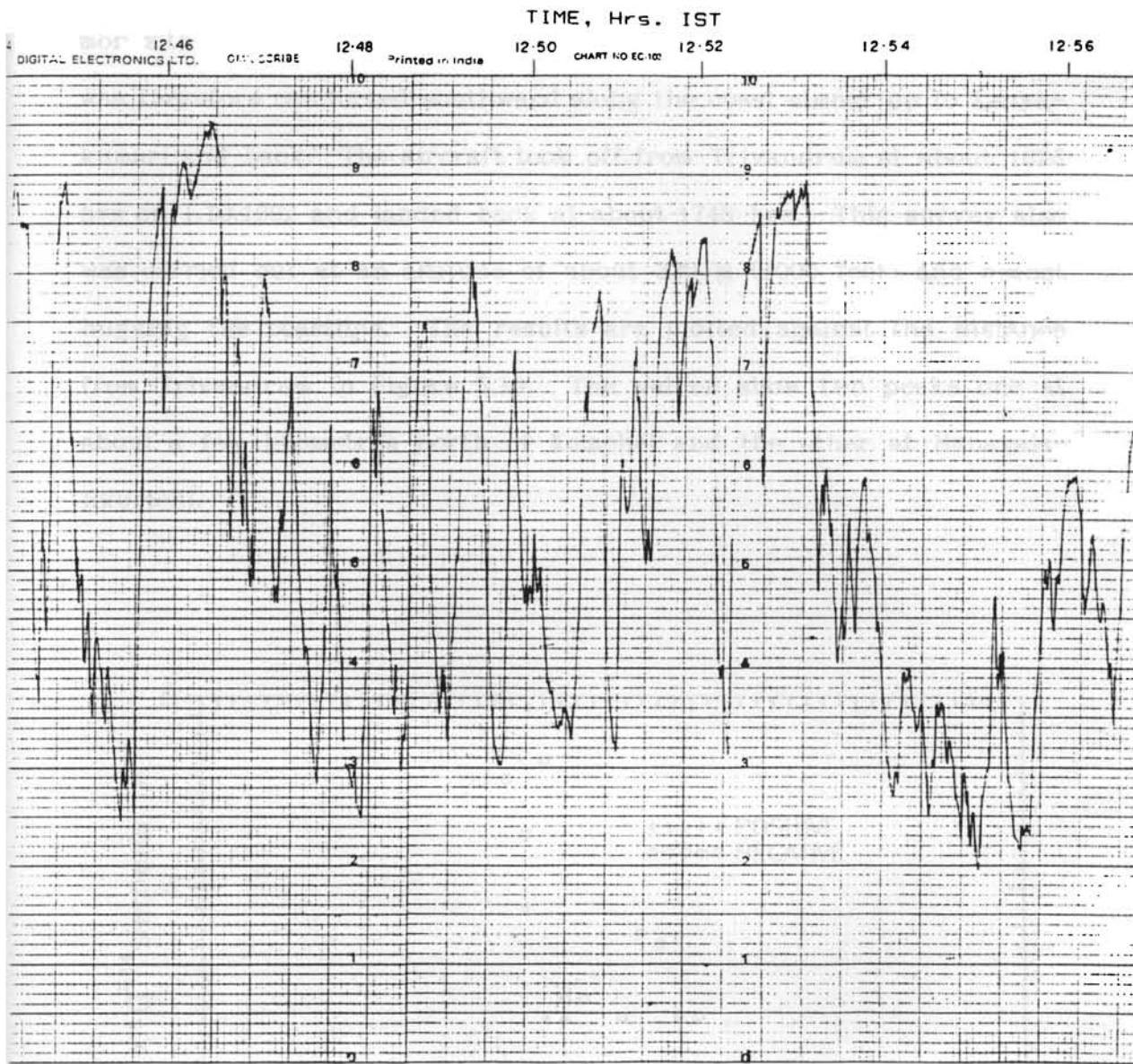


Figure 5.9 Sample portion of the chart from the survey between Trivandrum and Alleppey showing the large fluctuations.

5.3.2 Survey 2: Trivandrum - Kanyakumari

Apart from the Chavara region of Kerala State, large deposits of monazite are present around Manavalakkurichi in Tamil Nadu. A survey was therefore conducted southward along the coast almost up to Kanyakumari and back. The aircraft took off from Trivandrum at about 1625 hrs on 1.10.1992 and landed back at about 1745 hrs. This survey also was carried out at an altitude of about 330 m (1000 feet) and almost hugging the coastline. The results are plotted against the distance from Trivandrum in Figure 5.10. The values show two peaks one at about a few kilometres north of Kolachel and the other at Manavala-

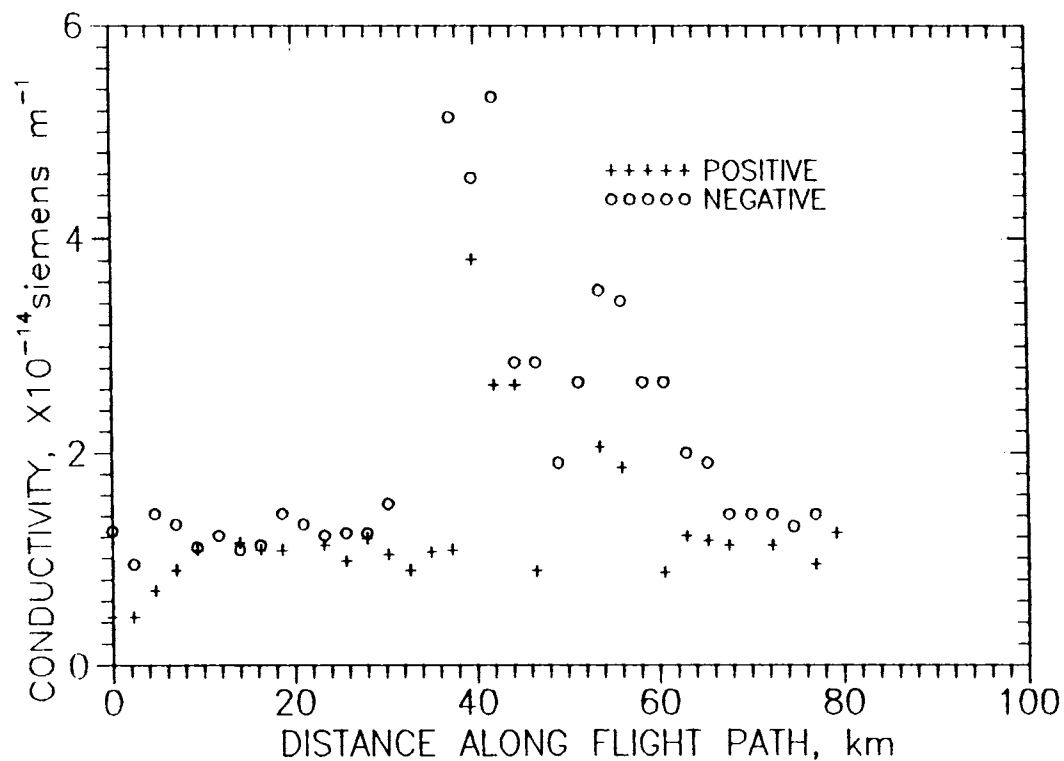


Figure 5.10 Conductivity values obtained in the survey between Trivandrum and Kanyakumari.

5.3.3 Survey 3: Trivandrum - Kottarakara - Chavara

To study the east-west extent of the effect of the radioactive deposits on the atmospheric electrical conductivity the third survey was conducted. This survey started from Trivandrum, went up to Kottarakara, and then turned west, flew over Chavara and a short distance over the sea, and then returned along the same route. In this survey the aircraft was maintained at about 2000 feet (650 m). The flight took off around 1340 hrs on 30.9.1992, and landed back at about 1515 hrs.

Mean values for each minute of the flight are shown in Figure 5.11. The data show the conductivity decreasing towards Kottarakara,

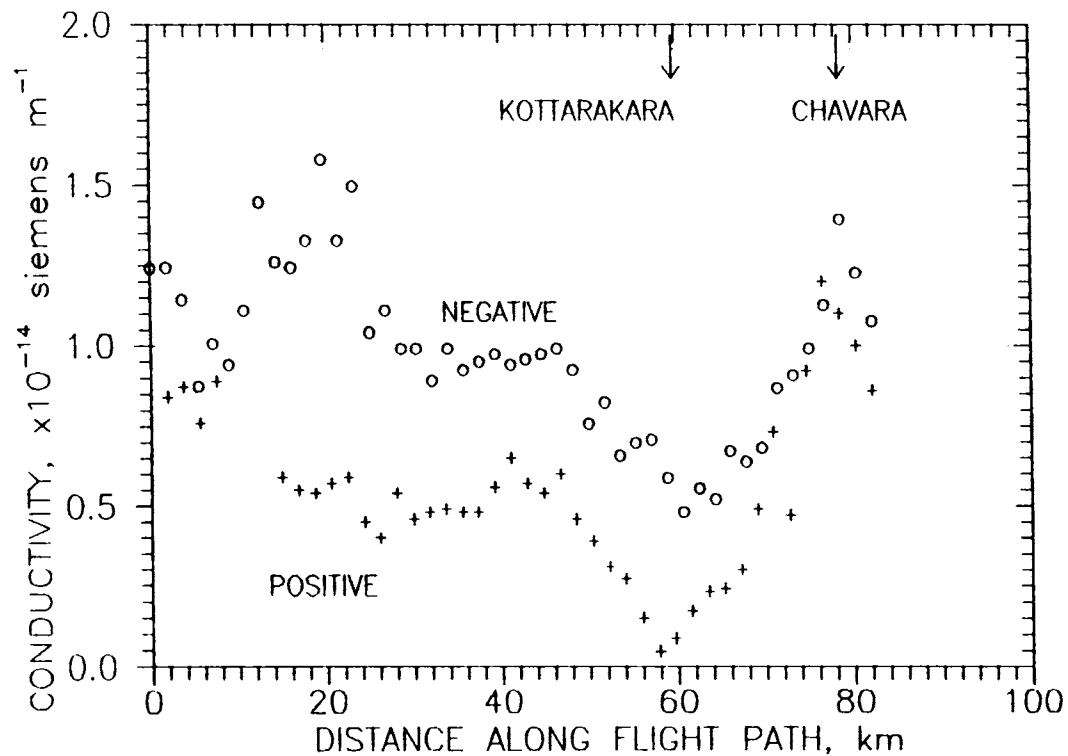


Figure 5.11 Conductivity data obtained in the survey between Trivandrum and Chavara via Kottarakara.

where it reaches a minimum, and then increasing up to Chavara. Monazite is present all along the coastal region and a few kilometres inland. Near and around Kottarakara the radioactivity is low. This is reflected in the conductivity being low over Kottarakara.

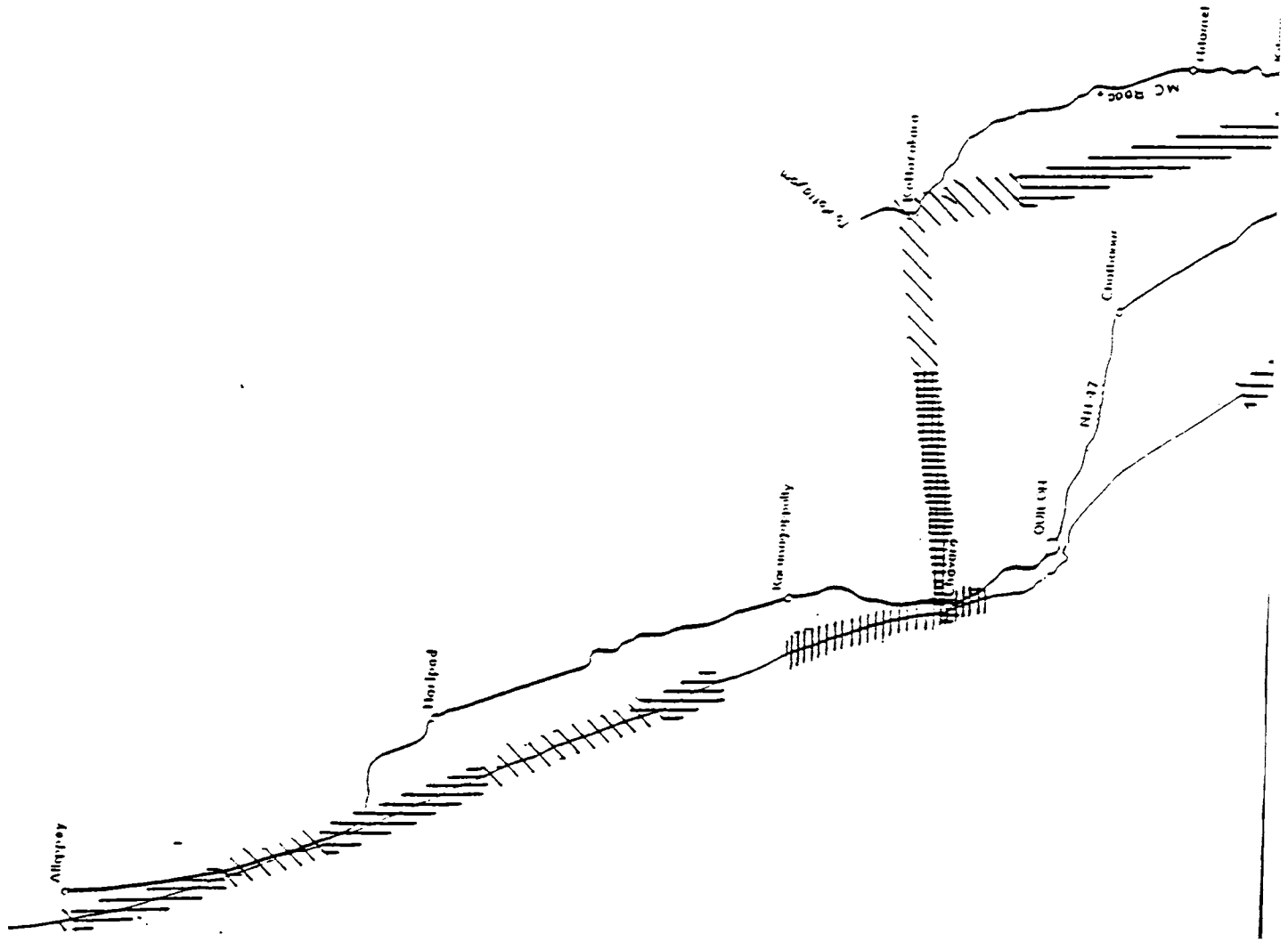
As the aircraft moves towards the coast after crossing Kottarakara, the conductivity increases, and reaches a peak at Chavara. The peak value at Chavara is lower than the one seen in the first survey because this survey was conducted at a higher altitude. During the short flight over the sea, the conductivity is seen to decrease rather rapidly. However the effect is seen to persist for the distance the flight went over the sea, the conductivity being larger than typical marine values. This has to be due to the transport of radon from over the land. Normally one would expect the conductivity to be high to the east of Chavara and decrease rapidly towards the sea. Because sea breeze is normally expected to carry away the radon and bring in fresh air from the sea, conductivity even at the coast should be close to that of marine air. This is not seen here. The ground station located at Chavara has also shown that conductivity values were higher than that of marine air even during periods when strong monsoon winds from the seaward side were present.

At a distance of around 20 km from Trivandrum, the negative polar conductivity measured during the return journey is seen to be much higher than positive. This is because the aircraft had taken a slightly different route during its return journey, and flew over a hill towards the north of Trivandrum. This hill is about 160 m high and has a somewhat higher level of radioactivity compared to its surround-

ings. The high negative values seen are therefore due to the reduction in ground height of the aircraft as it flew over the hill and the higher level of radioactivity there.

In the survey to Alleppey and back the positive and negative conductivity values are comparable. In the other two surveys the negative conductivities are higher than the positive conductivities. One possible cause for this difference is that the two polar conductivities are not measured simultaneously. Therefore, any change in polar conductivities with time will be reflected in the data. It is known that the conductivities do show a diurnal variation. Another possibility is that it could be due to a charging of the aircraft, as mentioned earlier. But since the first survey to Alleppey does not show any difference between the two polar conductivities, either the aircraft did not get charged during that flight, or the two processes could have combined to neutralize the effect of each other. Since the flights were carried out on consecutive days, when the weather remained more or less uniform, it is difficult to understand why the aircraft did not get charged in one flight alone. Therefore, the difference in polar conductivities could be due to a combination of these two causes.

The results of the conductivity surveys are plotted on a map of the region in Figure 5.12. The positive conductivity values alone are plotted in four convenient ranges. The ranges are different for the Kottarakara-Chavara survey because this survey was carried out at a different altitude from the other two. Over Chavara, therefore, polar conductivities have been obtained at two different altitudes, namely 1000 and 2000 feet, in addition to the data obtained at the surface. These



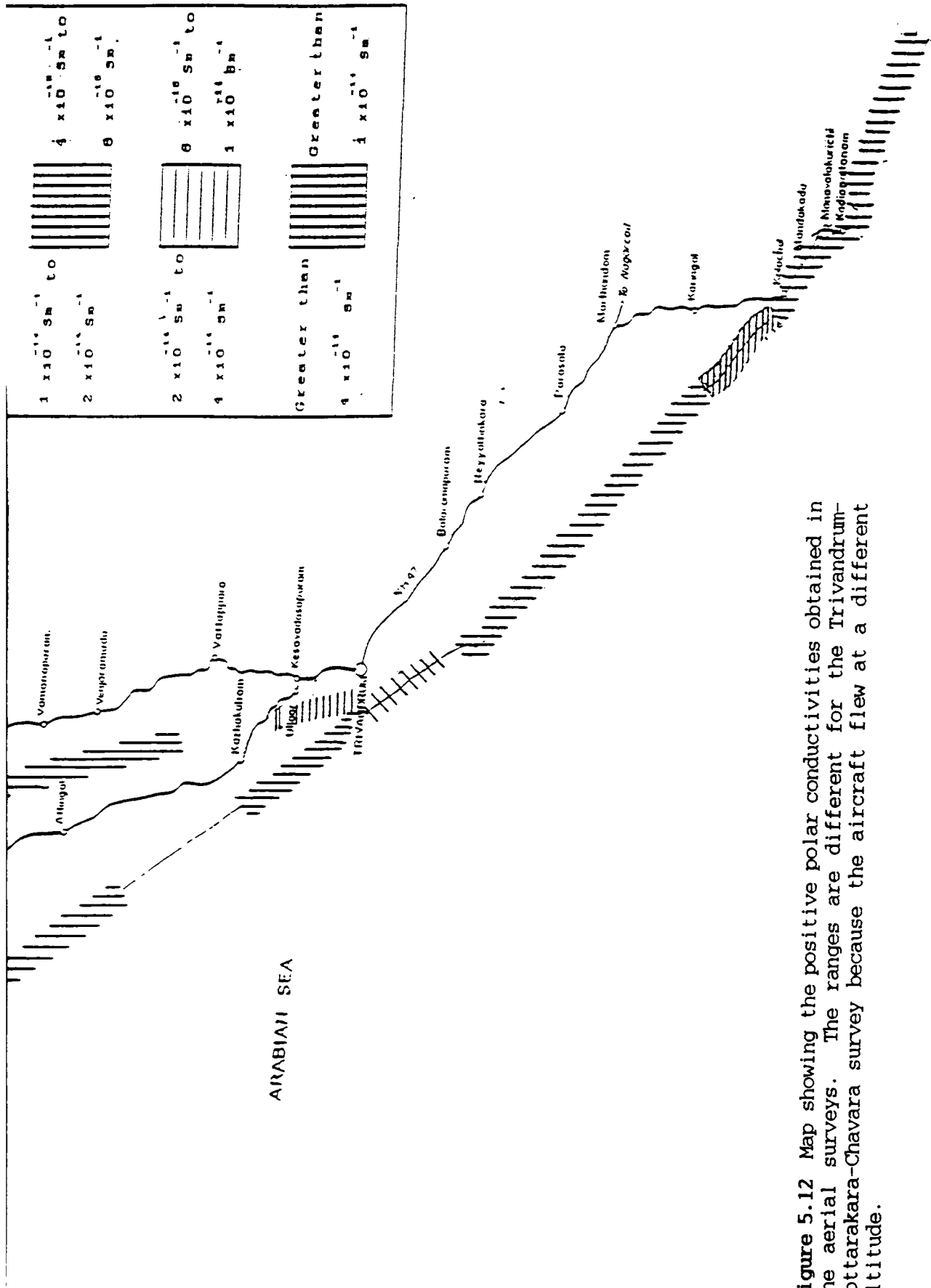


Figure 5.12 Map showing the positive polar conductivities obtained in the aerial surveys. The ranges are different for the Trivandrum-Kottarakara-Chavara survey because the aircraft flew at a different altitude.

measurements show that conductivity decreases with altitude in this region of the atmosphere. This is a direct result of the high radioactivity at the surface. In the horizontal plane, the higher conductivity is more or less confined to the region having the deposits.

The relationship between the polar conductivities at low altitudes and the presence of radioactive deposits at the surface points to the possibility of adapting this technique for preliminary surveys of radioactive deposits. The instrument is simple, light weight and inexpensive, and no special attachments or fixtures are needed on the aircraft. However, some more work has to be done to validate the technique and work out its feasibility.

CHAPTER VI

6 . SUMMARY AND CONCLUSION

6.1 RESUMÉ

This thesis presents the results of an investigation of the relationship between certain environmental factors and the behaviour of atmospheric electrical polar conductivities. The study was carried out in the southern part of Kerala State and the adjoining region of Tamil Nadu. One of the important environmental factors in this region is the large deposit of the radioactive mineral monazite in the coastal sands. This was, therefore, a major factor that was studied. Other environmental factors included rainfall, temperature, wind, etc. While the electrical conductivities were measured using instruments developed for the purpose, meteorological data were mostly obtained from the India Meteorological Department.

For the investigation, a Gerdien condenser instrument was designed and developed for continuous monitoring of atmospheric electrical polar conductivities. Three such instruments were fabricated and installed at suitable sites at Chavara, Ambalapuzha and Kottarakara. Positive and negative polar conductivities were measured for four to five months at these sites. Subsequently, one of these instruments was operated at the campus of our institute and data from here for about three months are used, along with rainfall measured simultaneously using a self recording rain gauge, to demonstrate the effect of rainfall on conductivity.

An electric field mill was developed for measuring the vertical electric field. It was test run for about one month at Kottarakara. Some modifications were found necessary, which were taken up.

A Gerdien condenser aircraft payload was also developed for conducting aerial surveys of polar conductivities using a Pushpak aircraft of the Kerala Aviation Training Centre, Trivandrum. Three surveys were carried out, namely, Trivandrum to Alleppey along the coast, Trivandrum to Kanyakumari along the coast, and Trivandrum to Chavara via Kottarakara. The third survey also went over the sea for about 1 km. Before the airborne surveys were conducted, the payload was tested by mounting it on a jeep and driving it along the highways. The highlights of the results are given below.

6.2 HIGHLIGHTS OF RESULTS

The data from the measurements at ground level indicate the following:

- (i) Polar conductivities have a similar behaviour in the region of study, as evidenced by the data from Kottarakara, Ambalapuzha and Trivandrum.
- (ii) Conductivity values are six to seven times higher at a site like Chavara having a rich deposit of radioactive minerals, compared to areas without significant deposits of these minerals.
- (iii) The diurnal variation pattern of polar conductivities is of the double oscillation type at all the sites, except during the

pre-monsoon period March to May at Chavara. Here the pattern is strongly influenced by wind during this period.

- (iv) The monthly mean amplitude of diurnal variation at Chavara during the pre-monsoon months is dependent on the mean maximum temperature. This can be attributed to the influence of temperature on the exhalation and atmospheric transport of radon.
- (v) The polar conductivities at Chavara show a sharp reduction after the onset of monsoon rainfall. The suppression of radon exhalation by rainfall must be the reason for this.
- (vi) Pre-monsoon rainfall, which is isolated, causes a reduction in conductivity, which recovers slowly after the rain.
- (vii) The vertical electric field at Kottarakara shows a double oscillation continental type behaviour that is more or less complementary to that of conductivity.
- (viii) The morning maximum in conductivity occurs around 0400 hrs and the minimum around 0700 to 0800 hrs at all the sites in all the seasons. This is seen to be more or less true even for a station like Athens where time of sunrise changes considerably over the year. This variation has a strong similarity to the semi-diurnal variation of atmospheric pressure.
- (ix) The aerial surveys have shown that the presence of natural radioactivity at the surface can be observed at 1000 to 2000 feet altitude, and possibly at higher altitudes also, by its influence on polar conductivities. This could be of use in preliminary surveys of radioactivity.

- (x) Surveys at ground level show that radioactivity from minerals in the soil and in rocks (in quarries) have a strong influence on atmospheric electrical conductivity.

In summary, the main findings of the study are:

- (a) the diurnal variation pattern of conductivity at a site having a large deposit of radioactive minerals is strongly influenced by meteorological factors like wind, rainfall and temperature, and can be different in different seasons;
- (b) rainfall causes a reduction in conductivity, and during periods of continuous rainfall, as in the monsoon season, the ratio of positive to negative polar conductivity becomes less than unity;
- (c) atmospheric pressure may play an important role in determining the diurnal variation of conductivity;
- (d) the presence of radioactive minerals at the surface can be detected from air-borne surveys of conductivity.

6.3 SUGGESTIONS FOR FURTHER STUDIES

The present study has made an attempt to understand some of the effects of environmental parameters like surface radioactivity, rainfall, atmospheric temperature, etc. on the behaviour of atmospheric electrical polar conductivities. While some interesting results have been obtained, the study also has brought to light some aspects of the behaviour of conductivities that need further investigation. Some of these aspects are discussed below.

An interesting observation made during the present study is that the morning maximum in conductivity is reached around 0400 hrs LT at almost all stations, rural and urban, and in all kinds of weather. Similarly, the morning minimum occurs between 0700 hrs and 0900 hrs. The usual explanation for the decrease in conductivity in the morning is based on sunrise and human activity, which seems to be unsatisfactory. There appears to be a relationship between the variation of conductivity and that of atmospheric pressure, their semi-diurnal components being almost exactly out of phase. The reason for the behaviour of conductivity in the early morning, therefore, has to be looked into more carefully. It would be useful to measure polar conductivities along with the small and large ion concentrations, the aerosol concentration, and meteorological parameters like pressure, temperature, humidity, etc.

Another point that needs to be looked into is the relationship between the amplitude of variation of conductivity and atmospheric temperature. The present study shows a dependence of the amplitude of variation of the monthly mean hourly values on the monthly mean maximum temperature. But a similar dependence of the daily amplitude of conductivity variation on the maximum temperature for the day is not seen. This is possibly due to the influence of other factors that may introduce random variations in the conductivity values. The explanation suggested here for the observed dependence is that of the influence of temperature on the exhalation and transport of radon. But an important influence on conductivity is that of aerosols. Explanations for conductivity variations at a site have mostly concentrated on the behaviour of aerosols. The effects of temperature and rainfall on

conductivity observed in the present study cannot be explained on this basis. It appears, therefore, that greater attention has to be given to the influence of meteorological parameters on radon exhalation and the consequences for atmospheric electricity.

REFERENCES

- Anderson, R.V., (1972): Atmospheric electricity, turbulence and a pseudo-sunrise effect resulting from a solar eclipse, *J Geophys Res*, 34, 567-572.
- Anderson, R.V. and H. Dolezalek, (1972): Atmospheric electricity measurements at Waldorf, Maryland, during the 7 March 1970 solar eclipse, *J Atmos Terr Phys*, 34, 561-566.
- Bricard, J., (1965): Action of radioactivity and of pollution upon parameters of atmospheric electricity, in S.C. Coroniti (Ed.) *Problems of Atmospheric and Space Electricity*, pp82-117.
- Callahan, R.C., S.C. Coroniti, A.J. Parziale and R. Patten, (1951): Electrical conductivity of air in the troposphere, *J Geophys Res*, 56, 545-551.
- Chalmers, J.A., (1951 a): The origin of the electric charge on rain, *Quart J Royal Meteorol Soc*, 77, 249-259.
- Chalmers, J.A., (1951 b): Point discharge currents, *J Atmos Terr Phys*, 2, 301.
- Chalmers, J.A., (1967): *Atmospheric Electricity*, Pergamon Press, New York.
- Chand, D. and N.C. Varshneya, (1973): Atmospheric convection and its effects on relaxation time and charge distribution, *J Atmos Terr Phys*, 35, 681-692.
- Chate, D.M. and A.K. Kamra, (1992): Charge separation associated with splashing of water drops on solid surfaces, *Atmos Res*, 29, 115-128.

- Cobb, W.E., (1967): Evidence of a solar influence on the atmospheric electric elements at Mauna Loa Observatory, *Mon Wea Rev*, **95**, 905.
- Cobb, W.E., (1973): Oceanic aerosol levels deduced from measurements of the electrical conductivity of the atmosphere, *J Geophys Res*, **30**, 101-106.
- Conley, T.D., (1974): Mesospheric positive ion concentration, mobilities, and loss rates obtained from rocket-borne Gerdien condenser measurements, *Radio Science*, **9**, 575-592.
- Conley, T.D., E.R. Hegblom and R.S. Narcisi, (1983): D-region positive and negative ion concentration and mobilities during the February 1979 eclipse, *J Atmos Terr Phys*, **45**, 499-513.
- Coroniti, S.C., A.J. Parziale, R.C. Callahan, and R. Patten, (1952): Effect of aircraft charge on airborne conductivity measurements, *J Geophys Res*, **57**, 197-205.
- Dhanorkar, S., (1992): *Characteristics of Atmospheric Ions Close to Ground*, Ph.D. thesis submitted to the University of Poona, Pune.
- Dhanorkar, S. and A.K. Kamra, (1991): Measurement of mobility spectrum and concentration of all atmospheric ions with a single apparatus, *J Geophys Res*, **20**, 18671-18678.
- Dutra, S.L.G., A.L.C. Gonzalez, W.D. Gonzalez and A.E.C. Ferreira, (1992): Downward mapping of quasi-static ionospheric electric fields at low altitudes during fair-weather, *J Atmos Terr Phys*, **54**, 223-230.
- Elster, J. and H. Geitel, (1899): On the existence of electric ions in the atmosphere, *Terr Magn Atmos Electr*, **4**, 213-234; cited in Israel (1971).
- Farrokh, H., (1975): Design of a simple Gerdien condenser for ionospheric D-region charged particle density and mobility measure-

ments, *Scientific Report 433*, Ionospheric Research Laboratory, Pennsylvania State University.

Gerdien, H., (1905): Demonstration eines apparatuses zur absoluten messung der electreschen leitfahigut der luft, *Terr Magn Atmos Electr*, 10, 65-79.

Gish, O.H. and G.R. Wait, (1950): Electric charge carried to ground through thunderstorms, *Report on Conference on Thunderstorm Electricity*, 193-203.

Hays, P.B., and R.G. Roble, (1979): A quasi-static model of global atmospheric electricity, 1. The lower atmosphere, *J Geophys Res*, 84, 3291-3305.

Holzworth, R.H. and F.S. Mozer, (1979): Direct evidence of solar flare modification of stratospheric electric fields, *J Geophys Res*, 84, 363-367.

Hoppel, W.A., (1967): Theory of the elctrode effect, *J Atmos Terr Phys*, 29, 709-721.

IMD, (1986): *Climate of Kerala State*, Government of India Publication, India Meteorological Department. Available from the Controller of Publications, Civil Lines, New Delhi 110 054.

Israel, H., (1958): Die natüliche Radioaktivität in Boden, Wasser und Luft, *Beitr Phys Atmosphäre*, 30, 177-188; cited in Israel, 1971.

Israel, H., (1971): *Atmospheric Electricity*, 2 vols., Israel Programme for Scientific Translations, Jerusalem.

Israelsson, S. and E. Knudsen, (1986): Effect of radioactive fallout from a nuclear power plant accident on electrical parameters, *J Geophys Res*, 91, 11909-11910.

- Johns, M.D. and K.S. Kreielsheimer, (1967): The side-on field mill, *J Atmos Terr Phys*, 29, 497-505.
- Jonassen, N. and M.H. Wilkening, (1965): Conductivity and concentration of small ions in the lower atmosphere, *J Geophys Res*, 70, 779-784.
- Junge, C.E., (1963): *Air Chemistry and Radioactivity*, Academic Press, New York.
- Kamra, A.K., (1969 a): Effect of wind on diurnal and seasonal variation of atmospheric electric field, *J Atmos Terr Phys*, 31, 1281-1286.
- Kamra, A.K., (1969 b): Electrification in an Indian dust storm, *Weather*, 24, 145-146.
- Kamra, A.K., (1972 a): Measurements of the electrical properties of dust storms, *J Geophys Res*, 77, 5183-5200.
- Kamra, A.K., (1972 b): Visual observation of sparks on gypsum dunes, *Nature*, 240, 143-144.
- Kamra, A.K., (1983): Spherical field meter for measurement of the electric field vector, *Rev Sci Instrum*, 54, 1401-1406.
- Kamra, A.K., (1989): Charge transfer by point discharge below dust storms, *Geophys Res Lett*, 16, 127-129.
- Kamra, A.K., (1991): Inadvertent modification of atmospheric electricity, *Current Sci*. 60, 639-646.
- Kamra, A.K. and A.B. Sathe, (1983): Raindrop charges, electric field and space charge measurements at a mountain station covered with monsoon clouds, *Arch Met Geophys Biocl, Ser A*, 32 145-153.
- Kamra, A.K. and N.C. Varshneya, (1967): Excess point-discharge current during rapid field changes, *J Atmos Terr Phys*, 29, 1519-1527.

- Kamra, A.K., and N.C. Varshneya, (1968): Agrimeter for measurement of atmospheric electric potential gradient, *India J Pure Appl Phys*, 6, 31-33.
- Kraakevic, J.H., (1958): The air-borne measurement of atmospheric conductivity, *J Geophys Res*, 63, 161-169.
- Lenard, P., (1892): Über die Electricität der Wasserfälle, *Ann Phys, Lpz.*, 46, 584-636; cited in Chalmers (1967).
- Liu, S.C., J.R.McAfee and R.J.Cicerone, (1984): Radon 222 and tropospheric vertical transport, *J Geophys Res*, 89, 7291-7297.
- Makino, M. and T. Ogawa, (1984): Responses of atmospheric electric field and air-earth current to variations of conductivity profile, *J Atmos Terr Phys*, 46, 431.
- Mani, A. and B.B. Huddar, (1975): Studies of dust and nuclei content of the air near the ground and their effect on atmospheric electricity parameters, *Indian J Meteorol Hydrol Geophys*, 26, 241-248.
- Markson, R., (1978): Solar modulation of atmospheric electrification and possible implications for the sun-weather relationship, *Nature*, 273, 103-109.
- Markson, R., (1985): Aircraft measurements of the atmospheric electrical global circuit during the period 1971-1984, *J Geophys Res*, 90, 5967-5977.
- Markson, R. and M.S. Muir, (1980): Solar wind control of the earth's electric field, *Science*, 208, 979-990.
- Meszaros, E., (1981): *Atmospheric Chemistry*, Elsevier Scientific Publishing Co., Amsterdam.

- Moses, H., Strehney A.F. and Lucas H.F. Jr., (1960): The effect of meteorological variables upon the vertical and temporal distribution of atmospheric radon, *J Geophys Res*, 65, 1223-1238.
- Muir, M.S., (1975): The ionosphere as the source of the atmospheric electric sunrise effect, *J Atmos Terr Phys*, 37, 553-559.
- Muir, M.S., (1977): Atmospheric electric space charge generated by the surf, *J Atmos Terr Phys*, 39, 1341-1346.
- Muir, M.S., (1979): A possible mechanism linking solar events and terrestrial weather, *S Afr J Phys*, 2, 33-35.
- Murali Das, S., S. Sampath and V. Sasi Kumar, (1991): Effect of surface radioactivity on vertical distribution of atmospheric electrical conductivities, *Indian J Radio Space Phys*, 20, 444-445.
- Nieuwolt, S., (1977): *Tropical Climatology*, John Wiley & Sons, Chichester.
- Nisbet, J.S., (1985): Currents to the ionosphere from thunderstorm generators: A model study, *J Geophys Res*, 90, 9831-9844.
- Paltridge, G.W., (1965): Experimental measurements of the small-ion density and electrical conductivity of the stratosphere, *J Geophys Res*, 70, 2751-2761.
- Paltridge, G.W., (1966): Stratospheric small ion density measurements from a high altitude jet aircraft, *J Geophys Res*, 71, 1945-1952.
- Park, C.G., (1976): Downward mapping of high latitude ionospheric electric fields to the ground, *J Geophys Res*, 81, 168.
- Park, C. and M. Dejnakintra, (1973): Penetration of thundercloud electric fields into the ionosphere, *J Geophys Res*, 78, 6623.

- Pierce, E.T., (1957): Nuclear explosions and a possible secular variation of the potential gradient in the atmosphere, *J Atmos Terr Phys*, 11, 71-72.
- Pierce, E.T., (1958): Some topics in atmospheric electricity, in *Recent Advances in Atmospheric Electricity*, edited by L.G. Smith, Pergamon Press, New York.
- Pierce, E.T., (1972): Radioactive fallout and secular effects in atmospheric electricity, *J Geophys Res*, 77, 482-487.
- Pierce, E.T. and A.L. Whitson, (1964): The variation of potential gradient with altitude above ground of high radioactivity, *J Geophys Res*, 69, 2895-2898.
- Pierce, E.T. and A.L. Whitson, (1965): Atmospheric electricity and the waterfalls of Yosemite valley, *J Atmos Sci*, 22, 314-319.
- Prakash, T.N., G.K. Raju and M. Prithviraj, (1991): Radioelement distribution in river, beach, and offshore areas and their significance to Chavara placer deposit, southern Kerala coast of India, *Geo-Marine Lett*, 11, 32-38.
- Raina, B.N. and R.C. Raina, (1988): Diurnal variation of some fair weather electrode effect parameters at Gulmarg, *J Atmos Terr Phys*, 50, 1-9.
- Reiter, R., (1969): Solar flares and their impact on potential gradient and air-earth current characteristics at high mountain stations, *Pure Appl Geophys*, 72, 259.
- Reiter, R., (1971): Further evidence of impact of solar flares on potential gradient and air-earth current characteristics at high mountain stations, *Pure Appl Geophys*, 86, 142.
- Retalis, D.A., (1983): Study of the large ion concentration in the air above Athens, *Arch Met Geophys Biocl, Ser A.*, 32, 135-143.

- Retalis, D.A., (1987): Chernobyl reactor accident consequences on small atmospheric ions concentration above Athens, *Pure Appl Geophys*, 125, 669-678.
- Retalis, D. and A. Pitta, (1989): Effects on electrical parameters at Athens, Greece, by radioactive fallout from a nuclear power plant accident, *J Geophys Res*, 94, 13093-13097.
- Retalis, D. and P.M. Zervos, (1976): Study of the electrical conductivity of the air above Athens, *J Atmos Terr Phys*, 38, 299-305.
- Roble, R.G., and P.B. Hays, (1979): A quasi-static model of global atmospheric electricity - 2. Electrical coupling between the upper and lower atmosphere, *J Geophys Res*, 84, 7247-7256.
- Rosen, J.M. and D.J. Hofmann, (1981): Balloon-borne measurements of the small ion concentration, *J Geophys Res*, 7399-7405.
- Sankaran, A.V., B. Jayaswal, K.S.V. Nambi and C.M. Sunta, (1986): *U, Th and K distributions inferred from regional geology and the terrestrial radiation profiles in India*, Publication of the Bhabha Atomic Research Centre, Trombay, Bombay, India.
- Sao, K., (1967): Correlation between solar activity and the atmospheric potential gradient at the earth's surface in the polar regions, *J Atmos Terr Phys*, 29, 213-215.
- Schery, S.D., D.H. Gaeddert, and M.H. Wilkening, (1984): Factors affecting exhalation of radon from a gravelly sandy loam, *J Geophys Res*, 89, 7299-7309.
- Takagi, M. and A. Iwata, (1980): A seasonal effect in diurnal variation of the atmospheric electric field on the Pacific coast of Japan, *Pure Appl Geophys*, 118, 953-963.
- Trevitt, A.C., (1984): Atmospheric electric modulation during a sea breeze, *J Geophys Res*, 89, 9663-9667.

- Tuomi, T.J., (1982): The atmospheric electrode effect over snow, *J Atmos Terr Phys*, **44**, 737-745.
- Twomey, S., (1977): *Atmospheric Aerosols*, Elsevier Scientific Publishing Co., Amsterdam.
- Varshneya, N.C., (1980): A mathematical model of global atmospheric electricity, *Proc. VI Internat. Conf. Atmos. Electr.*
- Whipple, E.C., (1960): An improved technique to obtain ion mobility distributions, *J Geophys Res*, **65**, 3679-3684.
- Wigand, A., (1927 a): Die erhaltung der Erdladung durch den blitzstrom (Conservation of the earth's charge by lightning current), *Phys Z*, **28**, 65-69; cited in Israel (1971).
- Wigand, A., (1927 b): Erdladung, blitzstrom und niederschlagsstrom (The earth's charge, the lightning current and the precipitation current), *Phys Z*, **28**, 261-263; cited in Israel (1971).
- Wilkening, M.H., (1959): Daily and annual courses of natural atmospheric radioactivity, *J Geophys Res*, **64**, 521-526.
- Wilkening, M.H. and V. Romero, (1981): ^{222}Rn and atmospheric electrical parameters in the Carlsbad caverns, *J Geophys Res*, **86**, 9911-9916.
- Willet, J.C., (1979): Fair-weather electric charge transfer by convection in an unstable planetary boundary layer, *J Geophys Res*, **84**, 703-718.
- Wilson, C.T.R., (1929): Investigations on lightning discharges and on the electric field of thunderstorms, *Phil Trans Royal Soc London*, (A) **221**, 73-115, 1920; and, Some thundercloud problems, *T J Franklin Insttt*, **208**, 1-12; cited in Israel (1971).
-

PUBLICATIONS

1. V. Sasi Kumar, S. Sampath and S. Murali Das, Effect of radioactive deposits at the surface on atmospheric electricity - Results of a study, *Proceedings of the 9th International Conference on Atmospheric Electricity*, St. Petersburg, Russia, June 15-19, 1992.
 2. V. Sasi Kumar, S. Murali Das and S. Sampath, Atmospheric electrical conductivities over a region of high radioactivity, accepted for publication in *Indian J Radio Space Phys*.
 3. S. Sampath, V. Sasi Kumar and S. Murali Das, Air-borne measurements of atmospheric electrical conductivities, communicated to *Pure Appl Geophys*.
 4. S. Murali Das, V. Sasi Kumar, S. Sampath, T.K. Krishnachandran Nair and M. Ismail, Aerial survey of atmospheric electrical conductivity over a region of high radioactivity using a Pushpak aircraft, communicated to *J Assoc Exploration Geophys*.
 5. V. Sasi Kumar, S. Sampath, S. Murali Das and K. Vijayakumar, Atmospheric electrical conductivity variations over different environments, communicated to *Geophys J Royal Astronom Soc*.
-